THE EFFICACY OF ASPERGILLOMARASMINE A

THE EFFICACY OF ASPERGILLOMARASMINE A TO OVERCOME β-LACTAM ANTIBIOTIC RESISTANCE

by CAITLYN M. ROTONDO, B.Sc., M.Sc.

A thesis submitted to the School of Graduate Studies in partial fulfillment
of the requirements for the degree of Doctor of Philosophy

DESCRIPTIVE NOTE

McMaster University, DOCTOR OF PHILOSOPHY (2022), Hamilton, Ontario (Biochemistry and Biomedical Sciences)

TITLE: The efficacy of aspergillomarasmine A to overcome β-lactam antibiotic resistance

AUTHOR: Caitlyn M. Rotondo, B.Sc., M.Sc.

SUPERVISOR: Gerard D. Wright, Ph.D.

NUMBER OF PAGES: xxii, 189

LAY ABSTRACT

Bacteria are all around us. While some bacteria can promote human health, others can cause serious infections. These infections are typically treated with antibiotics. β-Lactam antibiotics, such as penicillins and cephalosporins, are especially important to medicine. Unfortunately, an increasing number of bacteria employ enzymes, known as β-lactamases, which negate the effects of β-lactam antibiotics. Previous studies demonstrated that a natural product, known as aspergillomarasmine A (AMA), could inhibit some β-lactamase enzymes. Consequently, the inhibitory power of AMA was further explored against a larger number of β-lactamase enzymes and in combination with different β-lactam antibiotics. After discovering that AMA had more inhibitory power when combined with a β-lactam antibiotic known as meropenem, the efficacy of the AMA/meropenem pairing was evaluated against resistant bacteria in the presence and absence of avibactam, another β-lactamase inhibitor. The AMA/avibactam/meropenem combination was shown to be effective against some of the world's most antibiotic-resistant bacteria.

ABSTRACT

While antibiotics have saved the lives of millions of people since the discovery of the first β-lactam, penicillin, their continued effectiveness is being increasingly threatened by resistant bacteria. Bacterial resistance to β-lactams is mainly achieved through the production of serine-β-lactamases (SBLs) and metallo-β-lactamases (MBLs). Although both types of β-lactamases are commonly isolated in clinical settings, MBLs represent the greatest threat to public health since they are resistant to SBL inhibitors and most β-lactams. However, aspergillomarasmine A (AMA), a fungal natural product synthesized by *Aspergillus versicolor*, was shown to be a rapid and potent inhibitor against two clinically relevant MBLs: NDM-1 and VIM-2. In bacteria possessing these enzymes, AMA could rescue the activity of meropenem, a broad-spectrum β-lactam that is usually reserved for the treatment of the most severe bacterial infections. However, many questions remain revolving around AMA's inhibitory potency and spectrum. Therefore, the activity of AMA in combination with six β-lactams from three subclasses (carbapenem, penam, cephem) was explored against 19 MBLs from three subclasses (B1, B2, B3). After determining that AMA activity was linked to MBL zinc affinity and that AMA was more potent when paired with a carbapenem, the efficacy of an AMA/meropenem combination was evaluated with and without avibactam, a potent SBL inhibitor. This study used ten *Escherichia coli* and ten *Klebsiella pneumoniae* laboratory strains as well as 30 clinical strains producing at least one MBL and one SBL. Once establishing that the AMA/avibactam/meropenem combination was effective against carbapenemase-producing Enterobacterales, new *Acinetobacter* and *Pseudomonas* shuttle

vectors were created. With these shuttle vectors, it was determined that the AMA/avibactam/meropenem combination was effective against some of the bacteria topping the World Health Organization's priority pathogen list.

ACKNOWLEDGMENTS

The production of this doctoral dissertation was only made possible with the aid of some remarkable individuals who generously contributed to its success. Therefore, at this time, I would like to take a moment to thank everyone who kindly guided me throughout one of the most challenging and significant academic achievements of my career.

First and foremost, I would like to thank my supervisor, Dr. Gerry Wright. Without your profound belief in my research abilities, extensive knowledge, and infinite patience, the completion of my doctoral degree would not have been possible. In addition to my advisor, I express my sincere gratitude to my committee members, Dr. Eric Brown and Dr. Alfredo Capretta, for their insightful comments, hard-hitting questions, and honest feedback during our annual meetings. Lastly, a special thank you to Dr. Roberto Melano for agreeing to serve as an external reader for my doctoral dissertation. My utmost thanks go out to all of you for challenging me to do my best, expanding my knowledge base, and helping me to become an all-around better researcher.

Furthermore, I would like to extend my sincerest gratitude to all past and present members of the Wright laboratory. Over the years, your invaluable advice, immense kindness, and commitment to antibiotic resistance research have created a positive, enjoyable, and successful working environment that I will never forget. A special thank you to Haley Zubyk for cloning and transforming several resistance genes used throughout my research project. I would also like to extend my appreciation to Linda Ejim, who patiently taught me how to conduct minimal inhibitory concentration assays and potentiation assays. Many thanks as well to Allison Guitor and Dr. Wenliang Wang

for providing me with the clinical strain sequencing data and purified aspergillomarasmine A necessary for my research. Finally, I am deeply indebted to Dr. David Sychantha, Dr. Kalinka Koteva, Dr. Manpreet Kaur, and Matthew Surette as without your contributions my research projects would not have come to fruition.

Furthermore, words cannot express my infinite gratitude to my family and friends for being a constant source of patience, understanding, and strength throughout the entirety of my education. I am extremely grateful to my dear parents and my loving brother for their unconditional love, heartfelt prayers, steadfast encouragement, and continued support through both the good and bad moments encountered in the pursuit of my doctoral degree. Thank you for believing in me!

TABLE OF CONTENTS

LIST OF TABLES

CHAPTER 2

CHAPTER 3

CHAPTER 4

LIST OF FIGURES

CHAPTER 1

LIST OF ABBREVIATIONS

× *g* ..... Relative centrifugal force
°C ..... Degree Celsius
µF ..... Microfarad
µg ..... Microgram
µL ..... Microliter
µM ..... Micromolar
6×His ..... Polyhistidine
AAC ..... Aminoglycoside N-acetyltransferase
ACE ..... Angiotensin-converting enzyme
ACT ..... AmpC type
AMA ..... Aspergillomarasmine A
AMP ..... Ampicillin
AmpC ..... Ampicillinase
ANT ..... Aminoglycoside O-nucleotidyltransferase
APH ..... Aminoglycoside O-phosphotransferase
Arg ..... Arginine
Asn ..... Asparagine
ARP ..... Antibiotic resistance platform
Asp ..... Aspartic acid
AVI ..... Avibactam
ATCC ..... American Type Culture Collection
BBL ..... Class B β-lactamase
bla ..... β-Lactamase
BLI ..... β-Lactamase inhibitor
BzCl ..... Benzoyl chloride
CH_3CO_2K ..... Potassium acetate
Ca ..... Calcium
CA ..... California
$CaCl_2$ ..... Calcium chloride
CAMHB ..... Cation-adjusted Mueller Hinton II broth
CAR ..... Carbenicillin
CARD ..... Comprehensive Antibiotic Resistance Database
CEC ..... Cefaclor
CFU ..... Colony forming unit
CHDL ..... Carbapenem-hydrolyzing class D β-lactamase
CT ..... Connecticut
CTX ..... Cefotaxime
CTX-M ..... Cefotaximase
Cys ..... Cysteine
DBO ..... Diazobicyclooctane
DMSO ..... Dimethyl sulfoxide
DNA ..... Deoxyribonucleic acid

DOR ..... Doripenem
Dr. ..... Doctor
EASV ..... *Escherichia-Acinetobacter* shuttle vector
EDTA ..... Ethylenediaminetetraacetic acid
EPSV ..... *Escherichia-Pseudomonas* shuttle vector
erm ..... Erythromycin resistance methylase
ESBL ..... Extended-spectrum β-lactamase
ESKAPE ..... *Enterococcus faecium*, *Staphylococcus aureus*, *Klebsiella pneumoniae*, *Acinetobacter baumannii*, *Pseudomonas aeruginosa*, *Enterobacter* species
et al. ..... And others
EUCAST ..... European Committee on Antimicrobial Susceptibility Testing
FDA ..... Food and Drug Administration
FWD ..... Forward
FEP ..... Cefepime
g ..... Gram
GEN ..... Gentamicin
Gln ..... Glutamine
Glu ..... Glutamic acid
h ..... Hour
HEPES ..... *N*-2-hydroxyethylpiperazine-*N*′-2-ethanesulfonic acid
His ..... Histidine
HRP ..... Horseradish peroxidase
IA ..... Iowa
IDT ..... Integrated DNA Technologies
IL ..... Illinois
IMP ..... Imipenemase
IPTG ..... Isopropyl-*β*-D-thiogalactopyranoside
KAN ..... Kanamycin
kDa ..... Kilodalton
$K_{d,Zn2}$ ..... Zn^{2+} dissociation constant
KPC ..... *Klebsiella pneumoniae* carbapenemase
kV ..... Kilovolt
LB ..... Luria-Bertani
Lys ..... Lysine
M ..... Molar
m/z ..... Mass-to-charge ratio
MA ..... Massachusetts
MBL ..... Metallo-β-lactamase
MD ..... Maryland
msec ..... Millisecond
HCl ..... Hydrochloric acid
MCS ..... Multiple cloning site
MDR ..... Multidrug-resistant
ME ..... Maine

MEM ..... Meropenem
MeOH ..... Methanol
Mg ..... Milligram
$MgSO_4$ ..... Magnesium sulfate
MIC ..... Minimum inhibitory concentration
min ..... Minute
mL or ml ..... Milliliter
mM ..... Millimolar
MOPS ..... 3-(*N*-morpholino)propanesulfonic acid
$MnCl_2$ ..... Manganese chloride
mph ..... Macrolide phosphotransferase
MS/MS ..... Tandem mass spectrometry
NaCl ..... Sodium chloride
NAG ..... *N*-acetylglucosamine
NAM ..... *N*-acetylmuramic acid
NaOH ..... Sodium hydroxide
NDM ..... New Delhi metallo-β-lactamase
ng ..... Nanogram
NH_4OH ..... Ammonium hydroxide
Ni-NTA ..... Nickel-nitrilotriacetic acid
NJ ..... New Jersey
nl ..... Nanoliter
nM ..... Nanomolar
nm ..... Nanometer
OD ..... Optical density
ori ..... Origin of replication
OXA ..... Oxacillinase
PAGE ..... Polyacrylamide gel electrophoresis
PBP ..... Penicillin-binding protein
PCR ..... Polymerase chain reaction
PDB ..... Protein Data Bank
PIP ..... Piperacillin
PVDF ..... Polyvinylidene difluoride membrane
qnr ..... Quinolone resistance
Q-TOF ..... Quadrupole-time of flight
RbCl ..... Rubidium chloride
REV ..... Reverse
RGI ..... Resistance Gene Identifier
rpm ..... Revolutions per minute
RNA ..... Ribonucleic acid
RNase ..... Ribonuclease
RpoA ..... RNA polymerase subunit alpha
s ..... Second
SBL ..... Serine-β-lactamase

SDS ..... Sodium dodecyl sulfate
Ser ..... Serine
SHV ..... Sulf-hydryl variable
SIT ..... Spiro-indoline-thiadiazole
spp. ..... Several species
TEM ..... Temoniera
tet ..... Tetracycline
Tfb ..... Transformation buffer
TOB ..... Tobramycin
Tyr ..... Tyrosine
Ulp ..... Ubiquitin-like protein-specific protease
UPLC ..... Ultraperformance liquid chromatography
USA ..... United States of America
UV ..... Ultraviolet
VEB ..... Vietnamese extended-spectrum β-lactamase
VIM ..... Verona integron-encoded metallo-β-lactamase
v/v ..... Volume/Volume
Vis ..... Visible
VT ..... Vermont
WAC ..... Wright Actinomycete Collection
w/v or wt/vol ..... Weight/Volume
WHO ..... World Health Organization
Zn ..... Zinc
ZnCPD ..... Zn^{2+}-dependent carboxypeptidase A
$ZnSO_4$ ..... Zinc sulfate

DECLARATION OF ACADEMIC ACHIEVEMENT

I have performed all of the research in this body of work except where indicated in the preface of each chapter.

CHAPTER 1: Introduction

1.1 Penicillins: A brief history

Although Selman Waksman was credited with coining the term *antibiotic* in 1941, fungal and bacterial compounds capable of killing or hindering the growth of microorganisms have existed for millennia [1–3]. Over 3000 years ago, the Chinese exploited the antibacterial properties of fungi by treating infected wounds with moldy soya beans [3]. In modern medicine, the most common antibiotics synthesized by mold are penicillins. The discovery of the penicillins began in 1928 when Sir Alexander Fleming noticed something unusual on a petri dish containing the bacterium *Staphylococcus aureus* upon returning from vacation [4–7]. The mold, later identified as *Penicillium notatum*, which had contaminated the petri dish, was preventing the growth of *S. aureus* [4,6]. Upon growing and isolating the mold, Fleming concluded that a substance with antibacterial properties was being produced [5]. This substance was later named benzylpenicillin (or penicillin G) (Figure 1.1) [6]. Although Fleming published his findings in 1929 [5], he was never able to purify benzylpenicillin and, consequently, discontinued his research on this antibiotic [4,6]. His research would be completed in the 1940s with the successful production and purification of benzylpenicillin by Howard Flory, Ernst Chain and Norman Heatley [4,6–8].

1.2 β-lactam antibiotics: A highlight on carbapenems

Benzylpenicillin was the first member of the β-lactam family of antibiotics [9]. From 1941, when Albert Alexander became the first recipient of benzylpenicillin [7], to the present day, β-lactams remain among the most frequently prescribed antibiotics [10]. The β-lactam ring, a four-membered cyclic amide, is the namesake for this family of

antibiotics and is a distinctive feature present in the molecular structure of all β-lactams [11]. Although sharing a common structural feature, β-lactams can still be separated into five subclasses based on the structure of their β-lactam nucleus and side chain(s): 1) the penicillins (or penams), 2) the cephalosporins (or cephems), 3) the carbapenems, 4) the monobactams and 5) the clavams (Figure 1.1) [10]. Among these subclasses, the carbapenems are the β-lactams with the broadest antibacterial spectrum. Therefore, carbapenems are typically used as last-resort antibiotics to treat the most severe bacterial infections [12].

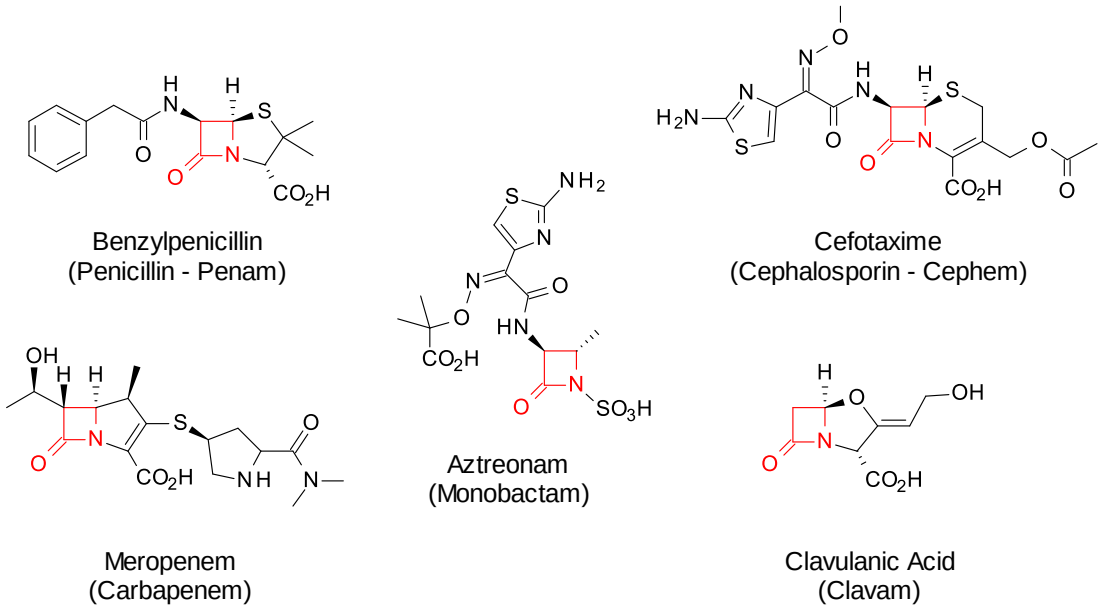

Figure 1.1: Structures of different β-lactam antibiotics. The β-lactam nucleus is highlighted in red. The five structural subclasses are shown in parentheses. Figure adapted from reference [13].

The history of carbapenems began in 1976 when Kahan and colleagues conducted a screen for peptidoglycan biosynthesis inhibitors using *Streptomyces* culture broths [14,15]. In 1979, following many attempts, the biologically active compound was purified

and named thienamycin (or thienpenem) [14]. Thienamycin, a natural product synthesized by *Streptomyces cattleya*, was the first carbapenem antibiotic and one of the most potent, broad-spectrum antibiotics ever discovered (Figure 1.2) [14,16]. However, thienamycin is chemically unstable and decomposes in the presence of water [12,17]. Therefore, a stable thienamycin-derivative named imipenem was the first clinically used carbapenem (Figure 1.2) [17]. Imipenem was developed by Merck & Co. [17] and approved for use in the United States of America (USA) by the Food and Drug Administration (FDA) in 1985 [12]. Imipenem is typically co-administered with the dehydropeptidase inhibitor cilastatin since this carbapenem is rapidly metabolized by a renal dipeptidase found in the human kidney [17]. Since the development of imipenem, three more carbapenems have been approved for use in clinics in the USA: 1) meropenem, 2) ertapenem, and 3) doripenem (Figure 1.2) [15].

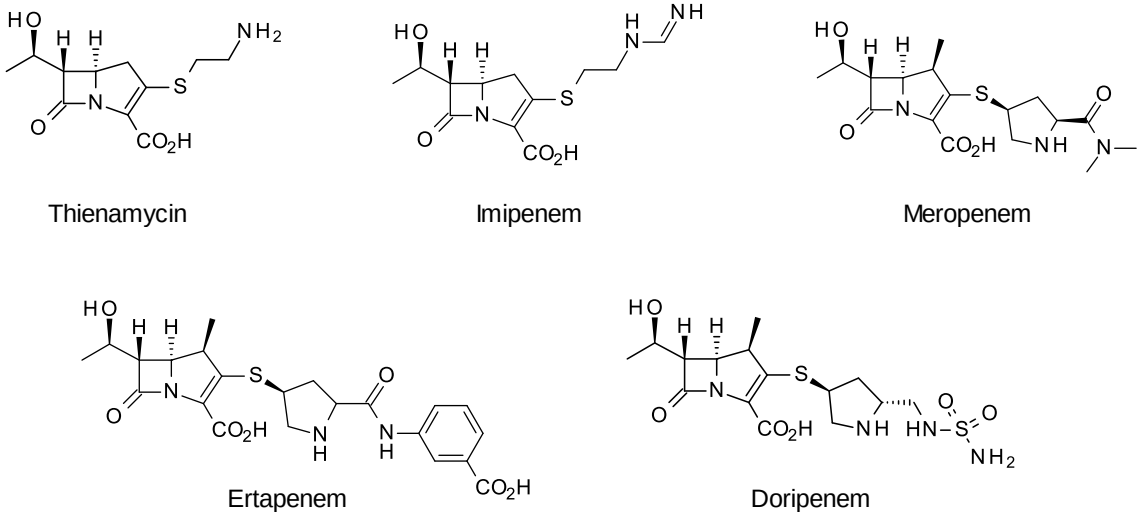

Figure 1.2: Structures of the different carbapenem antibiotics.

1.3 Mechanism of action of β-lactam antibiotics

Although carbapenems have the broadest spectrum of activity [12], all β-lactams function by inhibiting the final stage of bacterial cell wall synthesis [18]. The cell wall is a critical component of bacterial cells, composed of many elements, including a peptidoglycan layer [19]. The basic structure of the peptidoglycan layer is formed by alternating *N*-acetylglucosamine (NAG) and *N*-acetylmuramic acid (NAM) subunits (Figure 1.3) [20]. A specific pentapeptide attached to each NAM subunit allows for the cross-linking of different peptidoglycan layers [9,20]. The cross-linking of these pentapeptides is mediated by transpeptidase enzymes known as penicillin-binding proteins (PBPs) [9,21]. PBPs assist in the cross-linking of two peptidoglycan strands by removing the C-terminal D-alanine residue from one of the pentapeptides [21].

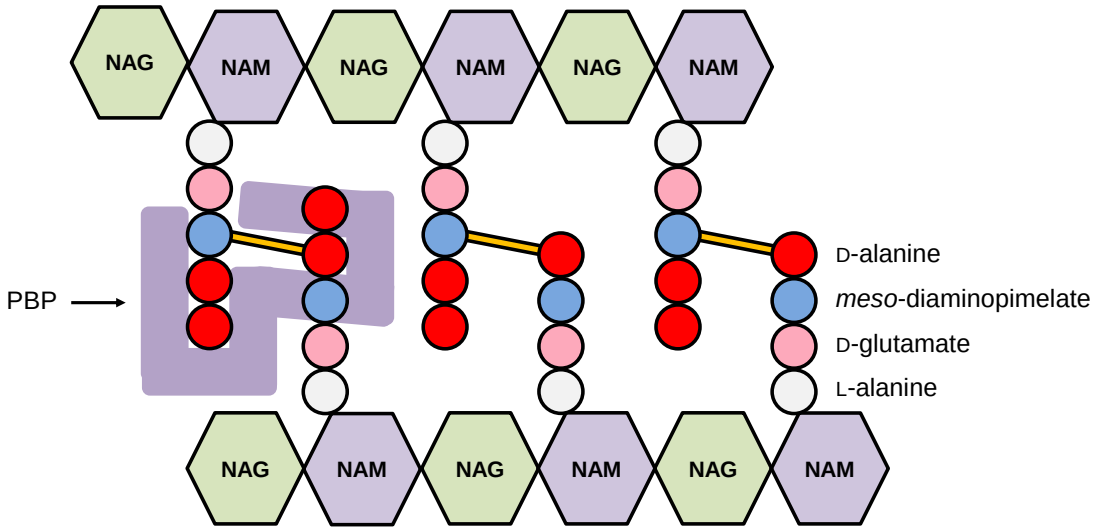

Figure 1.3: Structure of the peptidoglycan forming the cell wall of most Gram-negative bacteria.

β-Lactams are structural analogues of the D-alanine-D-alanine sequence motif of the pentapeptide terminus of the NAM subunits [9,22]. This structural similarity allows β-

lactams to irreversibly bind the PBPs, preventing the cross-linking of different peptidoglycan strands [9,22]. The peptidoglycan subunit cross-linking creates a rigid cell wall that protects bacteria cells from osmotic forces that would otherwise cause cell rupture [18,22]. Therefore, the inhibition of this step of cell wall synthesis ultimately causes the loss of integrity of the cell wall, and consequently, the lysis and death of the bacterial cell due to the β-lactam antibiotics triggering the activity of cell wall lytic enzymes (e.g., endopeptidases, lytic transglycosylases) [9,23,24].

1.4 Emergence of antibiotic resistance

Since benzylpenicillin was shown to successfully inhibit bacterial cell wall synthesis, the β-lactams have been the most widely used antimicrobial agents worldwide in treating bacterial infections [9,10,25]. Therefore, it is not surprising that the effectiveness of these antibiotics has severely decreased over the years due to their misuse in modern medicine and the increasing number of bacteria presenting antibiotic resistance mechanisms [26].

1.4.1 Causes of antibiotic resistance

A common cause of antibiotic resistance is their over-prescription, especially for the flu, colds, and coughs, which are infections caused primarily by viruses, which are not affected by antibiotics [26,27]. In 2015, more than 25 million prescriptions for antibiotics were filled in Canada alone [28]. Furthermore, people often do not finish their antibiotic treatment, which only eradicates the most susceptible bacteria while the resistant bacteria survive [26,29]. Antibiotics are also overused in livestock and fish farming [26]. In 2015, the FDA reported that 34 million pounds of antibiotics sold in the USA were used for animals [30]. In addition, poor infection control in hospitals and lack of hygiene have

been associated with antibiotic resistance since contaminated medical devices such as stethoscopes and catheters can lead to cross-contamination of multiple patients by resistant microorganisms [31]. Finally, the antibiotic resistance crisis is intensified due to the lack of new antibiotics being discovered [32]. Indeed, for almost 30 years, from the discovery of the lipopeptide antibiotics (e.g., daptomycin) in 1987 [33] until the report of teixobactin in 2015 [34], there had been no new chemical class of antibiotics reported.

1.4.2 Mechanisms of antibiotic resistance

Although antibiotics have been misused in human medicine and agriculture, these are not the only causes of the emergence of bacterial antibiotic resistance [26]. Over the years, bacteria themselves have evolved to resist the adverse effects of antibacterial agents through several mechanisms. Some of the most common include: 1) decreased permeability of the cell wall through loss or mutations of porins, 2) active efflux of the antibiotic by efflux pumps, 3) target alteration resulting in reduced susceptibility, and 4) enzymatic inactivation of the antibiotic (Figure 1.4) [25,26,35]. The predominant mechanism employed by Gram-negative bacteria to counteract the effects of β-lactams is the production of enzymes capable of degrading these antibiotics [25,36,37]. β-Lactamases are enzymes that hydrolyze the amide bond of the β-lactam ring [37,38]. As the β-lactam ring is a core structural feature present in all β-lactams, the hydrolysis of one of its bonds will inactivate these antimicrobial agents [36]. As first suggested by Ambler in 1980 [39], β-lactamases can be separated into four different classes (A, B, C, D) based on their catalytic and molecular properties [11].

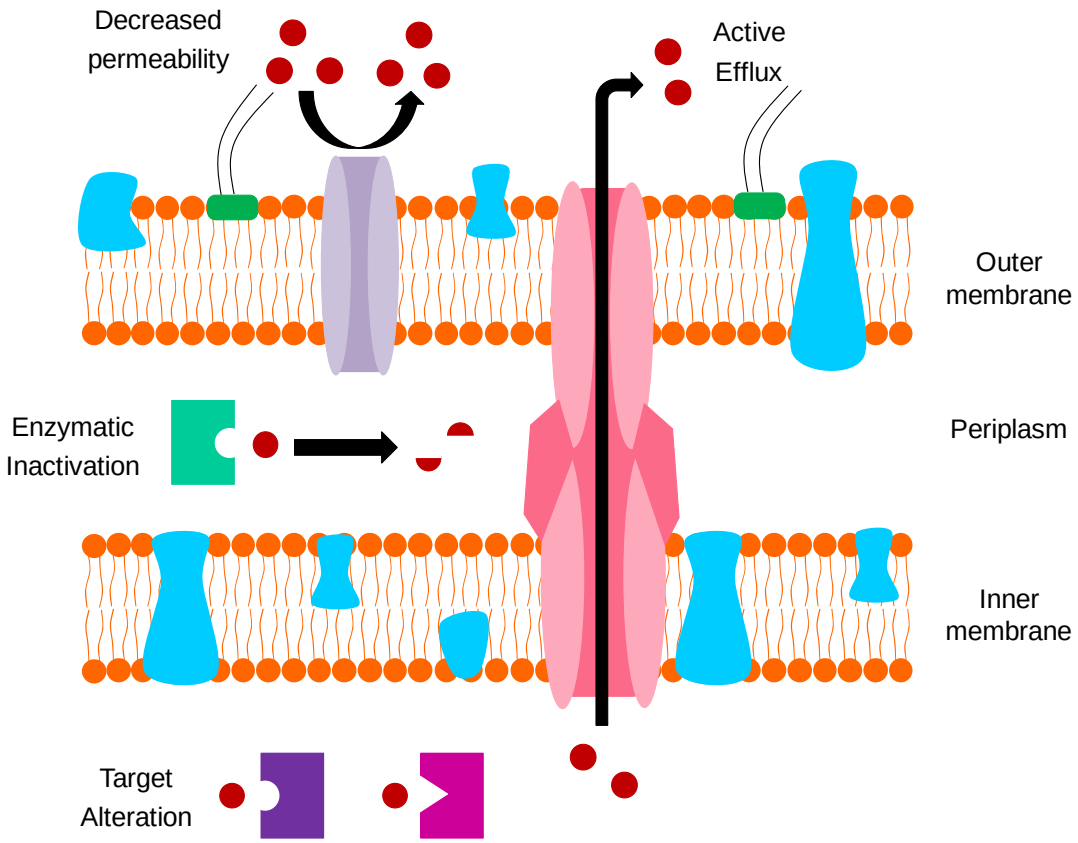

Figure 1.4: Mechanisms of antibiotic resistance in bacteria. The four most common strategies used by bacteria to counteract the effects of antibiotics are depicted: decreased permeability, active efflux, enzymatic inactivation, and target alteration. Antibiotics are represented by the red circles in the figure.

1.5 Serine-β-lactamases

Ambler classes A, C, and D are known as serine-β-lactamases (SBLs) since a serine residue is employed as the nucleophile that cleaves the β-lactam ring (Figure 1.5) [38]. Enzymes from all three classes share a serine-X-X-lysine motif [11,38,40]. The serine residue in this motif is the same nucleophilic serine residue that resides in the active site of these enzymes [11,38]. Although sharing a common motif, the three classes of SBLs can still be separated based on their sequences and substrate specificity [11,38].

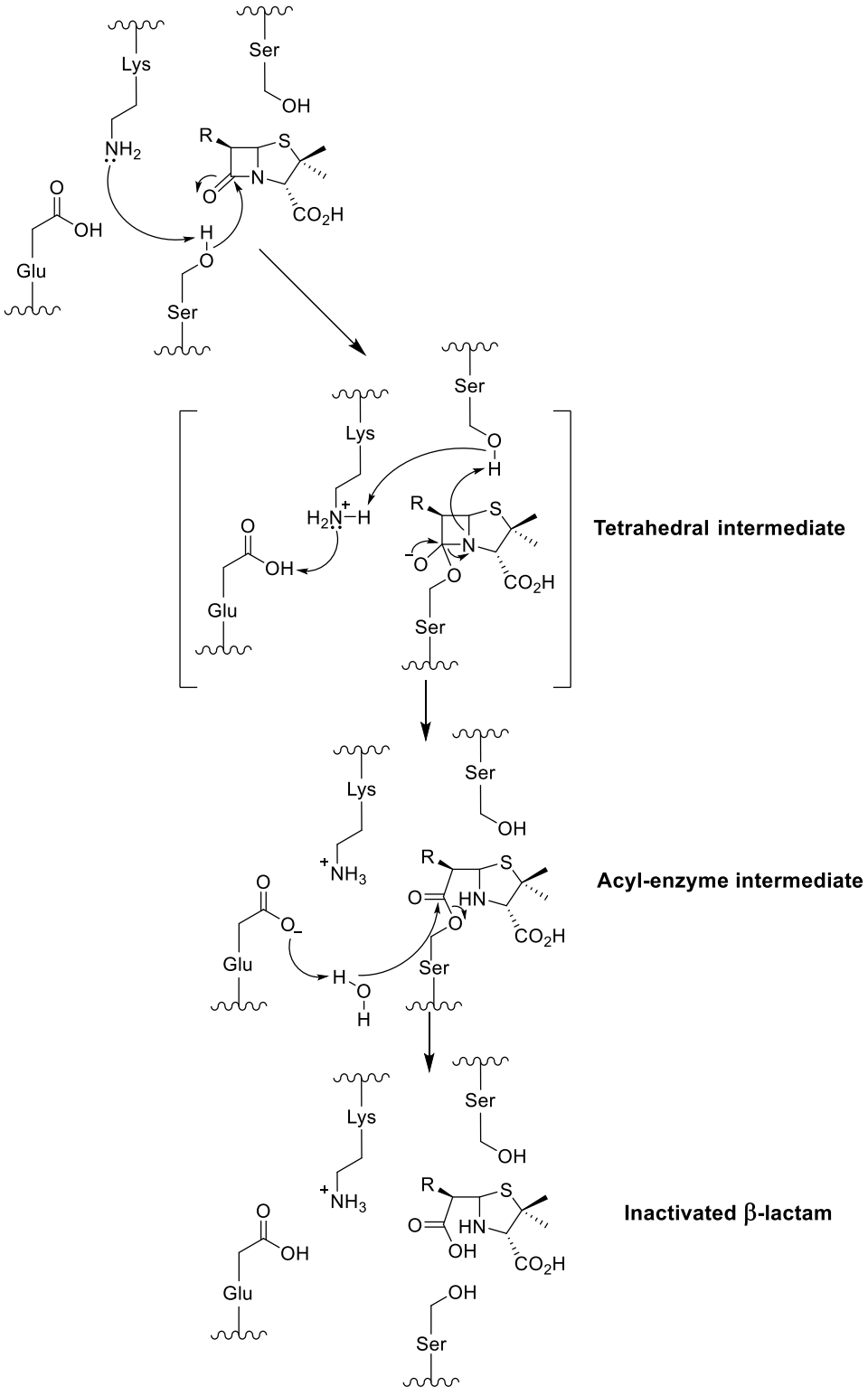

Figure 1.5: Proposed mechanism of class A serine-β-lactamases. Figure adapted from [11,41,42].

1.5.1 Class A serine-β-lactamases

Class A enzymes are frequently found on plasmids in numerous Gram-negative bacteria and are typically known as penicillinases since they are incredibly efficient at hydrolyzing penicillins [43]. The proposed mechanism of class A β-lactamases begins with the deprotonation of an active site serine by either a lysine [41,44] or a water molecule activated by a conserved glutamic acid [45]. Upon deprotonation, the serine is activated and attacks the β-lactam amide bond creating a tetrahedral intermediate [46]. The breakdown of this intermediate causes the expulsion of the nitrogen leaving group, which is subsequently protonated by a second serine, forming an acyl-enzyme intermediate [45]. Hydrolysis of the acyl bond of this intermediate is achieved by activating the nucleophilic water molecule by glutamic acid, resulting in the proton being donated back to serine and the release of the inactivated β-lactam from the active site (Figure 1.5) [47].

Class A contains the most encountered SBLs, such as enzymes from the TEM, SHV, KPC, and CTX-M families [48,49]. TEM-1, the first TEM variant and the first clinically relevant class A member, was initially described by Datta and Kontomichalou in 1965 (Figure 1.6) [50]. Initially isolated in 1963, this β-lactamase was found in a penicillin-resistant clinical isolate of *Escherichia coli* originating from a patient receiving treatment in Athens, Greece [50,51]. The patient's name, Temoniera, was used as the namesake for this family of enzymes [51].

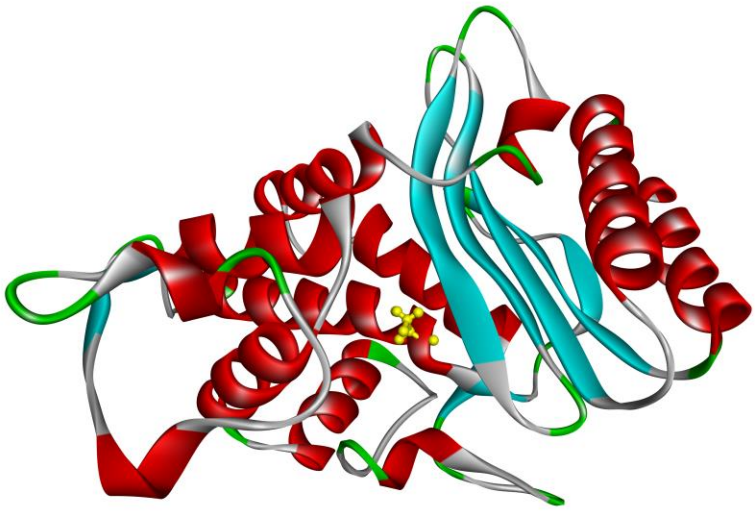

Figure 1.6: Crystal structure of TEM-1. The nucleophilic serine residue is depicted in yellow. PDB code 1M40.

Since the isolation of TEM-1, over 230 variants of this enzyme have been discovered according to the Comprehensive Antibiotic Resistance Database (CARD) [52]. However, among all these variants, TEM-1 remains one of the most frequently isolated class A β-lactamases and was responsible for as much as 90% of the ampicillin resistance encountered in *E. coli* by 1990 [53]. In addition, some TEM variants and other class A enzymes can hydrolyze cephalosporins and monobactams in addition to penicillins. These enzymes are known as extended-spectrum β-lactamases (ESBLs) [49]. Today, the CTX-M family of β-lactamases, named for their ability to confer cefotaxime resistance, includes the most prominent ESBLs isolated in clinics worldwide (e.g., CTX-M-3, CTX-M-9, CTX-M-14, CTX-M-15, CTX-M-32) [54]. Furthermore, a few class A enzymes have evolved the ability to hydrolyze most β-lactams, including carbapenems [55]. The first *Klebsiella pneumoniae* carbapenemase (KPC) was reported in 2001 and originated from a hospital in North Carolina, USA [56]. Today, according to the CARD, the KPC

family of β-lactamases contains over 70 members [57], with KPC-2 being the most frequently isolated class A carbapenemase worldwide (Figure 1.7) [58].

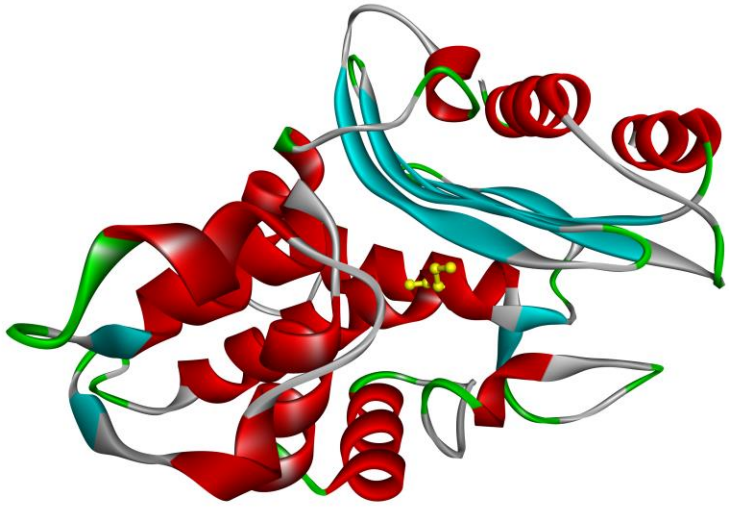

Figure 1.7: Crystal structure of KPC-2. The nucleophilic serine residue is depicted in yellow. PDB code 2V05.

1.5.2 Class C serine-β-lactamases

In 1940, before penicillin was clinically used, Abraham and Chain described an enzyme capable of degrading penicillin [59]. This enzyme, now referred to as an AmpC β-lactamase from *E. coli*, was the first β-lactamase ever reported and the first member of class C [60]. Today, class C enzymes are commonly referred to as AmpC β-lactamases or cephalosporinases as they are very proficient at inactivating cephalosporins and penicillins [60]. The general mechanism by which class C β-lactamases inactivate these β-lactams is similar to class A enzymes, except an active site tyrosine acts as the proton donor for the nitrogen leaving group upon acylation [61]. However, unlike class A serine-β-lactamases, class C members are generally under inducible expression and encoded on the chromosome of Gram-negative organisms, such as *Enterobacter cloacae, Citrobacter freundii*, *Serratia marcescens*, and *Pseudomonas aeruginosa* [62]. However, over the past

30 years, class C members have been increasingly discovered on mobile genetic elements such as plasmids [63]. Presently, CMY-2 is the most frequently encountered plasmid-encoded *ampC* gene from human and animal Enterobacterales isolates worldwide (Figure 1.8) [64].

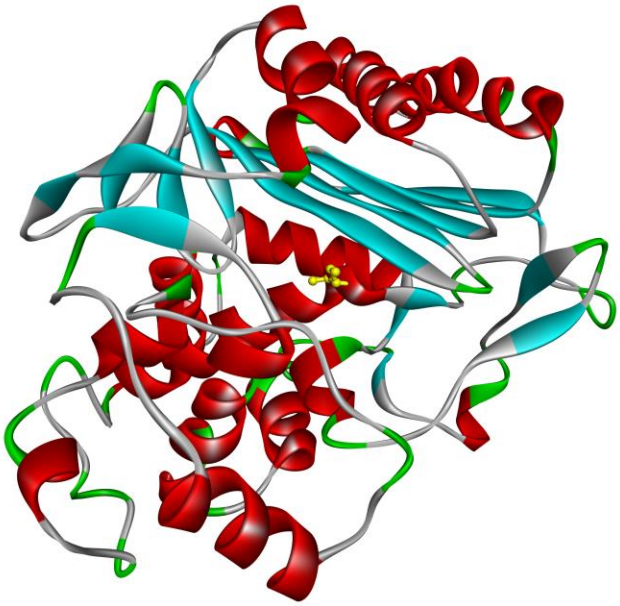

Figure 1.8: Crystal structure of CMY-2. The nucleophilic serine residue is depicted in yellow. PDB code 1ZC2.

1.5.3 Class D serine-β-lactamases

Class D enzymes or OXA-type β-lactamases are enzymes that hydrolyze oxacillin at a greater rate than benzylpenicillin [65–68]. In comparison to class A β-lactamases, class D members possess an *N*-carboxylated lysine and retain a serine as the nucleophile that attacks the amide bond of the β-lactam antibiotics [66,69]. Class D is the most diverse of the SBLs in term of amino acid sequence and substrate specificity since members possess several point mutations, resulting in either narrow or extended spectrum of activity against β-lactam antibiotics [67,68,70]. Indeed, some class D enzymes, such as OXA-2,

can only hydrolyze penicillins and some cephalosporins, while other class D members can inactivate most β-lactams, including carbapenems (e.g., meropenem) [65]. These extended-spectrum enzymes are known as carbapenem-hydrolyzing class D β-lactamases (CHDLs) [70]. The most widespread CHDLs are OXA-23, OXA-24/40, OXA-48, OXA-51, OXA-58, and OXA-143 [70]. Interestingly, although OXA-48 is capable of hydrolyzing carbapenems and penicillins, this CHDL demonstrates weak activity against extended-spectrum cephalosporins, such as ceftazidime and cefepime [71]. Furthermore, apart from OXA-48, which is predominantly produced by *K. pneumoniae* and *E. coli* isolates (Figure 1.9) [72], the remainder of the CHDL enzymes are mostly isolated from *Acinetobacter* spp., more specifically *A. baumannii* [70,71]. In 2017, the World Health Organization (WHO) published a list of priority pathogens that posed the greatest threat to human health, which identified carbapenem-resistant *A. baumannii* among the most critical [73,74].

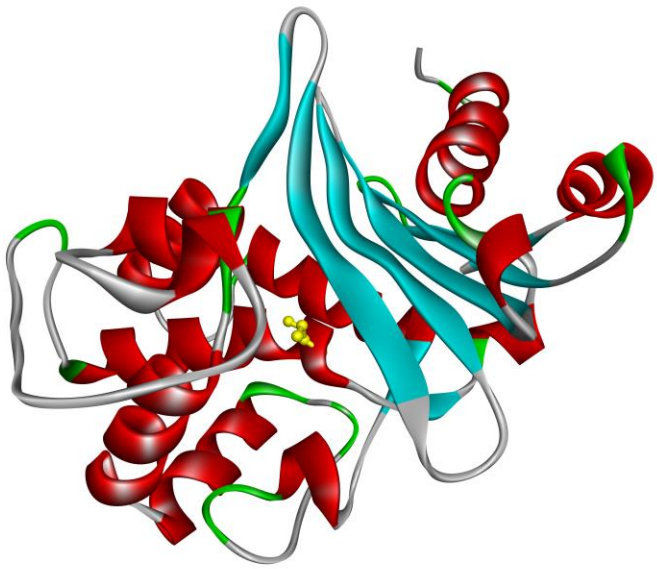

Figure 1.9: Crystal structure of OXA-48. The nucleophilic serine residue is depicted in yellow. PDB code 4S2P.

1.5.4 Serine-β-lactamase inhibitors

With the increasing number of SBL enzymes from all three subclasses being identified worldwide, several β-lactamase inhibitors (BLIs) have now been developed to control the spread of SBL-producing bacteria. Clavulanic acid, the first BLI to be approved for clinical use, was isolated from the soil bacterium *Streptomyces clavuligerus* in 1976 and possessed a β-lactam ring in its structure [75]. This inhibitor was discovered during a screen of natural products for compounds capable of inactivating β-lactamases [75]. Although showing little antimicrobial activity on its own, clavulanic acid could restore the activity of amoxicillin against *S. aureus* penicillinases, specifically the TEM β-lactamases [75,76]. Clavulanic acid is an irreversible mechanism-based (or suicide) inhibitor, which covalently binds the serine residue located in the active site of the SBL, forming an acyl-enzyme species [76,77]. Acylation and restructuring of the intermediate leads to the formation of an enamine intermediate [76]. The attack of this intermediate by a water molecule or another active site serine residue results in slow hydrolysis/ deacylation or prolonged irreversible inactivation of the SBL enzyme (Figure 1.10) [76,77].

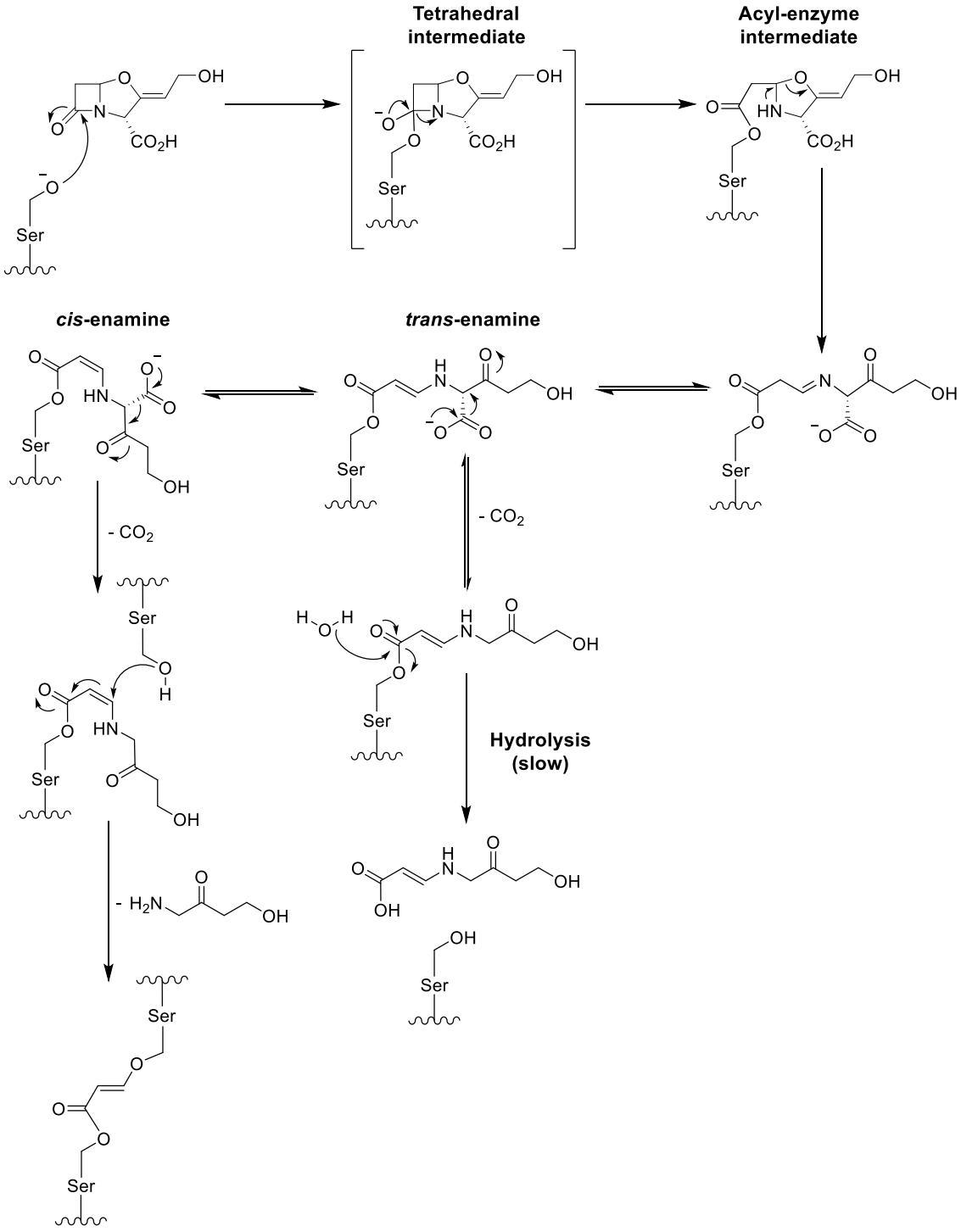

Figure 1.10: General mechanism of clavulanic acid in inactivation of serine-β-lactamases. Figure adapted from [78,79].

The discovery of clavulanic acid prompted the development of other BLIs such as sulbactam and tazobactam in 1978 and 1980, respectively [80,81]. Sulbactam and tazobactam are synthetic penicillanic acid sulfones. They contain a sulfonyl functional group, a penicillin core, and thus a β-lactam ring in their structure [82,83]. While both sulbactam and tazobactam demonstrate some antimicrobial activity on their own, they are typically combined with ampicillin or piperacillin, respectively, in the treatment of bacterial infections [76]. Although exhibiting potent activity against class A β-lactamases, especially against those belonging to the TEM family, sulbactam and tazobactam are less effective against class C and class D enzymes [60,71,76]. Sulbactam and tazobactam are mechanism-based inhibitors that inactive SBL enzymes through a similar mechanism of action as clavulanic acid (Figure 1.11) [76].

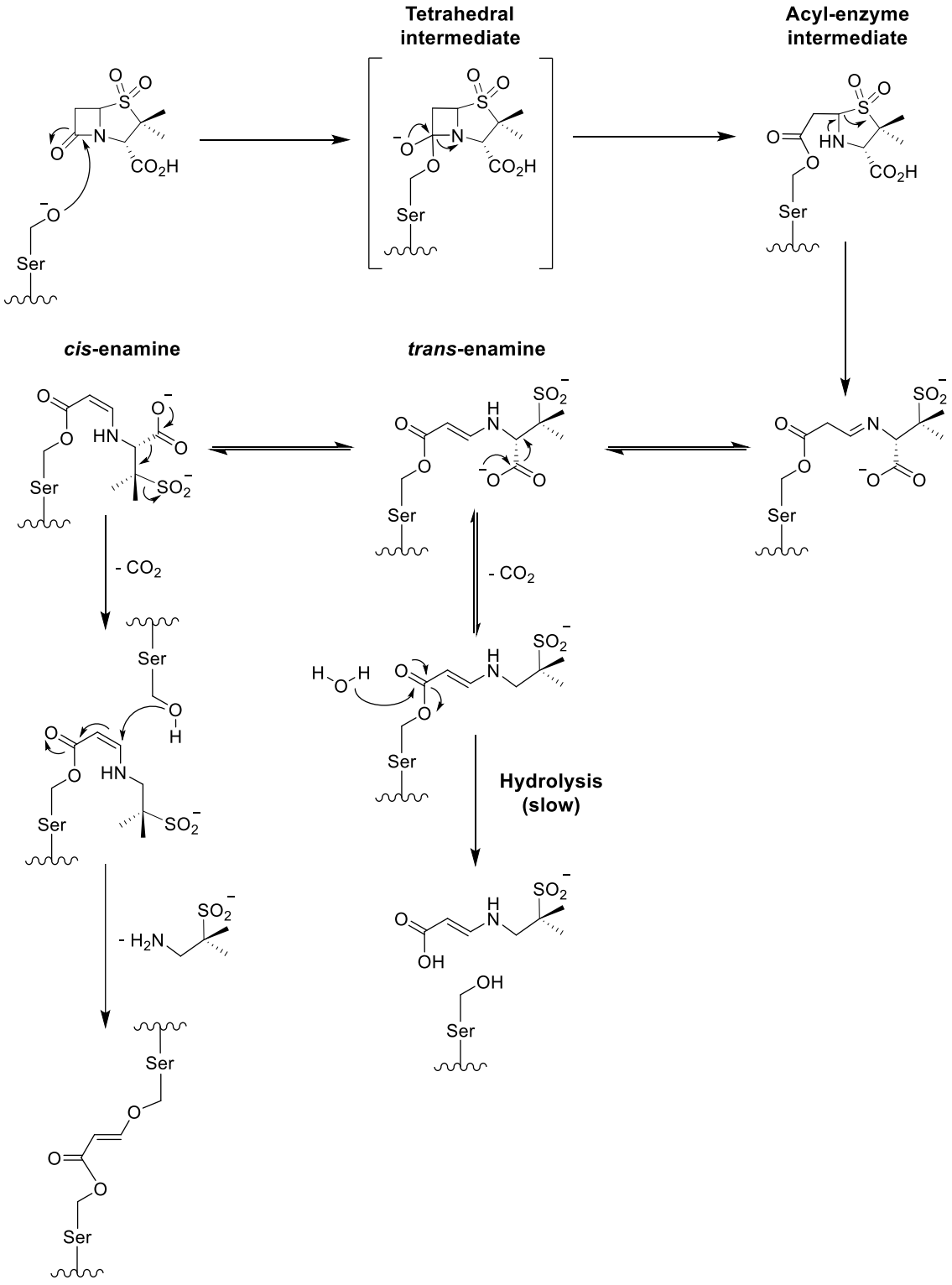

Figure 1.11: General mechanism of sulbactam in inactivation of serine-β-lactamases. Figure adapted from [79,84].

In the 1990s, the ongoing search for new SBL inhibitors capable of inactivating enzymes from classes A, C, and D led chemists at Hoechst Marion Roussel (now part of Sanofi-Aventis) in Germany to investigate diazobicyclooctanes (DBO) as β-lactam mimics [79,85]. Although early DBOs demonstrated poor antimicrobial activity, these compounds could weakly inhibit both class A and class C β-lactamases [85]. In 2015, avibactam became the first DBO BLI and the first non-β-lactam BLI to be approved for clinical use by the FDA [86,87]. Avibactam is a rapid and potent inhibitor of class A, class C, and some class D β-lactamases [88]. Although the inhibitory spectrum of avibactam includes class A ESBLs and carbapenemases, this BLI exhibited poor activity against most CHDLs [85,89]. Furthermore, similar to its predecessors (e.g., clavulanic acid), avibactam covalently modifies the active site serine residue of the SBL enzyme [79]. More specifically, the five-membered DBO ring contains an amide functional group that acylates the nucleophilic serine of the SBL, forming a carbamoyl-enzyme intermediate [85]. However, unlike previously discovered BLIs, avibactam acts via a reversible mechanism as the carbamoyl-enzyme intermediate can be deacylated and recyclized to regenerate the active inhibitor (Figure 1.12) [85,90]. Since the development of avibactam with its unique mechanism of action, modifications to the DBO scaffold have led to the discovery of relebactam, zidebactam, nacubactam, and durlobactam (Figure 1.13) [88]. Although relebactam has been approved for clinical use in the USA since 2019, the remaining DBOs are currently undergoing clinical trials [88,90]. The combination of durlobactam and sulbactam has even exhibited promising antimicrobial activity against CHDL-producing *Acinetobacter* spp. [88].

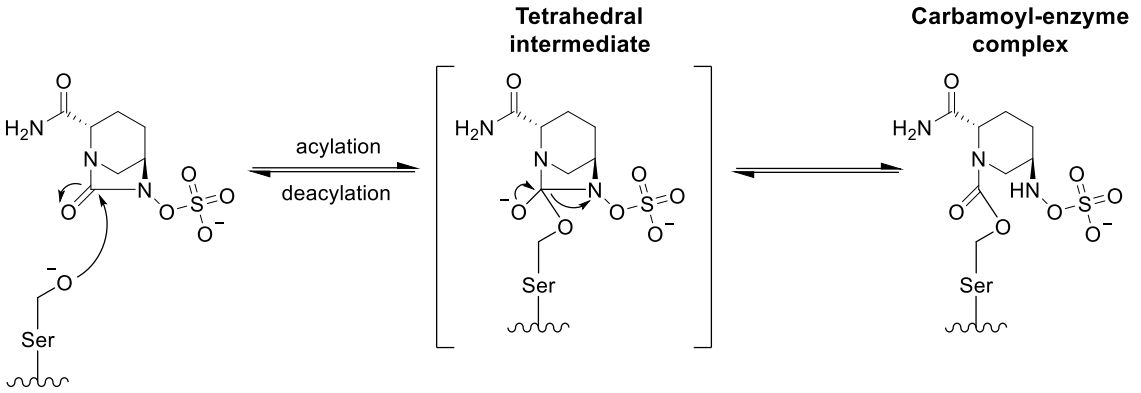

Figure 1.12: General mechanism of action of avibactam in inactivation of serine-β-lactamases. Figure adapted from [79].

Other non-β-lactam BLIs demonstrating promising antimicrobial activity across different β-lactamase classes are boronic acids [91]. Although articles describing the antimicrobial properties of boron-containing compounds have been published since 1882 [92], the ability of a boric acid-containing compound to inhibit SBLs would remain unknown until 1971 [93]. In subsequent studies, boronic acids demonstrated significant activity against SBLs and mammalian serine proteases [94]. Although this observation represented a major problem in the clinical usage of boronic acids, the development of cyclic boronates alleviated these concerns [88,95].

In 2017, vaborbactam, the first boron-containing BLI, was approved for clinical use (Figure 1.13) [91,96,97]. Vaborbactam interacts with the serine residue in the active site of the SBL enzyme, forming a covalent complex that mimics the tetrahedral intermediate crucial to SBL activity [97]. Since the discovery of vaborbactam, three new boronates have been developed and are currently undergoing clinical trials: 1) taniborbactam, 2) VNRX-7145, and 3) QPX7728 (Figure 1.13) [88]. Some cyclic boronates have even shown activity against class B β-lactamases [98].

Clavulanic acid and penicillanic acid sulfones

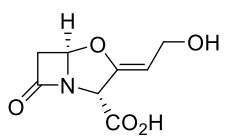

Clavulanic acid

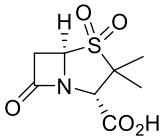

Sulbactam

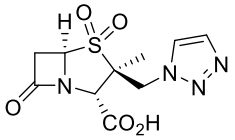

Tazobactam

Diazobicyclooctanes

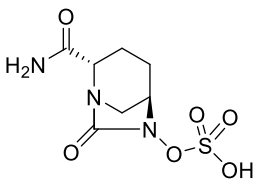

Avibactam

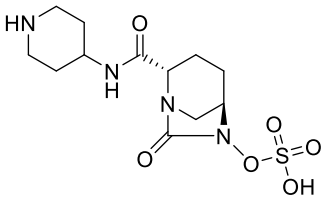

Relebactam

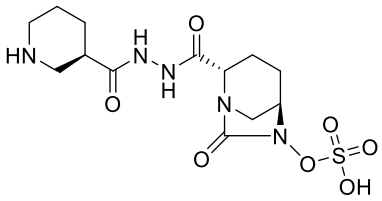

Zidebactam

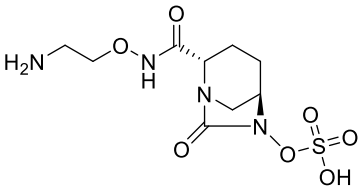

Nacubactam

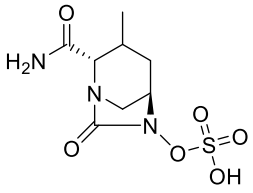

Durlobactam

Cyclic boronates

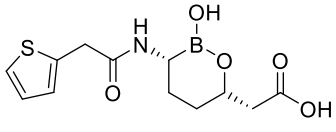

Vaborbactam

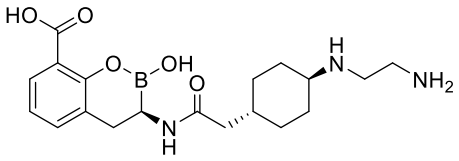

Taniborbactam

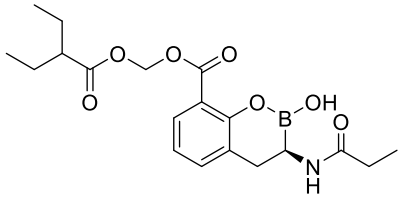

VNRX-7145

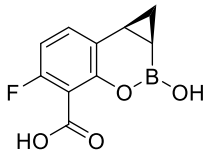

QPX7728

Figure 1.13: Inhibitors of serine-β-lactamases.

1.6 Metallo-β-lactamases

Ambler class B β-lactamases are metallo-β-lactamases (MBLs) requiring one or two zinc ions to stabilize a water (or hydroxide) molecule that acts as a nucleophile that cleaves the β-lactam ring (Figure 1.14) [13,36]. Other amino acids, such as a lysine (in NDM and IMP enzymes), an arginine (in VIM enzymes), and an asparagine can be found in the vicinity of the zinc-binding ligands [99]. These residues are situated in ideal positions to interact or stabilize the β-lactams found in the active site cleft of the MBLs [99]. MBLs can be separated into three subclasses (B1, B2, B3) based on their sequence similarity, zinc coordinating residues, and substrate specificity [100]. Although sharing a very low sequence similarity, MBLs from all three subclasses share a common four-layer fold known as an αβ/βα sandwich since the two central β-sheets are flanked by two α-helices (Figures 1.15A, 1.16A, 1.17A) [13,101]. Therefore, class B β-lactamases can still be aligned through their conserved secondary structures (e.g., α-helices and β-sheets from the αβ/βα fold) to create a standard numbering scheme known as the BBL numbering scheme [100,102]. This scheme facilitates the comparison of the structures and catalytic residues between members of the different MBL subclasses [36].

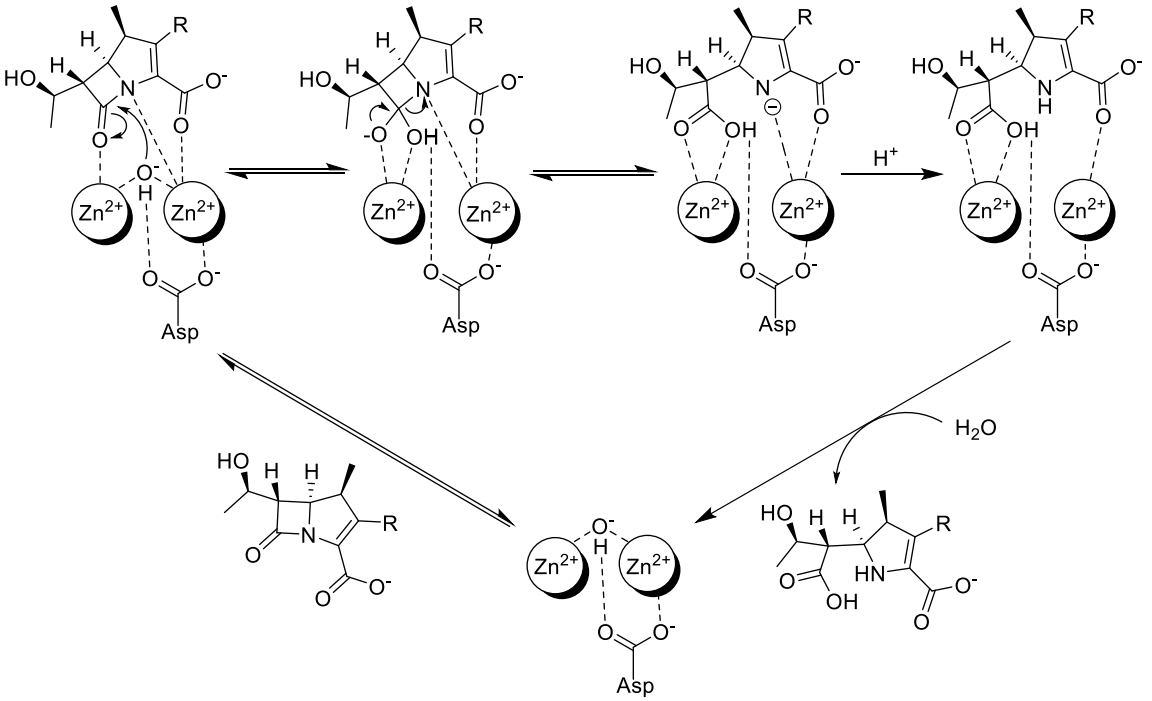

Figure 1.14: General chemical mechanism of di-zinc metallo-β-lactamases in inactivation of carbapenem antibiotics. Figure taken from [99]. Reprinted from Current Opinion in Microbiology, Volume 39, Caitlyn M. Rotondo and Gerard D. Wright, Inhibitors of metallo-β-lactamases, p. 97, Copyright (2022), with permission from Elsevier.

1.6.1 Subclass B1 metallo-β-lactamases

Subclass B1 is the biggest MBL subclass [103] and contains the largest number of clinically relevant MBLs, including NDM-, VIM-, and IMP-type enzymes [104]. These enzymes are monomeric, share a sequence identity of over 23%, and can cleave most β-lactams except for monobactams (e.g., aztreonam) [13,36,105]. Subclass B1 members contain two metal-binding sites and demonstrate more catalytic activity as dizinc enzymes (Figure 1.15B) [106]. The first zinc (Zn1) is tetrahedrally coordinated through three histidine residues. The second zinc (Zn2) is trigonal-pyramidally coordinated by an aspartic acid, a cysteine, a histidine, and one water molecule [13,105]. One additional

water (or hydroxide) molecule is also involved in coordinating and bridging both zinc ions (Figure 1.15B) [105].

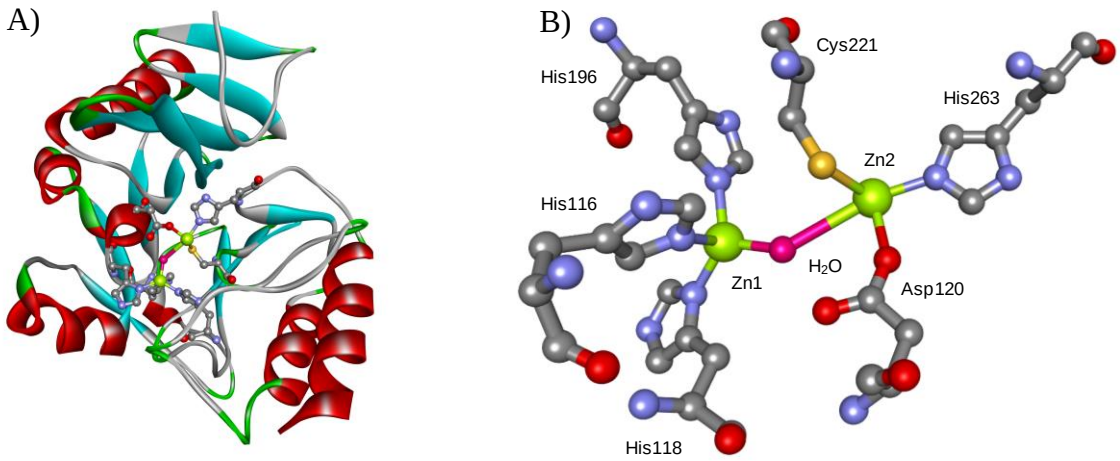

Figure 1.15: Crystal structure of dizinc NDM-1 from subclass B1. A) Overall αβ/βα fold characteristic of metallo-β-lactamases. B) Zinc coordinating residues forming the active site of NDM-1. Carbon, oxygen, nitrogen, and sulfur atoms are depicted in gray, blue, red, and yellow, respectively. PDB code 4EY2.

1.6.2 Subclass B2 metallo-β-lactamases

Subclass B2 is the least studied MBL subclass [107] and includes enzymes such as CphA2 from *Aeromonas hydrophila* [108]. These metalloenzymes are monomeric and only hydrolyze carbapenems (e.g., meropenem) [13]. Furthermore, members of subclass B2 only share an 11% sequence identity with enzymes from subclass B1 [36,102]. Subclass B1 and B2 enzymes share almost identical zinc-binding residues, except one histidine residue is replaced by an asparagine residue in the Zn1 site (Figure 1.16B) [13,105]. Although containing two zinc-binding sites, subclass B2 enzymes are active with only one zinc ion (in the Zn2 site) and are inhibited by the binding of a second zinc ion in the Zn1 site [109].

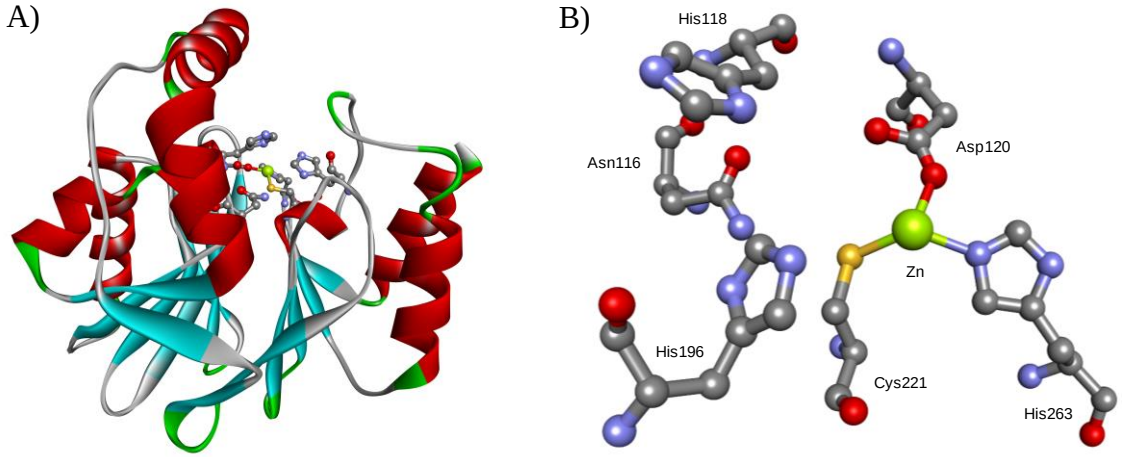

Figure 1.16: Crystal structure of mono-zinc CphA2 from subclass B2. A) Overall αβ/βα fold characteristic of metallo-β-lactamases. B) Zinc coordinating residues forming the active site of CphA2. Carbon, oxygen, nitrogen, and sulfur atoms are depicted in gray, blue, red, and yellow, respectively. PDB code 1X8G.

1.6.3 Subclass B3 metallo-β-lactamases

Subclass B3 enzymes demonstrate broad substrate specificity since they can hydrolyze most β-lactam antibiotics except for monobactams (e.g., aztreonam) [13]. Distinct from subclasses B1 and B2, enzymes from subclass B3 can be either monomeric (e.g., FEZ-1) or multimeric (e.g., L1, which is tetrameric) [110,111]. Furthermore, B3 enzymes share only a nine residue similarity with enzymes from subclasses B1 and B2, with most conserved residues being found in the active site of these metalloenzymes [36]. Distinct from subclass B1 and B2 enzymes, members of subclass B3 lack a cysteine residue in their Zn2 site, which is replaced by a histidine residue (Figure 1.17B). In addition, a glutamine residue can be found in the Zn1 site instead of a histidine residue in the case of the subclass B3 GOB enzymes [36,112]. Although retaining some activity with only one zinc ion, subclass B3 members demonstrate more catalytic activity as dizinc enzymes [13,105].

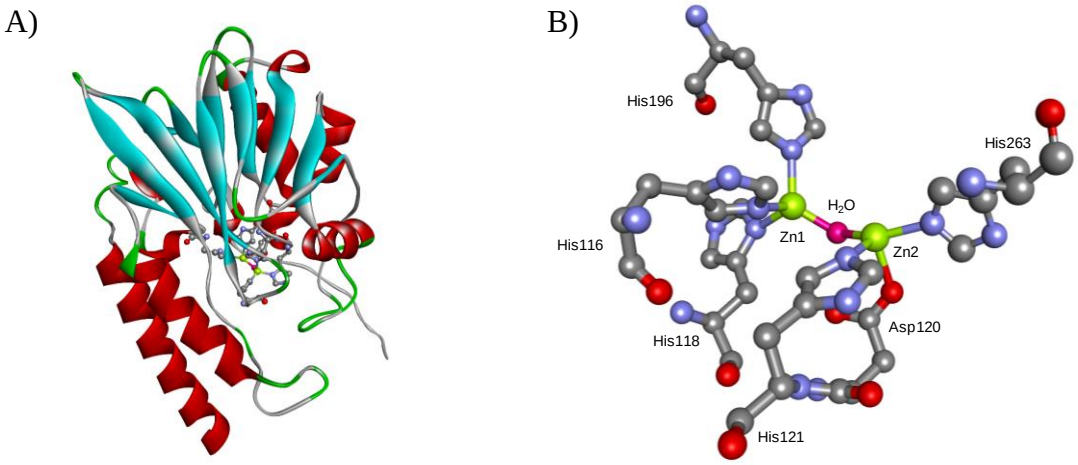

Figure 1.17: Crystal structure of dizinc L1 from subclass B3. A) Overall αβ/βα fold characteristic of metallo-β-lactamases. B) Zinc coordinating residues forming the active site of L1. Carbon, oxygen, and nitrogen atoms are depicted in gray, blue, and red, respectively. PDB code 1SML.

1.7 MBLs of Clinical Importance

Among the different classes of β-lactamases, MBLs are the most worrisome as they are resistant to clinically available SBL inhibitors (e.g., clavulanic acid, sulbactam, tazobactam, avibactam) [38], and are capable of inactivating most β-lactams including carbapenems [113]. Although several types of MBLs exist, the imipenemases (IMPs), the Verona integron-encoded metallo-β-lactamases (VIMs), and the New Delhi metallo-β-lactamases (NDMs) are the enzymes that are most commonly isolated in clinics around the world [98].

1.7.1 Imipenemase (IMP)

The first MBLs to be extensively studied were the IMP enzymes. These MBLs were found to have the ability to hydrolyze the carbapenem antibiotic known as imipenem, hence the origin of the name of this new family of metalloenzymes. The first IMP variant, IMP-1, was initially described by Watanabe et al. in 1991 [114]. This MBL was

originally isolated from a carbapenem-resistant strain of the Gram-negative bacterium *P. aeruginosa* in Japan in 1988 [114,115]. This was the first metallo-β-lactamase gene to be found on a transferable plasmid [114,116]. Since the isolation of IMP-1, over 80 variants of this enzyme have been reported according to the CARD [117]. However, among all of these variants, IMP-1 remains the most widespread and clinically-isolated IMP enzyme worldwide [118,119]. The fully active and mature IMP-1 has 228 amino acids, a molecular mass of 25 kDa, and two zinc ions in its active site (Figure 1.18) [120,121].

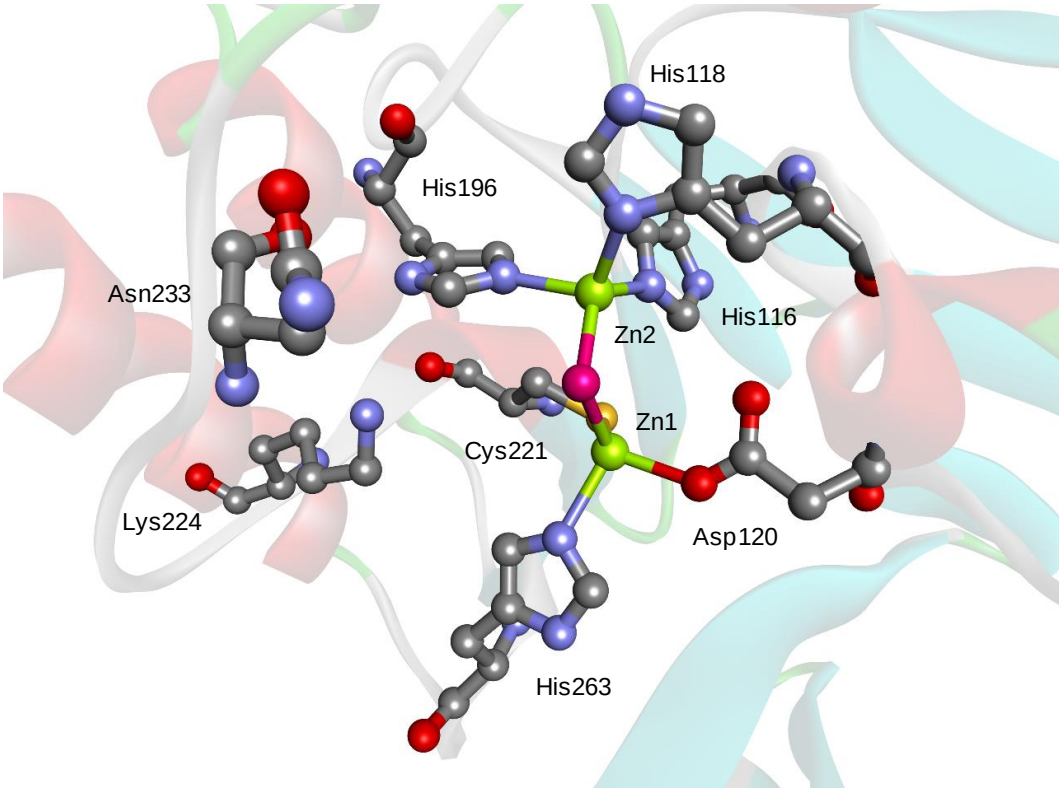

Figure 1.18: Structure of the active site of IMP-1. The zinc ions, associated invariant metal ligands, and conserved amino acids, Lys224 and Asn233, are depicted. PDB code 5ACU.

1.7.2 Verona integron-encoded metallo-β-lactamase (VIM)

VIM-1 was described by Lauretti et al. in 1999 [122]. Initially isolated in 1997, this MBL was found in a carbapenem-resistant clinical isolate of *P. aeruginosa* [121,123]. The *P. aeruginosa* strain carrying the *bla*$_{\text{VIM-1}}$ gene was originated from an Italian patient at the Verona University Hospital in Verona, Italy. This city was referenced as the namesake for this new family of metalloenzymes [122].

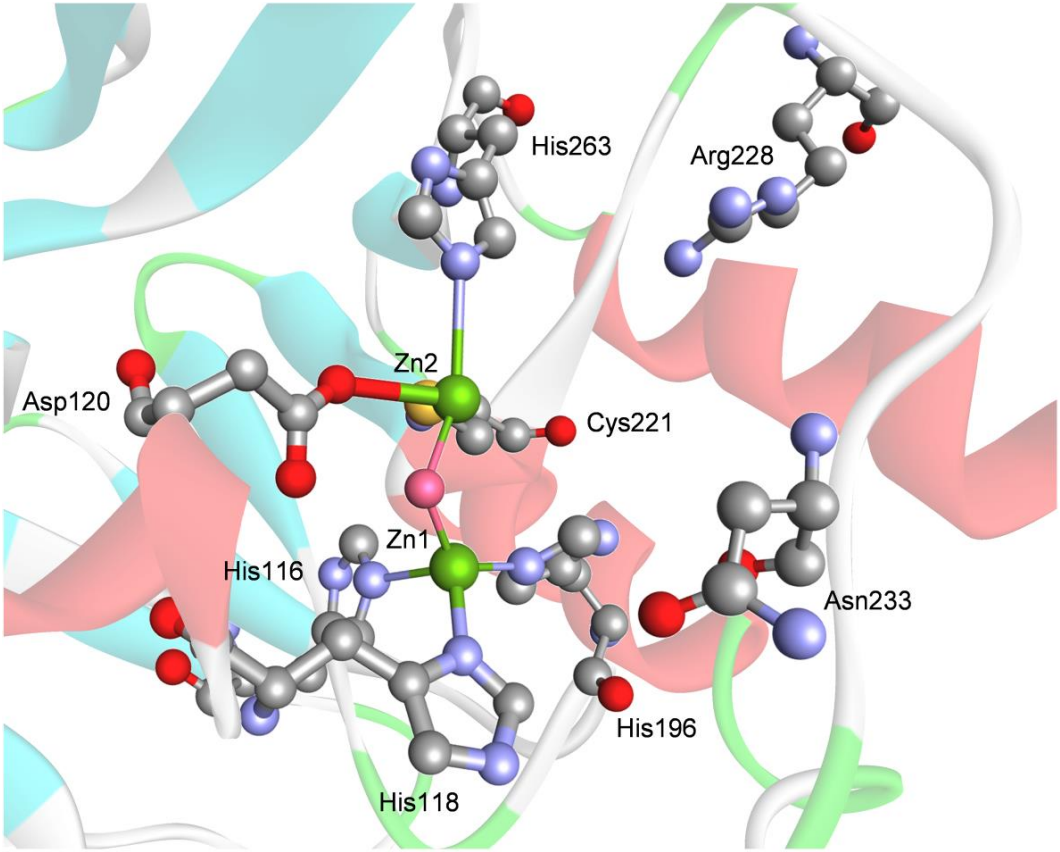

Figure 1.19: Structure of the active site of VIM-2. The Zn ions, associated invariant metal ligands, and conserved amino acids, Arg228 and Asn233, are depicted. PDB code 5ACU. Figure taken from reference [99]. Reprinted from Current Opinion in Microbiology, Volume 39, Caitlyn M. Rotondo and Gerard D. Wright, Inhibitors of metallo-β-lactamases, p. 98, Copyright (2022), with permission from Elsevier.

In 2000, a second VIM enzyme, sharing a 90% sequence identity with VIM-1, was described by Poirel et al. [124]. This variant, known as VIM-2, was isolated in 1996 from a 39-year-old French woman who had fallen ill with a carbapenem-resistant strain of *P. aeruginosa* after receiving a bone marrow transplant in a hospital in Marseille, France [116,124]. Since the isolation of VIM-1 and VIM-2, over 70 variants of these VIM enzymes have been discovered according to the CARD [125]. However, among all of these variants, VIM-2 remains the most widespread and clinically-isolated VIM enzyme worldwide [115]. The fully active and mature VIM-2 enzyme has 240 amino acids, a molecular mass of 25.5 kDa, and two zinc ions in its active site (Figure 1.19) [121].

1.7.3 New Delhi metallo-β-lactamase (NDM)

In 2009, a previously unknown MBL, NDM-1, was described by Yong et al. [126]. This MBL was isolated from a carbapenem-resistant strain of the Gram-negative bacterium *K. pneumoniae* and demonstrated low sequence identity with other MBLs. The most closely related MBLs, VIM-1 and VIM-2, only shared a 32.4% sequence identity with this NDM enzyme [126–128]. The resistant *K. pneumoniae* strain was isolated from a 59-year-old male patient from Sweden who acquired a urinary tract infection after receiving treatment in a hospital in New Delhi, India [116,126]. Therefore, this unknown MBL, now referred to as NDM-1, was named after the Indian capital as the authors believed that the $bla_{\text{NDM-1}}$ gene originated from the Indian subcontinent [126,127]. Nevertheless, since its isolation in 2009, the NDM family of enzymes has rapidly spread around the globe, and over 30 variants have been reported according to the CARD [129]. However, NDM-1 remains the most commonly isolated NDM variant in the clinical setting [128]. The full-length and

fully active NDM-1 enzyme had 270 amino acids, a molecular mass of 28 kDa, and two zinc ions in its active site (Figure 1.20) [130].

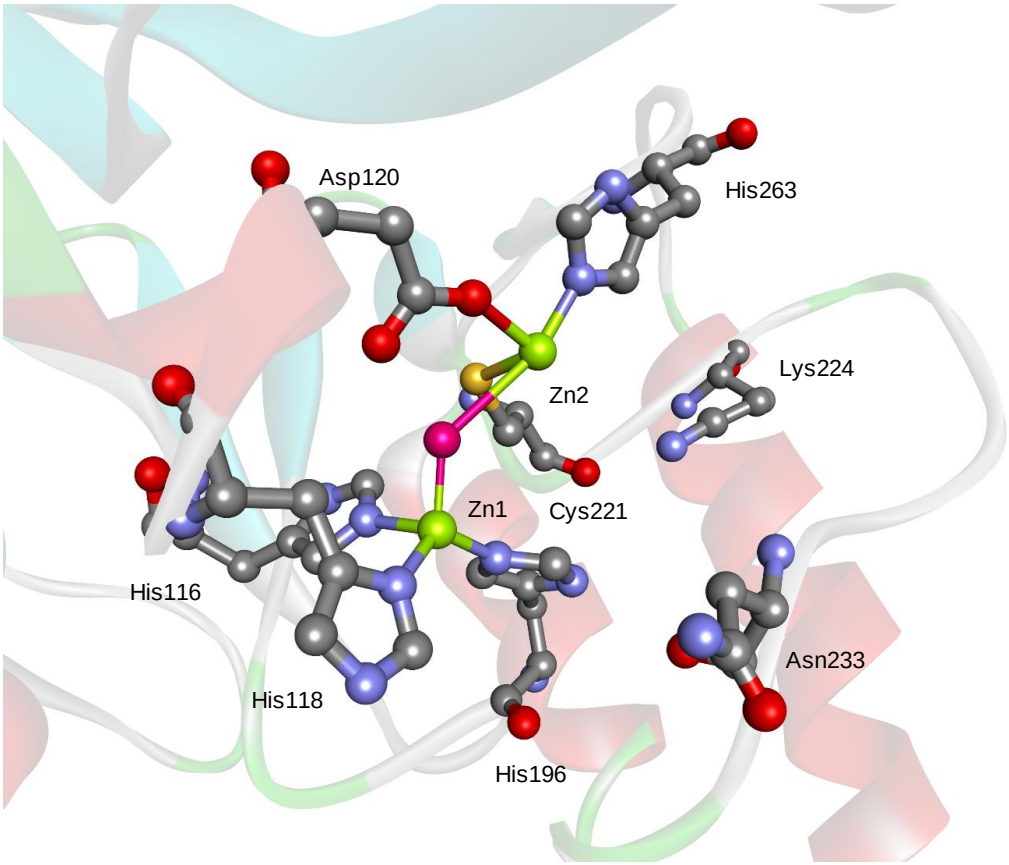

Figure 1.20: Active site of NDM-1. The Zn ions, associated invariant metal ligands, and conserved amino acids, Lys224 and Asn233, are depicted. PDB code 4EY2.

1.8 MBLs found on broad host range plasmids

Although the IMP, VIM, and NDM enzymes remain the most clinically isolated MBLs worldwide, all MBLs are becoming an increasing problem around the globe as they are rapidly spreading among different bacterial species [113]. This rapid spread is attributed to over 75% of MBL genes being located on mobile genetic elements such as transposons and plasmids. These mobile genetic elements allow the MBLs to be transferred from one bacterium to another through horizontal gene transfer [105,113,116].

One of the MBLs that has spread the fastest worldwide is NDM-1. Since its isolation in Sweden in 2009, the *bla*$_{\text{NDM-1}}$ gene has been isolated in over 50 countries spread out over every continent in the world, except for Antarctica [131]. Indeed, the rapid spread of NDM-1 across the United Kingdom in 2009 and around the globe in 2010 triggered warnings to be issued from the Health Protection Agency and the WHO, respectively [126,132]. The quick dissemination of NDM-1 is due to the *bla*$_{\text{NDM-1}}$ gene being found on broad host range plasmids. These self-transferable and easily replicated plasmids allow the *bla*$_{\text{NDM-1}}$ gene to be easily transferred between phylogenetically distinct bacterial hosts [133]. Therefore, although NDM was initially isolated from *K. pneumoniae* and *E. coli* in 2009, this MBL is now being expressed in a variety of distinct bacterial species. Today, NDM-1 is most commonly isolated from bacteria belonging to the Enterobacteriaceae family, *Acinetobacter* spp., and *P. aeruginosa* [128,133]. However, the *bla*$_{\text{NDM-1}}$ gene has also been found in the Gram-negative bacterium *Vibrio cholerae*. This is especially problematic as this bacterium had not previously been reported in carrying the gene for NDM-1, thus demonstrating the broad host range of the *bla*$_{\text{NDM-1}}$ gene [128,134].

1.9 Metallo-β-lactamase inhibitors

The worldwide dissemination of NDM-1 and other MBLs highlights the importance of finding an inhibitor of these metalloenzymes. Since all MBLs require zinc ions for their activity, most potential inhibitors developed thus far negate the effects of these metalloenzymes through a zinc-dependent approach [99]. However, in 2017, Dr. Christopher Schofield's group at the University of Oxford (Oxford, England) published an article detailing the discovery of a series of zinc-independent inhibitors with an

isoquinoline core structure (Figure 1.21) [135]. These inhibitors were identified during a structure-based virtual screen for compounds capable of interacting with some of the conserved amino acids residing in or around the active site of VIM-2, such as Arg228, Asn233, and Asp120 (Figure 1.19) [135]. Although these findings establish that zinc-independent MBL inhibition is possible, the diversity of the active site and catalytic residues of the MBLs makes targeting anything other than the conserved zinc ions quite challenging [99]. As for the zinc-dependent approach, MBL inhibitors can function by one of two mechanisms: 1) ligand displacement resulting in the formation of a reversible chelated complex or 2) zinc ion removal and sequestration [99].

1.9.1 Ligand replacement inhibitors

Captopril was first synthesized in 1975 [136,137] and has not only been shown to be a promising inhibitor of several clinically relevant MBLs (e.g., IMP-1, VIM-2, NDM-1) but was also the original angiotensin-converting enzyme (ACE) inhibitor [98,138,139]. Captopril was shown to have the ability to inhibit both the ACE and MBL enzymes through chelation of active site zinc ions using a free thiol [98,138,139]. In 2015, Dr. Schofield's laboratory demonstrated that the D-captopril, a stereoisomer of the clinically approved ACE inhibitor L-captopril, was the most active MBL inhibitor (Figure 1.21) [98].

In 2014, Klingler et al. reported a series of thiol-containing drugs with the ability to inhibit NDM-1, VIM-2, and IMP-7 [138]. Dimercaprol, the most promising MBL inhibitor detailed in this study, was developed by British biochemists at the University of

Oxford during World War II as a chelating agent used to treat heavy metal poisoning caused by arsenic-containing war gases (Figure 1.21) [138,140].

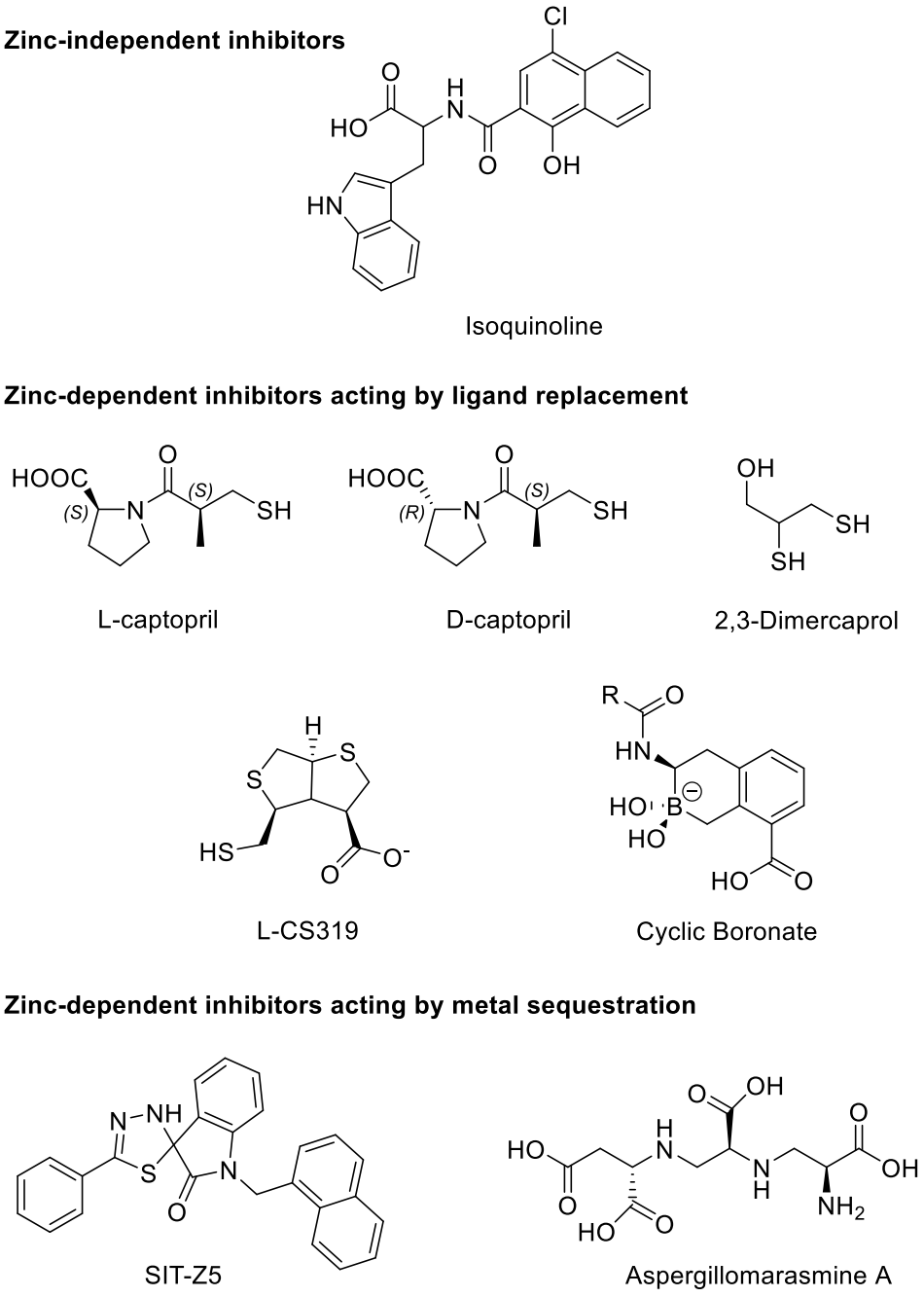

Figure 1.21: Inhibitors of metallo-β-lactamases. Figure adapted from reference [99].

In 2016, the laboratories of Dr. Robert Bonomo, Dr. Alejandro Vila, and Dr. James Spencer reported that bisthiazolidines, such as CS-319, could inhibit MBLs (Figure 1.21) [141,142]. Bisthiazolidines are small bicyclic compounds that mimic the penicillin scaffold and contain an additional thiol group that can interact with the zinc ions located in the MBL active site [141,142].

As previously mentioned in section 1.5.4, boronic acid-containing compounds, such as vaborbactam, are rapid and potent SBL inhibitors [97]. However, in 2016, Dr. Schofield's laboratory demonstrated that cyclic boronates could also rescue the activity of meropenem in NDM-1-producing bacteria by mimicking an intermediate of MBL hydrolysis (Figure 1.21) [98]. Indeed, the cyclic boronate, now known as taniborbactam (formerly VNRX-5133), is currently in phase III clinical trials and is the first β-lactamase inhibitor to demonstrate activity against enzymes from classes A, B, C, and D [88,143].

1.9.2 Metal sequestering inhibitors

MBL zinc ion removal represents a promising approach in inhibiting these metalloenzymes [99]. Indeed, various metal chelators have shown activity against MBL-producing bacteria [144]. For example, in 2010, when bound to calcium, ethylenediaminetetraacetic acid (EDTA), a chelating agent widely used to bind divalent and trivalent metal ions, was shown to have the ability to reduce the minimum inhibitory concentration of imipenem in MBL-producing *P. aeruginosa* isolates [145]. In mouse models of *P. aeruginosa* infections, calcium-EDTA was not only able to block MBL activity but could also neutralize tissue-damaging metalloproteases [145]. Furthermore, in 2015, Falconer et al. determined that a zinc-selective spiro-indoline-thiadiazole analogue,

known as SIT-Z5, could rescue the activity of meropenem in NDM-1-producing *K. pneumoniae* in both minimum inhibitory concentration assays and mouse models of infections (Figure 1.21) [146]. The EDTA and SIT-Z5 studies demonstrate that potent *in vivo* and *in vitro* MBL inhibition can be achieved with metal sequestering inhibitors [146]. Moreover, effective bioassay and animal model activity was observed for another recently discovered zinc-selective MBL inhibitor known as aspergillomarasmine A (Figure 1.21) [147].

1.10 Aspergillomarasmine A

In 1956, a French group called the *Société d'Étude et d'Applications Biologiques* isolated three unknown compounds from a strain of *Aspergillus flavus oryzae* [148]. These compounds were originally known as lycomarasmic acids due to their structural similarity to the compound lycomarasmine. Lycomarasmine was initially isolated from the fungal plant pathogen, *Fusarium lycopersici*, in 1944 by Clauson-Kaas, Plattner, and Gaumann [148,149]. However, as the lycomarasmic acids were isolated from *Aspergillus* and not *Fusarium* like their namesake, Haenni et al. proposed changing their name to 'aspergillomarasmine' in 1965 [148]. As a consequence of this proposition, the three compounds from 1956 would hereinafter be known as aspergillomarasmine A, aspergillomarasmine B, and anhydroaspergillomarasmine B (Figure 1.22) [148].

Aspergillomarasmine A

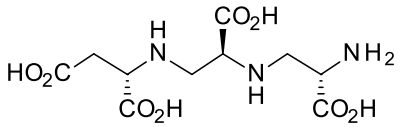

Lycomarasmine

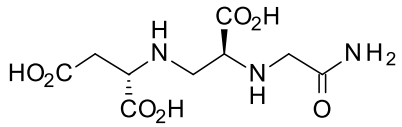

Aspergillomarasmine B

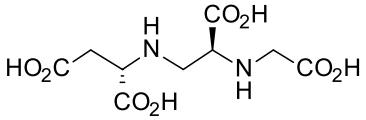

Anhydroaspergillomarasmine B

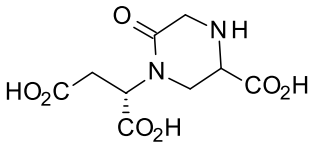

Figure 1.22: Structures of lycomarasmine, aspergillomarasmine A, aspergillomarasmine B and anhydroaspergillomarasmine B. Figure adapted from reference [148].

As aspergillomarasmine A (AMA) was discovered to be the causative agent in the wilting of leaves of tomato plants [148], the role of this compound in plant pathogenesis was further investigated. Throughout the years, AMA was isolated as the biologically active compound from different fungal plant pathogens such as *Fusarium oxysporum* f. sp. *melonis*, which causes Fusarium wilt (especially in melon plants) and *Pyrenophora teres*, which produces net-spot blotch disease in barley [150,151]. However, almost 60 years after its initial discovery, it was revealed that AMA not only functions as a plant toxin but also as a potent MBL inhibitor [147]. In 2014, King et al. conducted a targeted cell-based screen for new MBL inhibitors using microbial natural product extracts [147]. AMA, synthesized by *Aspergillus versicolor*, was discovered in a soil sample obtained from Kejimkujik National Park in Nova Scotia, Canada [152]. Although exhibiting no antimicrobial activity on its own, AMA could inhibit the activity of two clinically relevant MBLs, NDM-1 and VIM-2 [147]. However, this inhibitor was less potent against

another clinically relevant MBL, IMP-7 [147]. Furthermore, the activity of meropenem against Enterobacteriaceae, *Acinetobacter,* and *Pseudomonas* clinical isolates producing either NDM-1 or VIM-2 was restored when this antibiotic was given in conjunction with AMA [147]. Rescue of meropenem activity was also observed when the AMA/ meropenem combination was tested against NDM-1-producing *K. pneumoniae* in a mouse model of infection [147]. However, toxicity was observed in a canine model of infection upon usage of higher concentrations of AMA (unpublished). Since AMA was revealed to be a potent MBL inhibitor [147], further studies were conducted into its specific mechanism of action. In 2021, Sychantha et al. demonstrated that AMA acts as a selective zinc scavenger, which sequesters zinc from the low-affinity binding site of the MBLs [153].

1.11 Combination Therapy

Although previous studies portrayed the therapeutic potential of an AMA/meropenem combination against bacteria producing a single MBL enzyme, an increasing number of clinical isolates contain multiple β-lactamases from each different class to resist multiple antibiotics [154–156]. Due to the emergence of these multidrug-resistant bacteria, antimicrobial combination therapy is rapidly gaining popularity worldwide [157,158]. This type of therapy has many advantages in treating bacterial infections, such as the broadening of the antibacterial spectrum [158]. Furthermore, the utilization of multiple compounds which function through different mechanisms decreases the likelihood of the emergence of resistant mutants [159]. In addition, antimicrobial combinations represent an excellent treatment option for polymicrobial infections such as gastrointestinal

infections, which require more than one antibiotic to eradicate all the bacterial pathogens in the gut [158]. Furthermore, synergy is usually observed upon combining two or more antimicrobial agents. For example, a combination of meropenem-piperacillin and tazobactam was shown to have the ability to inhibit methicillin-resistant *S. aureus*, one of the most drug-resistant pathogens being isolated in clinics around the world [155,160].

1.12 Research hypotheses and objectives

With the growing number of MBL-producing bacteria, the development of new MBL inhibitors is crucial in quenching the spread of these antibiotic resistance genes. Previous studies have demonstrated that AMA was a rapid and potent inhibitor of two clinically relevant MBLs known as NDM-1 and VIM-2. However, the results of this study also revealed that AMA was less effective in inhibiting IMP-7, another widespread MBL. Therefore, it was hypothesized that the inhibitory potency of AMA would differ between different MBL families and subclasses. Consequently, the primary objective of my research project was to determine the effect of AMA against a broader panel of MBLs. Henceforth, AMA was paired with six different β-lactam antibiotic partners from three subclasses (penicillin, cephalosporin, carbapenem), and the efficacy of each pairing was evaluated against 19 MBLs from each subclass (B1, B2, B3).

The second objective of my research project revolved around the observation that multiple β-lactamase enzymes can be expressed by one bacterial strain. It was hypothesized that treating infections caused by these multidrug-resistant bacteria could be achieved through combination therapy with different β-lactamase inhibitors and β-lactam antibiotics. Therefore, in this study, the efficacy of an AMA (an MBL inhibitor),

avibactam (an SBL inhibitor), and meropenem (a β-lactam antibiotic) combination was evaluated against 20 laboratory strains and 30 clinical strains producing at least one MBL and one SBL.

Finally, carbapenem-resistant *Acinetobacter* and *Pseudomonas* species are among the bacteria posing the greatest threat to human health. Therefore, it was hypothesized that infections caused by these pathogens could be treated with an AMA/avibactam/ meropenem combination as this pairing proved to be effective against carbapenemase-producing Enterobacteriaceae. Consequently, new broad host range shuttle vectors for cloning and expression in *Acinetobacter* and *Pseudomonas* species were developed.

Overall, a better understanding of the inhibitory potency and spectrum of activity of AMA could be utilized in the development of future MBL inhibitors.

CHAPTER 2: Suppression of β-lactam resistance by aspergillomarasmine A is influenced by both the metallo-β-lactamase target and the antibiotic partner

2.1 PREFACE

The work presented in this chapter is used with permission of the American Society for Microbiology from:

Rotondo, C.M., Sychantha, D., Koteva, K., and Wright, G.D. Suppression of *β*-Lactam Resistance by Aspergillomarasmine A Is Influenced by both the Metallo-*β*-Lactamase Target and the Antibiotic Partner. *Antimicrob. Agents Chemother.*, **64**: e01386-19. Copyright (2022).

Permission conveyed through Copyright Clearance Center, Inc.

2.2 AUTHOR CONTRIBUTIONS

C.M.R., D.S., K.K. and G.D.W. designed the experiments discussed in this chapter. C.M.R. and D.S. conducted the cloning, bacterial transformations, and purification of various MBL genes employed to conduct these experiments. C.M.R. performed all the AMA and meropenem combination assays while D.S. performed all the *in vitro* enzyme assays. C.M.R., D.S and K.K. carried out the intracellular accumulation assays. C.M.R. and D.S. wrote the manuscript whereas K.K. and G.D.W. revised the manuscript.

C.M.R. and D.S. contributed equally to this article. Author order was determined alphabetically.

2.3 ABSTRACT

The rise of Gram-negative pathogens expressing metallo-*β*-lactamases (MBLs) is a growing concern, threatening the efficacy of β-lactam antibiotics, in particular, the carbapenems. There are no inhibitors of MBLs in current clinical use. Aspergillomarasmine A (AMA) is an MBL inhibitor isolated from *Aspergillus versicolor* with the ability to rescue meropenem activity in MBL-producing bacteria both *in vitro* and *in vivo*. Here we systematically explored the pairing of AMA with six *β*-lactam antibiotic partners against 19 MBLs from each subclass (B1, B2, and B3). Cell-based assays performed with *Escherichia coli* and *Klebsiella pneumoniae* showed that bacteria producing NDM-1 and VIM-2 of subclass B1 were the most susceptible to AMA inhibition, whereas bacteria producing CphA2 and AIM-1 of subclasses B2 and B3, respectively, were the least sensitive. Intracellular antibiotic accumulation assays and *in vitro* enzyme assays demonstrated that the efficacy of AMA/*β*-lactam combinations did not correlate with outer membrane permeability or drug efflux. We determined that the optimal *β*-lactam partners for AMA are the carbapenem antibiotics and the efficacy of AMA is linked to the Zn^{2+} affinity of specific MBLs.

KEYWORDS: antibiotic resistance, aspergillomarasmine A, beta-lactams, carbapenems, cephems, metallo-beta-lactamases, penams

2.4 INTRODUCTION

β-Lactams are the most commonly prescribed family of antibiotics and are increasingly ineffective against many serious bacterial infections (1). Resistance to *β*-lactam antibiotics occurs predominantly through the production of β-lactamases. These enzymes are divided into four classes based on their structure and amino acid sequence. Classes A, C, and D are serine-β-lactamases (SBLs) that employ an active site serine residue to promote hydrolysis of the β-lactam ring (1). Class B enzymes are metallo-*β*-lactamases (MBLs) that require active site Zn^{2+} ions for their catalytic activity (2). MBLs are further organized into three subclasses (B1, B2, and B3). The B1 subclass is the largest and incorporates most of the clinically relevant MBLs, including the NDM, VIM, and IMP families (3–5). The enzymes from subclasses B2 (e.g., CphA2) and B3 (e.g., L1, AIM-1) are less common in pathogens (6–8).

Several co-formulations of *β*-lactam antibiotics with *β*-lactamase inhibitors, including avibactam, relebactam, vaborbactam, sulbactam, tazobactam, and clavulanic acid, are in clinical use (9, 10). These inhibitors are specific to SBLs and do not affect MBLs, revealing a growing therapeutic gap as MBL producers increase in frequency across the globe. Selective inhibition of MBLs has proven challenging as a result of their low sequence similarity, structurally fluid active sites, and poor selectivity over human metalloenzymes (11, 12). Furthermore, while many MBL inhibitors display potent activity *in vitro*, few exhibit comparable efficacy in whole-cell assays or *in vivo* animal models.

In a targeted screen for new MBL inhibitors, we discovered the fungal natural product, aspergillomarasmine A (AMA), a potent inhibitor of the clinically important enzymes NDM-1 and VIM-2 (13). AMA restores the *in vitro* activity of meropenem in MBL-producing *Enterobacteriaceae*, *Acinetobacter*, and *Pseudomonas* isolates and was previously shown to be effective in rescuing meropenem activity against NDM-1-producing *Klebsiella pneumoniae* in a murine model of systemic infection (13). While these findings establish the potential of AMA as an MBL inhibitor, the effect of AMA against a broader panel of MBLs remains unknown.

In this study, we carried out a systematic analysis of the efficacy of AMA in combination with six *β*-lactam antibiotic partners from three subclasses (carbapenem, cephem, and penam). For susceptibility testing of the various antibiotic/inhibitor combinations, we selected 19 MBLs from three subclasses. The potency of each combination was evaluated using biochemical and cell-based assays, where individual MBLs were expressed in isogenic *Escherichia coli* and *K. pneumoniae* strains. The resulting data serve as a guide for the *in vivo* implementation of AMA and related MBL inhibitors.

2.5 RESULTS

2.5.1 The potency of AMA and meropenem combinations depends on the MBL subclass and allelic variant

We previously demonstrated that AMA could inhibit two clinically relevant MBLs, NDM-1 and VIM-2, but was less effective toward IMP-7 (13). Consequently, we sought to rigorously establish the inhibitory spectrum of AMA against 19 MBLs from each

subclass (B1, B2, B3). Using cell-based assays, we evaluated the efficacy of AMA in combination with meropenem. We scored efficacy based on the minimum concentration needed to restore the level of meropenem growth inhibition to its EUCAST (European Committee on Antimicrobial Susceptibility Testing) susceptibility breakpoint (2 μg/ml). To ensure consistency between the different enzymes tested, all MBL genes were identically cloned into the pGDP2 vector (low-copy-number plasmid with a P_{lac} promoter) (14) and transformed into *E. coli* BW25113. The MIC values of meropenem against the wild-type and MBL-producing strains were measured in the absence of AMA to serve as a benchmark for resistance (see Supplemental Table 2.1).

The results revealed that *E. coli* strains producing subclass B1 enzymes could be resensitized to meropenem (≤2 μg/ml) over AMA concentrations ranging from 4 to 32 μg/mL (Table 2.1; see also Supplemental Table 2.4). Producers of NDM-1, VIM-1, VIM-2, VIM-7, CAM-1, and IND-1 from subclass B1 were the most susceptible to AMA (4 to 8 μg/mL). Cells producing NDM-4, NDM-5, NDM-6, NDM-7, IMP-1, IMP-7, and IMP-27 were moderately sensitive (12 to 16 μg/ml). *E. coli* producing B2 or B3 enzymes, except for L1, were the least sensitive to AMA (no rescue of meropenem at 2 μg/ml at AMA ≥64 μg/mL) (Table 2.1; see also Supplemental Table 2.4). The extent of meropenem potentiation by AMA was not necessarily related to the degree of antibiotic resistance conferred by the MBL. For example, while IMP-7 conferred an MIC of 16 μg/mL, it was less susceptible to AMA inhibition than other MBLs that conferred MIC values of 64 μg/mL.

Table 2.1: Concentration of AMA needed to restore the activity of different *β*-lactam antibiotics to the level seen with their EUCAST susceptibility breakpoint concentration in MBL-producing *E. coli* BW25113[a]

	[AMA] at the susceptibility breakpoint of the antibiotic (*μ*g/mL)[b]					
MBL	**Meropenem**	**Doripenem**	**Ertapenem**	**Imipenem**	**Cefotaxime**	**Ampicillin**
NDM-1	8	12	24	12	64	64
NDM-4	16	16	64	16	>64	>64
NDM-5	12	24	64	16	>64	>64
NDM-6	16	16	64	16	64	>64
NDM-7	16	24	64	24	>64	>64
VIM-1	8	8	12	12	24	64
VIM-2	8	8	8	8	12	16
VIM-7	8	8	8	8	8	16
CAM-1	4	12	8	8	24	64
DIM-1	12	12	16	8	24	64
IND-1	8	8	12	12	24	>64
GIM-1	12	12	32	12	>64	>64
IMP-1	16	12	64	24	>64	64
IMP-7	24	12	>64	16	>64	32
IMP-27	32	24	>64	≤0.5	>64	12
SPM-1	16	24	64	8	>64	>64
CphA2	>64	64	>64	>64	≤0.5	≤0.5
L1	12	12	24	8	≤0.5	>64
AIM-1	64	64	>64	24	>64	>64

[a]All 19 MBL genes were cloned into the pGDP2 vector. All bioassays were conducted in duplicate. This table shows the results from replicate 1.

[b]The EUCAST susceptibility breakpoint concentrations for meropenem, doripenem, ertapenem, imipenem, cefotaxime, and ampicillin are 2, 1, 0.5, 2, 1 and 8 *μ*g/mL, respectively.

To examine whether the inhibitory potency of AMA was simply dependent on different levels of *β*-lactamase expression, a FLAG-tag was engineered at the C termini of eight representative MBLs. These MBLs were specifically chosen because they covered a broad range of sensitivity to various combinations of AMA and meropenem. The level of

MBL production was quantified using an anti-FLAG monoclonal antibody via Western blotting. The installation of the tag did not affect resistance. The relative protein levels of NDM-4, NDM-5, NDM-6, NDM-7, VIM-2, and IMP-7 were all within a 2-fold range (see Supplemental Figures 2.1, 2.2). Although NDM-1 demonstrated the highest sensitivity to AMA inhibition, its relative expression was ~3-fold higher than any other enzyme. In contrast, IMP-7, which has a low sensitivity to AMA inhibition, showed lower protein levels. Together with our bioassay data, these results indicate that the MBL inhibition spectrum of AMA is broad but that it is more active toward class B1 enzymes.

2.5.2 The efficacy of AMA depends on the β-lactam antibiotic partner

We partnered AMA with three different carbapenems (doripenem, ertapenem, and imipenem), a cephem (cefotaxime), and a penam (ampicillin) to explore the optimal AMA/antibiotic combination. We graded the efficacy of AMA based on its ability to restore the activity of each antibiotic to its EUCAST susceptibility breakpoint concentration (for doripenem, ertapenem, imipenem, cefotaxime, and ampicillin, 1, 0.5, 2, 1, and 8 μg/mL, respectively). As described above, the individual drug MIC values for each antibiotic against MBL-producing *E. coli* served as benchmarks for resistance (see Supplemental Table 2.1). We found that the carbapenem and cephem susceptibilities of MBL-producing *E. coli* BW25113 were well (>7-fold) above the breakpoints. However, as this strain of *E. coli* encodes a chromosomal cephalosporinase (AmpC), it showed a baseline ampicillin MIC of 4 μg/mL and was much closer to the susceptibility breakpoint (see Supplemental Table 2.1).

The levels of β-lactam potentiation by AMA were comparable for most of the

carbapenems tested. Testing with AMA, the majority of strains producing MBLs showed either equivalent or 2-fold increased susceptibility for doripenem and imipenem relative to meropenem. Ertapenem, however, showed more variation. In particular, the IMP and NDM alleles were 3-fold to 5-fold less sensitive to AMA when paired with ertapenem relative to other carbapenems (Table 2.1; see also Supplemental Table 2.4). This pattern of reduced susceptibility to AMA inhibition involving the VIM, IMP, and NDM enzymes was also evident when cefotaxime and ampicillin were the partner antibiotics (Table 2.1; see also Supplemental Table 2.4). *E. coli* producing CphA2 was the most refractory to AMA combinations and showed high-level resistance against all carbapenem antibiotics (Table 2.1; see also Supplemental Table 2.4).

2.5.3 *β*-Lactam potentiation by AMA is also MBL class-dependent in *K. pneumoniae*

To investigate whether the inhibitory potency of AMA with different *β*-lactam antibiotics was pathogen dependent, we transformed *K. pneumoniae* ATCC 33495 with plasmids carrying one of eight selected MBL genes. The MIC values of the different *β*-lactams against the wild-type and MBL-producing *K. pneumoniae* were measured in the absence of AMA to serve as a control (see Supplemental Table 2.2). *K. pneumoniae* encodes a chromosomal penicillinase (SHV) and is consequently resistant to ampicillin with a drug MIC value of 64 μg/mL.

Similar to the results in *E. coli*, the potency of AMA combinations against MBLs produced in *K. pneumoniae* varied with the subclass of the *β*-lactam antibiotic partner. *K. pneumoniae* strains producing NDM-1 or VIM-2 were the most susceptible to

carbapenems (Table 2.2; see also Supplemental Table 2.5). However, *K. pneumoniae* producing other NDM variants demonstrated less sensitivity to AMA/carbapenem combinations, requiring higher AMA concentrations to achieve efficacy (Table 2.2; see also Supplemental Table 2.5). Meropenem was the *β*-lactam partner most strongly potentiated by AMA. Concentrations of AMA ranging from 8 to 16 μg/mL reduced the MIC values of this carbapenem for most MBL-producing *K. pneumoniae* to ≤2 μg/mL (Table 2.2; see also Supplemental Table 2.5). Since the MIC of meropenem with most MBL-producing *K. pneumoniae* strains was ≥32 μg/mL, this represents at least a 16-fold improvement of the antibiotic's activity (see Supplemental Table 2.2). The AMA and ampicillin pairing resulted in the poorest efficacy overall since all MBL-producing *K. pneumoniae* strains remained resistant to this antibiotic due to the production of an endogenous serine-dependent penicillinase (Table 2.2; see also Supplemental Table 2.5). Like *E. coli*, CphA2 and AIM-1 were the least sensitive to AMA inhibition (Table 2.2; see also Supplemental Table 2.5). These results suggest that the alteration of the potency of the AMA combinations contributed by the antibiotic partner was not pathogen dependent for two representative *Enterobacteriaceae* strains. Furthermore, the basal levels of *β*-lactam resistance shown by chromosomal *β*-lactamases play a significant role in determination of the appropriate *β*-lactam to be paired with AMA.

Table 2.2: Concentration of AMA needed to restore the activity of different *β*-lactam antibiotics to the level seen with their EUCAST susceptibility breakpoint concentration in MBL-producing *K. pneumoniae* ATCC 33495[a]

	[AMA] at the susceptibility breakpoint of the antibiotic (*μ*g/mL)[b]					
MBL	**Meropenem**	**Doripenem**	**Ertapenem**	**Imipenem**	**Cefotaxime**	**Ampicillin**
NDM-1	12	16	24	12	64	>64
NDM-4	16	24	64	24	>64	>64
NDM-5	16	24	64	24	>64	>64
NDM-6	12	16	64	24	>64	>64
VIM-2	8	8	8	12	16	>64
IMP-7	24	24	>64	64	>64	>64
CphA2	>64	>64	>64	>64	≤0.5	>64
AIM-1	64	64	>64	>64	>64	>64

[a]All 8 MBL genes were cloned into the pGDP2 vector. All bioassays were conducted in duplicate. This table shows the results from replicate 1.

[b]The EUCAST susceptibility breakpoint concentrations for meropenem, doripenem, ertapenem, imipenem, cefotaxime, and ampicillin are 2, 1, 0.5, 2, 1 and 8 *μ*g/mL, respectively.

2.5.4 Outer membrane permeability and efflux do not influence the activity of different *β*-lactam antibiotics against MBL-producing bacteria

To probe whether the observed differences in the effects of *β*-lactam specificity on the efficacy of AMA were the result of differences in outer membrane penetration or efflux of these antibiotics, potentiation assays were conducted with hyperpermeable *bamB*/*tolC* deletion strains of *E. coli* BW25113 expressing eight different MBL genes. The BamB lipoprotein and the TolC outer membrane protein play essential roles in outer membrane permeability and the efflux of antibiotics, respectively (15, 16). We found that apart from ampicillin, for which the baseline MIC value decreased 8-fold, the carbapenem MIC values against the Δ*bamB* Δ*tolC* strain were similar to those seen with the wild-type.

Likewise, the levels of resistance shown by MBL-producing strains were comparable (see Supplemental Table 2.3).

Table 2.3: Concentration of AMA needed to restore the activity of different *β*-lactam antibiotics to the level seen with their EUCAST susceptibility breakpoint concentration in MBL-producing *E. coli* BW25113 Δ*bamB* Δ*tolC*[a]

	[AMA] at the susceptibility breakpoint of the antibiotic (*μ*g/mL)[b]		
MBL	**Meropenem**	**Doripenem**	**Ampicillin**
NDM-1	8	12	32
NDM-4	16	24	> 64
NDM-5	16	24	> 64
NDM-6	12	24	> 64
VIM-2	8	8	24
IMP-7	24	24	> 64
CphA2	64	> 64	≤ 0.5
AIM-1	64	64	> 64

[a]All 8 MBL genes were cloned into the pGDP2 vector. All bioassays were conducted in duplicate. This table shows the results from replicate 1.
[b]The EUCAST susceptibility breakpoint concentrations for meropenem, doripenem, and ampicillin are 2, 1 and 8 *μ*g/mL, respectively.

AMA treatment of the MBL-producing Δ*bamB* Δ*tolC* strains revealed that the extent of potentiation of each *β*-lactam was very similar to that seen with wild-type *E. coli* (Table 2.3; see also Supplemental Table 2.6). We further probed the efficacy of the *β*-lactams by directly measuring the intracellular accumulation of AMA and each antibiotic in both the *E. coli* wild-type and Δ*bamB* Δ*tolC* strains. Although it was not possible to determine how much drug was lost to surface binding and periplasmic leeching, we reasoned that this would be a constant for each *β*-lactam in both the wild-type and Δ*bamB* Δ*tolC* strains. Any differences in accumulation should then be a result of increased penetration and/or decreased efflux (17). We found that AMA and the carbapenem

antibiotics were detectable in cell extracts in wild-type bacteria but that the extent of accumulation varied with the subclass of the *β*-lactam antibiotic. Despite the drug MIC values being similar to those seen with the wild-type, *E. coli* Δ*bamB* Δ*tolC* showed 5-fold, 2-fold, and 1.5-fold increases in accumulation for meropenem, doripenem, and imipenem, respectively (Figure 2.1). Ertapenem was the only member of the carbapenems which showed no such change between the strains.

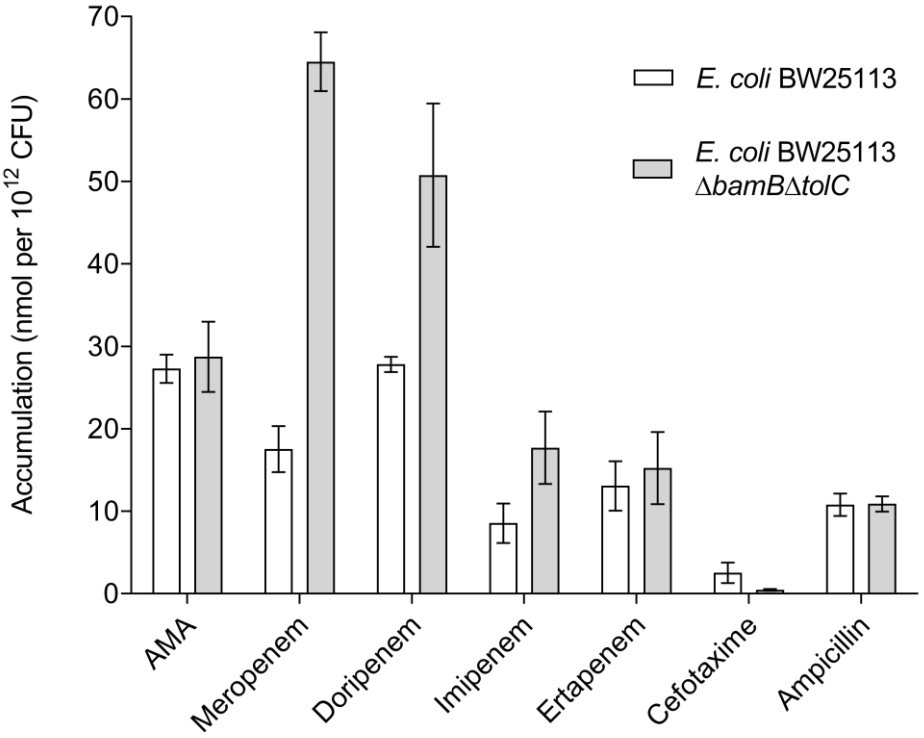

Figure 2.1: Accumulation assay data for different *β*-lactam antibiotics in *E. coli* BW25113 and *E. coli* BW25113 Δ*bamB* Δ*tolC*. All assays were performed in biological triplicate and technical duplicate. The error bars represent the standard deviations.

Our initial attempts to detect the accumulation of ampicillin failed and were likely hampered by its susceptibility to endogenous AmpC. To circumvent AmpC-mediated hydrolysis, we cotreated the cells with avibactam. The treatment enabled for the detection of ampicillin, which we found had accumulated similarly in the two strains, despite

having a lower MIC in the hyperpermeable strain. It is possible that some of the ampicillin had been hydrolyzed, resulting in an underestimation of the precise amount present. We also faced challenges with cefotaxime since, despite several attempts, we could not demonstrate robust accumulation levels for this antibiotic.

2.5.5 *β*-Lactam inactivation is affected by substrate-specific zinc requirements of MBLs

Previous work had shown that Zn^{2+} dissociates from MBLs during catalytic turnover of *β*-lactams and that this can lead to enzyme inactivation (18, 19). This phenomenon is particularly pronounced under conditions where excess Zn^{2+} is unavailable to replenish the enzyme. Since AMA binds to free Zn^{2+}, it could potentially withhold Zn^{2+} from MBLs, and the *β*-lactam could promote inactivation. We therefore hypothesized that different *β*-lactam substrates could uniquely influence Zn^{2+} dissociation from MBLs and affect the efficacy of AMA.

We tested this hypothesis with a series of *in vitro* enzyme assays involving a subset of purified MBLs and the panel of *β*-lactam substrates used in cell-based assays. In each enzyme stock (20 μM), a limited amount of AMA (100 nM) was included to sequester any residual Zn^{2+} in the Chelex-treated buffer. The reaction mixtures contained enzyme (4 to 10 nM), saturating amounts of substrate, and various concentrations of $ZnSO_4$ (0.001 to 20 μM). The resulting reaction rates exhibited clear Zn^{2+} dependence for each substrate. From the progress curves of the initial reaction rates, the Zn^{2+} dissociation constant ($K_{d,Zn2}$) could be calculated as the concentration of $ZnSO_4$ required to achieve half-maximal velocity. We presume on the basis of previous observations made by several

different research groups (20) that metal dissociation occurs primarily from the second zinc site (Zn^2) of the MBLs.

Table 2.4: Zinc-dependence of metallo-β-lactamase-catalysed hydrolysis of β-lactam antibiotics[a]

	Metallo-*β*-lactamase zinc dissociation constants[b] ($K_{d,Zn2}$)					
Substrate	**NDM-1**	**NDM-4**	**NDM-6**	**VIM-2**	**IMP-7**	**AIM-1**
Ampicillin	0.91 ± 0.07	0.15 ± 0.02	0.23 ± 0.02	0.45 ± 0.05	0.24 ± 0.04	0.19 ± 0.05
Cefotaxime	1.4 ± 0.3	0.17 ± 0.03	0.24 ± 0.02	0.21 ± 0.03	0.80 ± 0.4	0.33 ± 0.07
Meropenem	3.2 ± 0.5	0.3 ± 0.06	0.64 ± 0.08	0.63 ± 0.1	0.46 ± 0.08	0.52 ± 0.08
Imipenem	0.4 ± 0.04	0.06 ± 0.007	0.14 ± 0.01	0.34 ± 0.09	0.95 ± 0.3	0.59 ± 0.07
Ertapenem	2.8 ± 1	4.3 ± 2.6	2.0 ± 0.3	2.3 ± 1	2.0 ± 0.4	0.95 ± 0.2
Doripenem	1.1 ± 0.1	0.18 ± 0.02	0.14 ± 0.08	0.38 ± 0.03	0.082 ± 0.01	0.90 ± 0.1

[a]Reactions were carried out with enzyme (4 to 10 nM) in Chelex-treated HEPES-NaOH, pH 7.5 (50 mM), supplemented with AMA (100 nM).

[b]All constants are reported in micromolar (μM).

The levels of substrate-specific zinc dependence for each MBL differed greatly among the MBLs and ranged from nanomolar to micromolar $K_{d,Zn2}$ values. In reaction mixtures containing ampicillin, cefotaxime, meropenem, and doripenem, NDM-1 showed the lowest average level of affinity for Zn^{2+} during catalysis, with substrate-specific $K_{d,Zn2}$ values that were mostly in the low micromolar range (0.9 to 3.2 μM; Table 4; see also Supplemental Figure 2.3). This finding contrasted with the results seen with other MBLs, for which nanomolar (140 to 950 nM) Zn^{2+} affinity was observed. Intriguingly, the Zn^{2+} dependence of imipenem and ertapenem hydrolysis did not follow this trend. For imipenem, the $K_{d,Zn2}$ values for NDM-1, VIM-2, IMP-7, and AIM-1 fell within a 2-fold range (400 to 950 nM), while NDM-4 and NDM-6 showed the highest affinity for Zn^{2+} during hydrolysis of this carbapenem (60 and 140 nM, respectively). Surprisingly, ertapenem showed low micromolar Zn^{2+} affinity (0.95 to 4.3 μM) for every MBL tested,

which contrasted with the trends that we observed for the other substrates (Table 2.4; see also Supplemental Figure 2.3). Overall, these data allowed for the general estimation of Zn^{2+} affinity for each MBL and showed that the specific choice of β-lactam influences the $K_{d,Zn2}$ within a 3-fold range for each enzyme.

The $K_{d,Zn2}$ values failed to explain our observations where AMA differentially potentiated β-lactams. The results further support the hypothesis that the level of β-lactam resistance conferred by each MBL is the primary factor that dictates AMA susceptibility. However, the general level of Zn^{2+} affinity determined for each MBL was consistent with previous studies, where enzymes with higher affinity for Zn^{2+} were found to be better suited to withstanding its associated limitation in general (21). For example, NDM alleles, other than NDM-1, have evolved to increase metal affinity. This was evident in the current study as the concentrations of AMA needed to restore the activity of the antibiotics to their susceptibility breakpoints were generally lower for NDM-1 than for NDM-4, NDM-5, NDM-6, NDM-7, IMP-7, CphA2, and AIM-1. Interestingly, VIM-2 stands out as a particular case in that its low $K_{d,Zn2}$ values do not correlate well with the bioassay data, suggesting that this enzyme has an unknown property which increases its sensitivity to AMA.

2.6 DISCUSSION

AMA is an inhibitor of MBLs and potentiates the activity of meropenem against MBL-producing bacteria. Here, we explored the inhibitory activity of AMA paired with five other β-lactam antibiotics against 19 MBL enzymes produced in three bacterial strains.

Potentiation assays indicated that AMA achieved the highest inhibitory potency when

combined with a carbapenem antibiotic. This was not influenced by the bacterial species or strain used during the bioassays (Tables 2.1, 2.2, 2.3). The results of the intracellular accumulation assays suggest that the inhibitory activity of AMA together with the different *β*-lactam antibiotics is not correlated with outer membrane permeability or drug efflux (Figure 2.1). One possible explanation for the advantage of using AMA/carbapenem pairings may be related to the affinity of these drugs for their targets, the penicillin-binding proteins (PBPs). Kocaoglu and Carlson determined that each *β*-lactam antibiotic is selective for a subset of PBPs (22). While ampicillin targets a broader spectrum of PBPs, none of them are not solely essential for bacterial growth, and the bactericidal effect is the result of inhibition of several of these enzymes.

On the other hand, meropenem, doripenem, and cefotaxime all inhibit at least one essential PBP and do so with high potency. Furthermore, unlike penams, which are prone to hydrolysis by class C SBLs (e.g., AmpC) and low-molecular-weight PBPs, carbapenems are not substrates for these enzymes. These observations are consistent with previous studies which demonstrated that meropenem, doripenem, and imipenem are the carbapenem antibiotics with the highest potencies and the broadest spectra of activity against different bacterial species (23), including extended-spectrum *β*-lactamase (ESBL)-producing isolates of *E. coli* and *K. pneumoniae* (24).

Our work supports previous studies indicating that MBL-mediated carbapenem resistance is weaker than cefotaxime and ampicillin (21, 25–27). Considering our data in conjunction with the current knowledge available for *β*-lactam efficacy and resistance, AMA is most likely to succeed when paired with a carbapenem, in particular,

meropenem, doripenem, or imipenem.

Given our observations that the *β*-lactam substrate uniquely influences AMA susceptibility of different MBLs, we wondered if its inhibitory activity was mechanistically dependent on substrate interactions. Substrate-induced Zn^{2+} dissociation (i.e., reduced Zn^{2+} affinity) is well documented in several MBL studies (18, 19, 28–30) and those results inspired us to develop the mechanistic basis for the following hypothesis: *β*-lactams promote the release of Zn^{2+} from MBLs (presumably by increasing the rate constant for dissociation), and then AMA acts as a recipient for the free metal. In effect, AMA would withhold Zn^{2+}, leading to essentially irreversible inhibition. Precedents for this hypothesis can be found in the mechanism of inhibition proposed for D-penicillamine (D-Pen) toward human Zn^{2+}-dependent carboxypeptidase A (ZnCPD). D-Pen directly catalyzes the removal of Zn^{2+} from ZnCPD through increased metal dissociation, but the high-affinity apoenzyme can rebind the metal and outcompete D-Pen. However, if a potent chelator such as EDTA is present, Zn^{2+} is sequestered, and ZnCPD is wholly inhibited (31, 32). In general, our data show that Zn^{2+} affinity seen during *β*-lactam hydrolysis correlated well with the potency of AMA for numerous MBL/*β*-lactam pairs. This was consistent with several studies that have shown that increased affinity can overcome Zn^{2+} scarcity. For example, NDM variants contain single-point or multiple-point mutations which increase Zn^{2+} affinity. Furthermore, this increases the thermostability of these MBLs, which has been associated with an increase in resistance (21). This is also consistent with our observation that CphA2 is refractory to AMA, as this MBL is a mono-Zn^{2+} enzyme with a strong metal affinity ($K_{d,Zn}$ value of 6 pM (33)).

Curiously, not all of the $K_{d,Zn2}$ values correlated with the biological activity of AMA and some of the results were counterintuitive. For example, the hydrolysis of ertapenem resulted in the highest $K_{d,Zn2}$ values for every MBL tested, which currently eludes explanation. Moreover, VIM-2 has a high Zn^{2+} affinity during hydrolysis of most β-lactams, although it is one of the most sensitive MBLs in our bioassays. Recently, it was shown that membrane anchoring stabilizes NDM variants when Zn^{2+} is scarce in the environment (34). All other MBLs contain cleavable signal peptides and are released into the periplasmic space and can be rapidly degraded in a manner depending on their stability. In the case of VIM-2, González et al. have shown that it is particularly susceptible to degradation (34), which could explain why, despite high Zn^{2+} affinity, VIM-producing bacteria are more susceptible to AMA.

Our results demonstrate that an AMA/carbapenem pairing would be the most effective combination for treating infections caused by MBL-producing bacteria in the clinics, though higher concentrations of AMA are required to cover recently emerging NDM alleles.

2.7 MATERIALS AND METHODS

2.7.1 DNA manipulations and pGDP2 plasmid construction

All oligonucleotide primers were purchased from IDT (Coralville, IA). The MBL genes used in this study were also purchased from IDT as gBlock gene fragments, except for bla_{NDM-4}, bla_{NDM-5}, bla_{NDM-6}, and bla_{NDM-7}. The gBlock sequences for each MBL gene were obtained from the Comprehensive Antibiotic Resistance Database (CARD; https://card.mcmaster.ca/). The sequence of bla_{AIM-1} from the CARD was codon

optimized for *E. coli* K-12 to facilitate its expression in the *E. coli* and *K. pneumoniae* strains. Each MBL gene fragment was subsequently cloned into the pGDP2 vector. As *bla*$_{\text{NDM-4}}$, *bla*$_{\text{NDM-5}}$, *bla*$_{\text{NDM-6}}$, and *bla*$_{\text{NDM-7}}$ differ from *bla*$_{\text{NDM-1}}$ by only a few point mutations, constructs of these variants were generated by site-directed mutagenesis of pGDP2:*bla*$_{\text{NDM-1}}$ using the primers listed in Supplemental Table 2.7. In comparison to NDM-1, the NDM-4 (M154L) and NDM-6 (A233V) variants required a single nucleotide substitution whereas the NDM-5 (M154L and V88L) and NDM-7 (D130N and M154L) variants needed two nucleotide substitutions. All MBL gene sequences were verified by Sanger sequencing. For antibiotic susceptibility and AMA potentiation assays, the purified plasmids were transformed into chemically competent *E. coli* BW25113 cells, *E. coli* BW25113 Δ*bamB* Δ*tolC* cells, or *K. pneumoniae* ATCC 33495 cells. The freeze-thaw transformation procedure of the *K. pneumoniae* cells followed the protocol described in reference (35). These bacterial strains were chosen for the transformation because *E. coli* BW25113, and *K. pneumoniae* ATCC 33495 are carbapenem-susceptible (see Supplemental Tables 2.1, 2.2, 2.3).

2.7.2 pE-SUMOstar and pET-28b plasmid construction

For protein overproduction and purification, the MBL genes previously cloned into the pGDP2 vectors were used as templates for cloning into overexpression vectors using the primers listed in Supplemental Table 2.8. SignalP (http://www.cbs.dtu.dk/services/SignalP/) was used to determine the sequence of the signal peptide, which was excluded from the final constructs to facilitate cytoplasmic accumulation. The VIM-2, IMP-7, and AIM-1 genes were ligated in a pET-28b vector in frame with a cleavable N-terminus

6×His tag. All NDM genes were ligated into a pE-SUMOstar vector in frame with an N-terminus 6×His-Smt3 tag. Smt3 is a ubiquitin-like protein from *Saccharomyces cerevisiae*. The purified plasmids were then transformed into chemically competent *E. coli* BL21(DE3) cells. Mature MBL gene sequences were verified by Sanger sequencing before overexpression.

2.7.3 Western blot analysis

Engineering FLAG-tagged variants of each MBL was achieved through a PCR-based procedure. The MBL genes previously cloned into the pGDP2 vectors were used as templates for the addition of the protein tag by using the primers listed in Supplemental Table 2.8. To allow for the addition of the FLAG-tag to the C terminal of the protein, the stop codon needed to be removed from the C-terminal of the MBL gene. The tagged MBL genes were ligated into the pGDP2 vector and transformed into chemically competent *E. coli* BW25113 cells. Gene sequences were verified by Sanger sequencing before immunodetection.

Cation-adjusted Mueller Hinton II broth (CAMHB) supplemented with kanamycin (50 μg/mL) was inoculated with *E. coli* BW25113 cells containing the FLAG-tagged MBL. The inoculated medium was incubated at 37°C until the optical density at 600 nm (OD_{600}) reached 1.0. Cells (1 ml) were harvested by centrifugation (17,000 × *g*, 2 min, room temperature). The cell pellet was resuspended in 100 μL of double-distilled water (ddH_2O) and mixed with 100 μL of 2× SDS running buffer. Proteins resolved by sodium dodecyl sulfate-polyacrylamide gel electrophoresis (SDS-PAGE) were transferred to a polyvinylidene difluoride membrane (PVDF) and probed with mouse-derived anti-FLAG

monoclonal antibodies conjugated to horseradish peroxidase (HRP; GenScript, Piscataway, NJ) (1:5,000). Chemiluminescence signals were detected using a ChemiDoc MP imaging system (Bio-Rad, Hercules, CA). Following imaging, irreversible inhibition of HRP was conducted by incubating the Western blot with 30% hydrogen peroxide for 15 min at 37°C (36). The Western blot was then reprobed with mouse-derived anti-RpoA antibodies (BioLegend, San Diego, CA) (1:5,000) and anti-mouse IgG antibodies conjugated to HRP (Cell Signaling Technology, Danvers, MA) (1:5,000). Chemiluminescence signals were detected using a ChemiDoc MP imaging system. Protein band intensities were quantified using Image Lab software (Bio-Rad). These results were then plotted and analyzed using GraphPad Prism 8 (GraphPad, La Jolla, CA) to determine the relative protein expression levels. The antibodies targeting the alpha subunit of RNA polymerase (RpoA) served as loading controls for the analysis.

2.7.4 Protein purification

For each MBL, LB medium supplemented with kanamycin (50 μg/ml) was inoculated with *E. coli* BL21(DE3) cells containing the appropriate plasmid. The inoculated medium was incubated at 37°C until the OD_{600} reached 0.6 to 0.8. Expression of the constructs was induced by the use of isopropyl-β-D-thiogalactopyranoside (IPTG) at a final concentration of 1 mM. Cultures were then incubated at 16°C for 16 to 20 h. Cells were harvested by centrifugation (6,000 × *g*, 20 min, 4°C) using a Beckman Coulter Avanti J-25 centrifuge with a JLA 9.1000 rotor (Beckman Coulter, Fullerton, CA) and frozen at –20°C until required. For purification, the cell pellet was resuspended in lysis buffer (25 mM HEPES-NaOH, 300 mM NaCl, 10 mM imidazole, 100 μM $ZnSO_4$, pH 7.5). Cells

were then disrupted by sonication (8-s intervals for 8 min) using a Microson XL-2000 ultrasonic liquid processor (Qsonica, Newtown, CT) set at level 12. Unbroken cells were removed by centrifugation (40,000 × *g*, 20 min, 4°C) using a Beckman JLA 25.50 rotor (Beckman Coulter). His-tagged proteins were then bound to 2 ml of HisPur nickel-nitrilotriacetic acid (Ni-NTA) resin (Pierce, Rockford, IL) and applied to a gravity column. The resin was washed three times with lysis buffer (60 ml total volume), and the protein eluted with lysis buffer containing 300 mM imidazole. Fractions were analyzed using SDS-PAGE. All fractions shown to contain purified β-lactamase were combined and dialyzed for 16 to 20 h at 4°C in dialysis buffer (25 mM HEPES-NaOH, 150 mM NaCl, 100 μM $ZnSO_4$, pH 7.5). Following dialysis, the 6×His tag was removed from the protein using thrombin (Sigma-Aldrich, St-Louis, MO). The 6×His tag and undigested protein were removed by passage through HisPur Ni-NTA resin equilibrated in dialysis buffer. Subsequently, thrombin was removed with *p*-aminobenzamidine-agarose resin. Protein samples were then analyzed by SDS-PAGE to confirm tag removal. The purified proteins were stored at 4°C or frozen at –20°C.

Purification of NDM-1 proceeded as described above, except for the addition of the Ulp-1 (ubiquitin-like protein-specific protease 1) to the dialysis buffer. The dialyzed protein was then applied to 2 ml of HisPur Ni-NTA resin to remove any uncleaved NDM-1 as well as Ulp-1. Fractions containing cleaved NDM-1, as assessed by SDS-PAGE, were pooled and stored at 4°C. NDM-4, NDM-5, and NDM-6 were purified using the same procedure as that used for NDM-1 purification.

AIM-1 was produced in an insoluble form and was acquired from the pellet obtained after centrifugation of the cell lysate. The AIM-1-containing protein pellet was solubilized using denaturation buffer (50 mM HEPES-NaOH, 150 mM NaCl, 6 M guanidine HCl, pH 7.5), followed by centrifugation (30,000 × *g*, 20 min, 4°C). The denatured protein sample (10 ml) was subsequently refolded in renaturation buffer (50 mM HEPES-NaOH, 150 mM NaCl, 50 mM L-arginine, 10 μM $ZnSO_4$, pH 7.5) using a slow dialysis method. The dialysis membrane containing AIM-1 was subjected to buffer exchange in 50-ml volumes once per hour for a total of 8 h at room temperature. Precipitated protein was removed by centrifugation (30,000 × *g*, 10 min, 4°C), and the supernatant was then applied to HisPur Ni-NTA resin. The protein was eluted as described above, concentrated, and further purified to remove aggregates using a size exclusion column (HiLoad Superdex 200 16/600; GE Healthcare Bio-Sciences AB, Uppsala, Sweden) that was equilibrated and operated with dialysis buffer. SDS-PAGE-analyzed fractions containing monomeric protein were combined, and the His tag was removed as described above. The enzyme activity was tested and was comparable to previously published kinetic data (8).

2.7.5 β-Lactam potentiation assays

Bacterial antibiotic susceptibility assays were conducted using AMA in combination with a β-lactam antibiotic based on the protocol described in reference (37). β-Lactam antibiotics were dissolved in water, and AMA was diluted in water containing ≤5% (vol/vol) ammonium hydroxide to ensure that the final pH was between 7.5 to 8.5. Compounds were subjected to filter sterilization. All assays were conducted in a 96-well

format with 10 dilutions of AMA (0.5, 1, 2, 4, 8, 12, 16, 24, 32, and 64 μg/mL) being added to columns 1 to 10 while 8 2-fold dilutions of the β-lactam antibiotic (0.5–64 μg/mL) were added to rows A to H. The dilutions of the β-lactam antibiotics were also added to column 11 to confirm the MIC value of the β-lactam antibiotic with each different strain. The dilutions of AMA and the β-lactam antibiotic were conducted manually or with a Labcyte Echo 550 liquid dispenser (Labcyte, San Jose, CA) or with a Thermo Scientific Multidrop Combi nL reagent dispenser (Thermo Fisher Scientific, Waltham, MA). A bacterial inoculum was prepared from the bacterial cells of interest using colonies picked from overnight plates whose OD_{625} was adjusted to 0.08 to 0.10. Once the optimal OD_{625} was reached, a 200-fold dilution of the inoculum was conducted before its addition to the MIC plate. The dilution of the inoculum was performed using CAMHB. The final inoculum cell density was 5×10^5 CFU/mL. The inoculum was added to columns 1 through 11. The bacterial inoculum and the CAMHB were then added alternatively to column 12 to serve as growth and sterility controls. The final assay volume was 100 μl when the assay was conducted in a 96-well round-base microtest plate (Sarstedt, Nümbrecht, Germany) or 50 μl when the assay was scaled to a 384-well format (flat bottom, clear, tissue culture treated, polystyrene; Corning, Kennebunk, ME). Following a 20-h static incubation at 37°C, bioassay plates containing *E. coli* were shaken for 5 min to resuspend the bacterial cells. However, *K. pneumoniae* cells were resuspended manually using a pipette to minimize the formation of aerosols. The bioassay plates were read spectrophotometrically at a wavelength of 600 nm using a SpectraMax 384 Plus UV/Vis spectrophotometer/microplate reader (Molecular Devices, San Jose,

CA). All potentiation assays were done with at least two replicates. The susceptibility breakpoints published by the European Committee on Antimicrobial Susceptibility Testing (EUCAST; http://www.eucast.org/clinical_breakpoints/) were used as a reference.

2.7.6 Accumulation assays

Antibiotic accumulation was conducted as previously described using the *E. coli* wild-type and Δ*bamB* Δ*tolC* strains (38). Briefly, meropenem, doripenem, imipenem, ertapenem, cefotaxime, ampicillin, or AMA was added to cells in a volume of 875 μl ([β-lactam] = 50 μM and [AMA] = 100 μM). Avibactam (50 μM) was added to the assays containing either cefotaxime or ampicillin. Avibactam was used to inhibit the AmpC β-lactamase, which is chromosomally encoded by the *E. coli* strains and prevented the detection of these antibiotics. The antibiotics were incubated with the bacteria (10 min, 37°C), and 800 μl of the suspension was subsequently washed through 700 μl of ice-cold silicone oil (9:1 AR20/Sigma High Temperature) by centrifugation (12,000 × *g*, 2 min, room temperature). The cells were resuspended in 200 μl water and lysed by three freeze-thaw cycles. Cell debris was collected by centrifugation (17,000 × *g*, 2 min, room temperature) using a Fisher Scientific accuSpin Micro 17 microcentrifuge (Thermo Fisher Scientific), and the pellet was extracted with 100 μl methanol (MeOH). The cell extracts were pooled and quantitatively analyzed by the used of ultraperformance liquid chromatography (UPLC) coupled to a high-resolution quadrupole-time of flight (Q-TOF) 6550 mass spectrometer (Agilent, Santa Clara, CA). In order to detect AMA, samples were derivatized with benzoyl chloride (BzCl) based on the protocol described in

reference (39). Briefly, samples were mixed with acetonitrile (1:1), and 0.5 volumes of sodium carbonate (100 mM) and BzCl (2%) were added, and the mixture was subjected to vortex mixing. Any precipitated material was removed by centrifugation (17,000 × *g*, 2 min, room temperature). Samples were loaded onto a C_8 column (Agilent Eclipse XDB-C8) (100 mm by 2.1 mm; 3.5-μm pore size) that had previously been equilibrated with solvent A (water, 0.1% formic acid) and 5% solvent B (acetonitrile, 0.1% formic acid), and they were resolved using a linear gradient of 5% to 97% solvent B over 7 min, followed by a 1-min wash step at 97% solvent B at a flow rate of 0.4 ml/min. The Q-TOF was operated in extended dynamic range positive-ion targeted tandem mass spectrometry (MS/MS) modes with an *m/z* range of 100 to 1,700 *m/z* and a capillary voltage of 0.5 kV. The collision energies and respective parent-daughter ion transitions used for AMA and each β-lactam antibiotic are listed in Supplemental Table 2.9. Quantification was carried out with a calibration curve of each antibiotic using Agilent MassHunter Quantitative Analysis software. For each compound, biological and technical replicates were conducted in triplicate and duplicate, respectively.

2.7.7 *In vitro* enzymes assays

MBL-catalyzed hydrolysis of β-lactam substrates was monitored spectrophotometrically by measuring the decrease in UV absorbance at 300 nm (meropenem, doripenem, imipenem, and ertapenem), 265 nm (cefotaxime), or 235 nm (ampicillin) in UV-grade 96-well flat-bottom microplates (Thermo Fisher Scientific). Before use in assays, enzymes (20 μM) were preincubated with AMA (0.5 mM; 16 h, 4°C) and subsequently dialyzed into reaction buffer (50 mM HEPES-NaOH [pH 7.5], 100 nM AMA; 4°C) to ensure that

residual Zn^{2+} was removed from the enzyme preparation. HEPES-NaOH (1 M) buffer was pretreated with 5% (wt/vol) Chelex 100 prior to use (24 h, 25°C). Enzyme (4 to 10 nM) in reaction buffer was added to varying concentrations $ZnSO_4$ (0.0007, 0.0015, 0.03, 0.15, 0.31, 0.62, 1.2, 2.5, 5, 10, and 20 μM) containing carbapenem (0.5 mM), ampicillin (0.5 mM), or cefotaxime (0.25 mM) substrate to initiate the reaction. The reactions were monitored using a BioTek Synergy H1 plate reader (Biotek, Winooski, VT) over 5 min at 25°C. To obtain $K_{d,Zn2}$ values, the initial rates of substrate hydrolysis at each $ZnSO_4$ concentration were plotted and analyzed using nonlinear regression by fitting the data to equation 1 using GraphPad Prism 8. In cases where zinc inhibition was apparent, equation 2 was used. All enzyme assays were performed in duplicate.

$$v_0 = \frac{V_{max}\,[ZnSO_4]}{K_{d,Zn2} + [ZnSO_4]} \tag{1}$$

$$v_0 = \frac{V_{max}\,[ZnSO_4]}{K_{d,Zn2} + [ZnSO_4]\,(1 + [ZnSO_4] / K_i)} \tag{2}$$

2.8 ACKNOWLEDGEMENTS

This research was funded by a Canadian Institutes of Health Research grant (FRN-148463), a Canadian Institutes of Health Research Fellowship award (to D.S.), a Canada Research Chair in Antibiotic Biochemistry (to G.D.W.), and an Ontario Graduate Scholarship and Queen Elizabeth II Graduate Scholarship (to C.M.R).

We thank Haley Zubyk for conducting the cloning and bacterial transformation of several MBL genes employed in this research and Susan McCusker for assistance with liquid handling instrumentation.

2.9 REFERENCES

1. King DT, Sobhanifar S, Strynadka NCJ. 2016. One ring to rule them all: Current trends in combating bacterial resistance to the β-lactams. Protein Sci 25:787–803. https://doi.org/10.1002/pro.2889.

2. Bebrone C. 2007. Metallo-β-lactamases (classification, activity, genetic organization, structure, zinc coordination) and their superfamily. Biochem Pharmacol 74:1686–1701. https://doi.org/10.1016/j.bcp.2007.05.021.

3. Guo Y, Wang J, Niu G, Shui W, Sun Y, Zhou H, Zhang Y, Yang C, Lou Z, Rao Z. 2011. A structural view of the antibiotic degradation enzyme NDM-1 from a superbug. Protein Cell 2:384–394. https://doi.org/10.1007/s13238-011-1055-9.

4. García-Sáez I, Docquier J-D, Rossolini GM, Dideberg O. 2008. The three-dimensional structure of VIM-2, a Zn-β-lactamase from *Pseudomonas aeruginosa* in its reduced and oxidised form. J Mol Biol 375:604–611. https://doi.org/10.1016/j.jmb.2007.11.012.

5. Concha NO, Janson CA, Rowling P. 2000. Crystal Structure of the IMP-1 Metallo *β*-lactamase from *Pseudomonas aeruginosa* and Its Complex with a Mercaptocarboxylate Inhibitor: Binding Determinants of a Potent, Broad-spectrum Inhibitor. Biochemistry 39:4288–4298. https://doi.org/10.1021/bi992569m.

6. Villadares MH, Galleni M, Frère J-M, Felici A, Perilli M, Franceschini N, Rossolini GM, Oratore A, Amicosante G. 1996. Overproduction and Purification of the *Aeromonas hydrophila* CphA Metallo-*β*-Lactamase Expressed in *Escherichia coli*. Microb Drug Resist 2:253–256. https://doi.org/10.1089/mdr.1996.2.253.

7. Ullah JH, Walsh TR, Taylor IA, Emery DC, Verma CS, Gamblin SJ, Spencer J. 1998. The crystal structure of the L1 metallo-β-lactamase from *Stenotrophomonas maltophilia* at 1.7 Å resolution. J Mol Biol 284:125–136. https://doi.org/10.1006/jmbi.1998.2148.

8. Leiros H-KS, Borra PS, Brandsdal BO, Edvardsen KSW, Spencer J, Walsh TR, Samuelsen Ø. 2012. Crystal Structure of the Mobile Metallo-β-Lactamase AIM-1 from *Pseudomonas aeruginosa*: Insights into Antibiotic Binding and the Role of Gln157. Antimicrob Agents Chemother 56:4341–4353. https://doi.org/10.1128/AAC.00448-12.

9. Palzkill T. 2013. Metallo-β-lactamase structure and function. Ann N Y Acad Sci 1277:91–104. https://doi.org/10.1111/j.1749-6632.2012.06796.x.

10. Bush K, Bradford PA. 2019. Interplay between β-lactamases and new β-lactamase inhibitors. Nat Rev Microbiol 17:295–306. https://doi.org/10.1038/s41579-019-0159-8.

11. Rotondo CM, Wright GD. 2017. Inhibitors of metallo-β-lactamases. Curr Opin Microbiol 39:96–105. https://doi.org/10.1016/j.mib.2017.10.026.

12. Tehrani KHME, Martin NI. 2018. β-lactam/β-lactamase inhibitor combinations: an update. Med Chem Comm 9:1439–1456. https://doi.org/10.1039/c8md00342d.

13. King AM, Reid-Yu SA, Wang W, King DT, De Pascale G, Strynadka NC, Walsh TR, Coombes BK, Wright GD. 2014. Aspergillomarasmine A overcomes metallo-β-lactamase antibiotic resistance. Nature 510:503–506. https://doi.org/10.1038/nature13445.

14. Cox G, Sieron A, King AM, De Pascale G, Pawlowski AC, Koteva K, Wright GD. 2017. A Common Platform for Antibiotic Dereplication and Adjuvant Discovery. Cell Chem Biol 24:98–109. https://doi.org/10.1016/j.chembiol.2016.11.011.

15. Namdari F, Hurtado-Escobar GA, Abed N, Trotereau J, Fardini Y, Giraud E, Velge P, Virlogeux-Payant I. 2012. Deciphering the Roles of BamB and Its Interaction with BamA in Outer Membrane Biogenesis, T3SS Expression and Virulence in *Salmonella*. PLoS One 7:e46050. https://doi.org/10.1371/journal.pone.0046050.

16. Koronakis V, Eswaran J, Hughes C. 2004. Structure and Function of TolC: The Bacterial Exit Duct for Proteins and Drugs. Annu Rev Biochem 73:467–489. https://doi.org/10.1146/annurev.biochem.73.011303.074104.

17. Li X-Z, Ma D, Livermore DM, Nikaido H. 1994. Role of Efflux Pump(s) in Intrinsic Resistance of *Pseudomonas aeruginosa*: Active Efflux as a Contributing Factor to β-Lactam Resistance. Antimicrob Agents Chemother 38:1742–1752. https://doi.org/10.1128/aac.38.8.1742.

18. Badarau A, Page MI. 2006. Enzyme Deactivation Due to Metal-Ion Dissociation during Turnover of the Cobalt-*β*-Lactamase Catalyzed Hydrolysis of *β*-Lactams. Biochemistry 45:11012–11020. https://doi.org/10.1021/bi0610146.

19. Badarau A, Page MI. 2008. Loss of enzyme activity during turnover of the *Bacillus cereus β*-lactamase catalysed hydrolysis of *β*-lactams due to loss of zinc ion. J Biol Inorg Chem 13:919–928. https://doi.org/10.1007/s00775-008-0379-2.

20. Thomas PW, Zheng M, Wu S, Guo H, Liu D, Xu D, Fast W. 2011. Characterization of Purified New Delhi Metallo-*β*-lactamase-1. Biochemistry 50:10102–10113. https://doi.org/10.1021/bi201449r.

21. Cheng Z, Thomas PW, Ju L, Bergstrom A, Mason K, Clayton D, Miller C, Bethel CR, VanPelt J, Tierney DL, Page RC, Bonomo RA, Fast W, Crowder MW. 2018. Evolution of New Delhi metallo-*β*-lactamase (NDM) in the clinic: Effects of NDM mutations on stability, zinc affinity, and mono-zinc activity. J Biol Chem 293:12606–12618. https://doi.org/10.1074/jbc.RA118.003835.

22. Kocaoglu O, Carlson EE. 2015. Profiling of β-Lactam Selectivity for Penicillin-Binding Proteins in *Escherichia coli* Strain DC2. Antimicrob Agents Chemother 59:2785–2790. https://doi.org/10.1128/AAC.04552-14.

23. Zhanel GG, Wiebe R, Dilay L, Thomson K, Rubinstein E, Hoban DJ, Noreddin AM, Karlowsky J a. 2007. Comparative review of the carbapenems. Drugs 67:1027–1052. https://doi.org/10.2165/00003495-200767070-00006.

24. Jones RN, Sader HS, Fritsche TR. 2005. Comparative activity of doripenem and three other carbapenems tested against Gram-negative bacilli with various β-lactamase resistance mechanisms. Diagn Microbiol Infect Dis 52:71–74. https://doi.org/10.1016/j.diagmicrobio.2004.12.008.

25. Tada T, Miyoshi-Akiyama T, Shimada K, Shimojima M, Kirikae T. 2013. IMP-43 and IMP-44 Metallo-β-Lactamases with Increased Carbapenemase Activities in Multidrug-Resistant *Pseudomonas aeruginosa*. Antimicrob Agents Chemother 57:4427–4432. https://doi.org/10.1128/AAC.00716-13.

26. Poirel L, Naas T, Nicolas D, Collet L, Bellais S, Cavallo JD, Nordmann P. 2000. Characterization of VIM-2, a Carbapenem-Hydrolyzing Metallo-β-lactamase and Its Plasmid- and Integron-Borne Gene from a *Pseudomonas aeruginosa* Clinical Isolate in France. Antimicrob Agents Chemother 44:891–897. https://doi.org/10.1128/aac.44.4.891-897.2000.

27. Yong D, Toleman MA, Bell J, Ritchie B, Pratt R, Ryley H, Walsh TR. 2012. Genetic and Biochemical Characterization of an Acquired Subgroup B3 Metallo-β-Lactamase Gene, *bla*$_{\text{AIM-1}}$, and Its Unique Genetic Context in *Pseudomonas aeruginosa* from Australia. Antimicrob Agents Chemother 56:6154–6159. https://doi.org/10.1128/AAC.05654-11.

28. Wommer S, Rival S, Heinz U, Galleni M, Frère J-M, Franceschini N, Amicosante G, Rasmussen B, Bauer R, Adolph H-W. 2002. Substrate-activated Zinc Binding of Metallo-*β*-lactamases. J Biol Chem 277:24142–24147. https://doi.org/10.1074/jbc.M202467200.

29. Rasia RM, Vila AJ. 2002. Exploring the Role and the Binding Affinity of a Second Zinc Equivalent in *B. cereus* Metallo-*β*-lactamase. Biochemistry 41:1853–1860. https://doi.org/10.1021/bi010933n.

30. Bounaga S, Laws AP, Galleni M, Page MI. 1998. The mechanism of catalysis and the inhibition of the *Bacillus cereus* zinc-dependent *β*-lactamase. Biochem J 331:703–711. https://doi.org/10.1042/bj3310703.

31. Chong CR, Auld DS. 2000. Inhibition of Carboxypeptidase A by D-Penicillamine: Mechanism and Implications for Drug Design. Biochemistry 39:7580–7588. https://doi.org/10.1021/bi000101+.

32. Chong CR, Auld DS. 2007. Catalysis of Zinc Transfer by D-Penicillamine to Secondary Chelators. J Med Chem 50:5524–5527. https://doi.org/10.1021/jm070803y.

33. Villadares MH, Kiefer M, Heinz U, Soto RP, Meyer-Klaucke W, Nolting HF, Zeppezauer M, Galleni M, Frère J-M, Rossolini GM, Amicosante G, Adolph H-W. 2000. Kinetic and spectroscopic characterization of native and metal-substituted β-lactamase from *Aeromonas hydrophila* AE036. FEBS Lett 467:221–225. https://doi.org/10.1016/S0014-5793(00)01102-9.

34. González LJ, Bahr G, Nakashige TG, Nolan EM, Bonomo RA, Vila AJ. 2016. Membrane anchoring stabilizes and favors secretion of New Delhi metallo-β-lactamase. Nat Chem Biol 12:516–522. https://doi.org/10.1038/nchembio.2083.

35. Merrick MJ, Gibbins JR, Postgate JR. 1987. A Rapid and Efficient Method for Plasmid Transformation of *Klebsiella pneumoniae* and *Escherichia coli*. Microbiology 133:2053–2057. https://doi.org/10.1099/00221287-133-8-2053.

36. Sennepin AD, Charpentier S, Normand T, Sarré C, Legrand A, Mollet LM. 2009. Multiple reprobing of Western blots after inactivation of peroxidase activity by its substrate, hydrogen peroxide. Anal Biochem 393:129–131. https://doi.org/10.1016/j.ab.2009.06.004.

37. Clinical and Laboratory Standards Institute. 2012. Methods for Dilution Antimicrobial Susceptibility Tests for Bacteria That Grow Aerobically ; Approved Standard—Ninth Edition. CLSI, Wayne, PA.

38. Richter MF, Drown BS, Riley AP, Garcia A, Shirai T, Svec RL, Hergenrother PJ. 2017. Predictive rules for compound accumulation yield a broad-spectrum antibiotic. Nature 545:299–304. https://doi.org/10.1038/nature22308.

39. Wong JMT, Malec PA, Mabrouk OS, Ro J, Dus M, Kennedy RT. 2016. Benzoyl chloride derivatization with liquid chromatography–mass spectrometry for targeted metabolomics of neurochemicals in biological samples. J Chromatogr A 1446:78–90. https://doi.org/10.1016/j.chroma.2016.04.006.

2.10 SUPPLEMENTAL MATERIAL

Supplemental Table 2.1: Minimum inhibitory concentration (MIC) values of different β-lactam antibiotics against MBL-producing *E. coli* BW25113. All 19 MBL genes were cloned into the pGDP2 vector. *E. coli* BW25113 containing the pGDP2 plasmid, but no MBL gene was used as a control. All MIC assays were conducted in duplicate.

MBL	Minimum Inhibitory Concentration (μg/mL)					
	Meropenem	**Doripenem**	**Ertapenem**	**Imipenem**	**Cefotaxime**	**Ampicillin**
None	0.06	0.03	0.03	0.25–0.50	0.06	4
NDM-1	32	32	> 64	16	> 64	> 64
NDM-4	64	64	> 64	> 64	> 64	> 64
NDM-5	64	64	> 64	32	> 64	> 64
NDM-6	64	32	> 64	64	> 64	> 64
NDM-7	64	32	> 64	32	> 64	> 64
VIM-1	32	8–16	16	8–16	> 64	> 64
VIM-2	16	8	16–32	16	> 64	> 64
VIM-7	32	8	64	64	64	> 64
CAM-1	8	16	16	32	> 64	> 64
DIM-1	16	16	32	4	> 64	> 64
IND-1	16	8–16	32	64	> 64	> 64
GIM-1	16	8	64	4	> 64	> 64
IMP-1	16	8	32	16–32	64	> 64
IMP-7	16	8	32	4	> 64	> 64
IMP-27	32	32	64	4	> 64	16
SPM-1	32	16	64	16–32	> 64	> 64
CphA2	16–32	16–32	> 64	8–16	≤ 0.50	4–8
L1	16	16	16–32	4–8	1	> 64
AIM-1	32	16	> 64	64	64	> 64

Supplemental Table 2.2: Minimum inhibitory concentration (MIC) values of different β-lactam antibiotics against MBL-producing *K. pneumoniae* ATCC 33495. All 8 MBL genes were cloned into the pGDP2 vector. *K. pneumoniae* ATCC 33495 containing the pGDP2 plasmid, but no MBL gene was used as a control. All MIC assays were conducted in duplicate.

MBL	Minimum Inhibitory Concentration (μg/mL)					
	Meropenem	**Doripenem**	**Ertapenem**	**Imipenem**	**Cefotaxime**	**Ampicillin**
None	0.06	0.06–0.13	0.06	1	0.13	64
NDM-1	> 64	> 64	> 64	64	> 64	> 64
NDM-4	> 64	> 64	> 64	> 64	> 64	> 64
NDM-5	> 64	> 64	> 64	32	> 64	> 64
NDM-6	> 64	> 64	> 64	64	> 64	> 64
VIM-2	64	32	> 64	>64	> 64	> 64
IMP-7	32	32	32–64	8–16	> 64	> 64
CphA2	> 64	> 64	> 64	> 64	≤ 0.50	64
AIM-1	> 64	64	> 64	> 64	> 64	> 64

Supplemental Table 2.3: Minimum inhibitory concentration (MIC) values of different β-lactam antibiotics against MBL-producing *E. coli* BW25113 Δ*bamB*Δ*tolC*. All 8 MBL genes were cloned into the pGDP2 vector. *E. coli* BW25113 Δ*bamB*Δ*tolC* containing the pGDP2 plasmid, but no MBL gene was used as a control. All MIC assays were conducted in duplicate.

MBL	Minimum Inhibitory Concentration (μg/mL)		
	Meropenem	**Doripenem**	**Ampicillin**
None	0.06	0.06	0.50
NDM-1	32	64	> 64
NDM-4	64	> 64	> 64
NDM-5	64	32	> 64
NDM-6	64	64	> 64
VIM-2	16	8	> 64
IMP-7	16	16	> 64
CphA2	32	16	2
AIM-1	64	32	> 64

Supplemental Table 2.4: Concentration of AMA needed to restore the activity of different β-lactam antibiotics to their EUCAST susceptibility breakpoint concentration in MBL-producing *E. coli* BW25113. All 19 MBL genes were cloned into the pGDP2 vector. All bioassays were conducted in duplicate. This table shows the results from replicate 2.

MBL	[AMA] at the Susceptibility Breakpoint of the Antibiotic (μg/mL) [a]					
	Meropenem	**Doripenem**	**Ertapenem**	**Imipenem**	**Cefotaxime**	**Ampicillin**
NDM-1	8	12	16	12	64	64
NDM-4	16	16	64	16	> 64	> 64
NDM-5	12	24	64	16	> 64	> 64
NDM-6	16	16	32	12	64	> 64
NDM-7	16	24	64	24	> 64	> 64
VIM-1	8	8	12	12	24	64
VIM-2	8	8	8	8	12	16
VIM-7	8	8	8	8	8	12
CAM-1	4	12	8	8	24	> 64
DIM-1	12	12	16	4	24	64
IND-1	8	8	12	12	24	> 64
GIM-1	12	8	32	8	> 64	> 64
IMP-1	16	12	64	24	> 64	64
IMP-7	24	12	> 64	16	> 64	32
IMP-27	32	24	> 64	≤ 0.5	> 64	12
SPM-1	12	24	64	12	> 64	> 64
CphA2	> 64	64	> 64	> 64	≤ 0.5	≤ 0.5
L1	12	12	24	8	≤ 0.5	> 64
AIM-1	64	64	> 64	24	> 64	> 64

[a] The EUCAST susceptibility breakpoint concentrations for meropenem, doripenem, ertapenem, imipenem, cefotaxime and ampicillin are 2, 1, 0.5, 2, 1 and 8 μg/mL, respectively.

Supplemental Table 2.5: Concentration of AMA needed to restore the activity of different β-lactam antibiotics to their EUCAST susceptibility breakpoint concentration in MBL-producing *K. pneumoniae* ATCC 33495. All 8 MBL genes were cloned into the pGDP2 vector. All bioassays were conducted in duplicate. This table shows the results from replicate 2.

MBL	[AMA] at the Susceptibility Breakpoint of the Antibiotic (μg/mL) [a]					
	Meropenem	**Doripenem**	**Ertapenem**	**Imipenem**	**Cefotaxime**	**Ampicillin**
NDM-1	12	16	24	12	64	> 64
NDM-4	16	24	64	24	> 64	> 64
NDM-5	16	24	64	24	> 64	> 64
NDM-6	12	16	64	24	> 64	> 64
VIM-2	8	8	8	12	16	> 64
IMP-7	32	24	> 64	64	> 64	> 64
CphA2	> 64	> 64	> 64	> 64	≤ 0.5	> 64
AIM-1	64	64	> 64	> 64	> 64	> 64

[a] The EUCAST susceptibility breakpoint concentrations for meropenem, doripenem, ertapenem, imipenem, cefotaxime and ampicillin are 2, 1, 0.5, 2, 1 and 8 μg/mL, respectively.

Supplemental Table 2.6: Concentration of AMA needed to restore the activity of different β-lactam antibiotics to their EUCAST susceptibility breakpoint concentration in MBL-producing *E. coli* BW25113 Δ*bamB*Δ*tolC*. All 8 MBL genes were cloned into the pGDP2 vector. All bioassays were conducted in duplicate. This table shows the results from replicate 2.

MBL	[AMA] at the Susceptibility Breakpoint of the Antibiotic (μg/mL) [a]		
	Meropenem	**Doripenem**	**Ampicillin**
NDM-1	8	12	32
NDM-4	16	24	> 64
NDM-5	16	16	> 64
NDM-6	16	24	> 64
VIM-2	8	8	24
IMP-7	24	24	> 64
CphA2	> 64	> 64	≤ 0.5
AIM-1	64	64	> 64

[a] The EUCAST susceptibility breakpoint concentrations for meropenem, doripenem and ampicillin are 2, 1 and 8 μg/mL, respectively.

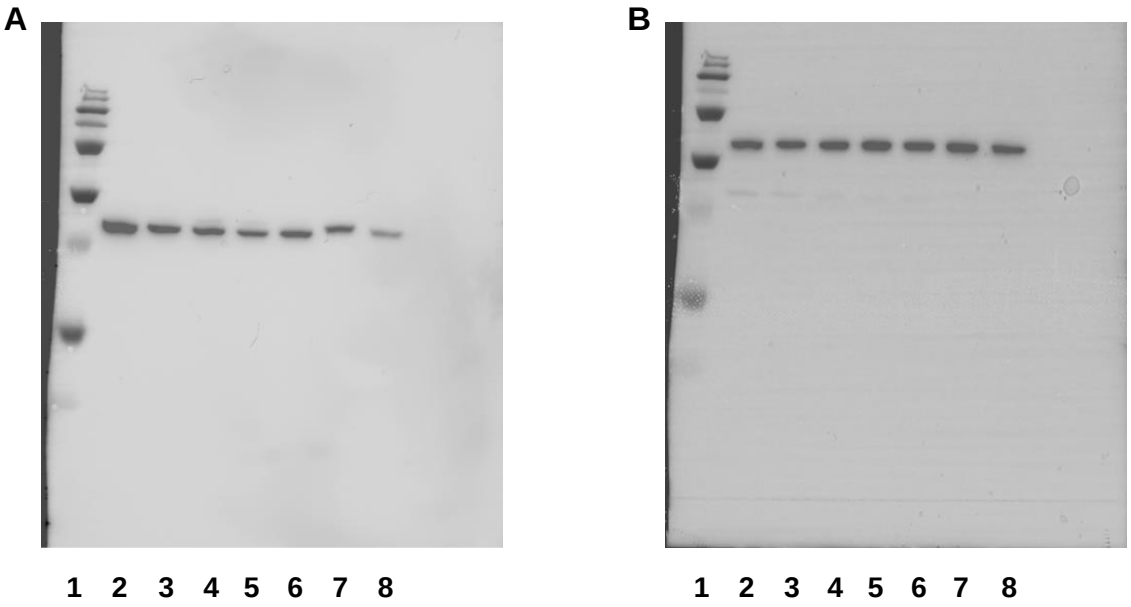

Supplemental Figure 2.1: Protein expression levels of MBL enzymes in *E. coli* BW25113. The Western blot was conducted as described in the Materials and Methods section. The antibodies used to probe the Western blot were a) mouse-derived anti-FLAG antibodies conjugated to HRP, and b) mouse-derived anti-RpoA antibodies and anti-mouse IgG antibodies conjugated to HRP. Lane 1: PageRuler Prestained Protein Ladder, lane 2: NDM-1, lane 3: NDM-4, lane 4: NDM-5, lane 5: NDM-6, lane 6: NDM-7, lane 7: VIM-2, lane 8: IMP-7.

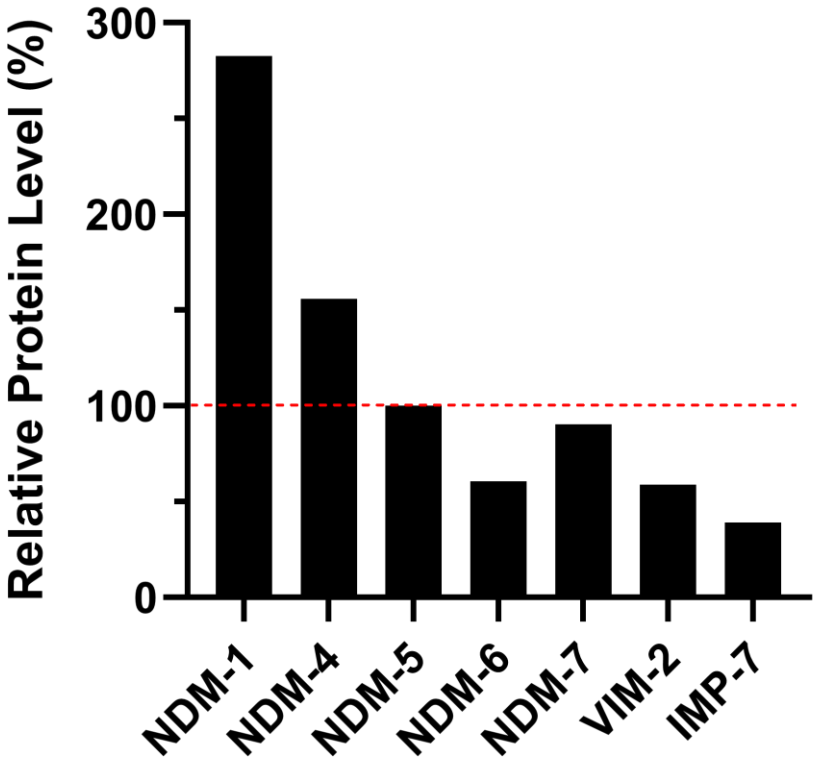

Supplemental Figure 2.2: Relative protein expression levels of MBL enzymes in *E. coli* BW25113. Proteins expression levels were detected using a Western blot probed with mouse-derived anti-FLAG antibodies conjugated to HRP. The Western blot was conducted as described in the Materials and Methods section. Antibodies targeting RpoA served as loading controls. Protein band intensities were quantified using Image Lab. These results were then plotted and analyzed using GraphPad Prism 8. The protein expression levels of the MBL enzymes are shown in relation to NDM-5.

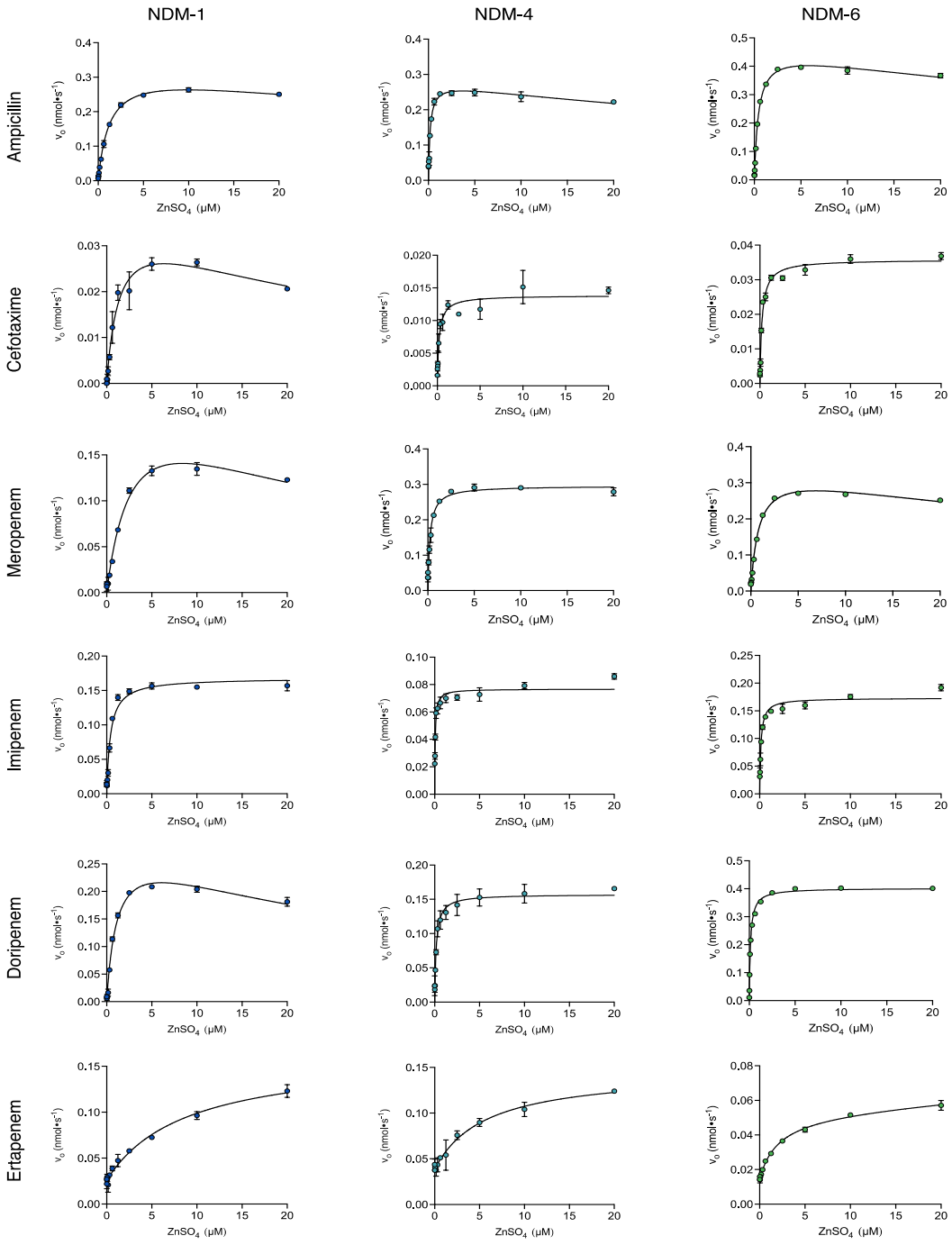

Supplemental Figure 2.3: Zinc-dependence of MBL-catalyzed hydrolysis of β-lactam antibiotics. Kinetic analysis of each MBL and substrate used the initial rates of reaction of enzyme (4–10 nM) in Chelex-treated 25 mM HEPES:NaOH buffer (pH 7.5) with 100 nM AMA at 25°C. Reaction mixtures contained saturating substrate concentrations (0.25–0.5 mM) and included varying amounts of $ZnSO_4$ (0.0007, 0.0015, 0.03, 0.15, 0.31, 0.62, 1.2, 2.5, 5, 10, 20 μM). Nonlinear regression analysis was performed using GraphPad Prism 8.

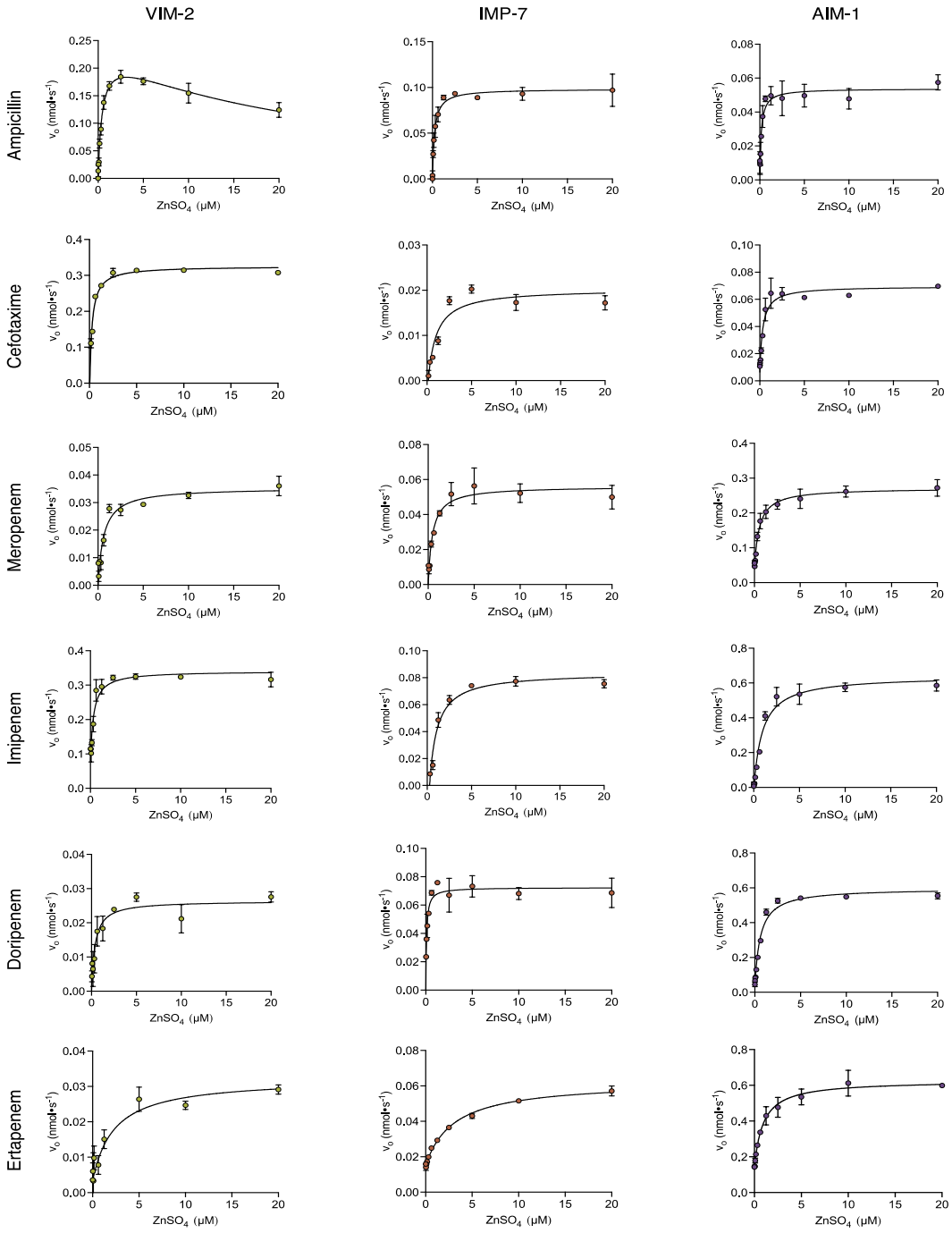

Supplemental Figure 2.3: Continued.

Supplemental Table 2.7: Sequences of the primers used to create the NDM variants by site-directed mutagenesis. The changed nucleotide is indicated in red in the primer sequence. The restriction enzyme recognition sites are underlined in the primer sequence.

Primer Name	Primer Sequence
NDM FWD	5′–TACCCTCATATGGAATTGCCCAATATTATGCACC–3′
NDM REV	5′–TACCCTAAGCTTTCAGCGCAGCTTGTCGGC–3′
V88L FWD	5′– CCGCGTGCTGTTGGTCGATACCGCCTG –3′
V88L FWD	5′– TATCGACCAACAGCACGCGGCCGCCATC–3′
D130N FWD	5′–GCGGTATGAACGCGCTGCATGCG–3′
D130N REV	5′–GCAGCGCGTTCATACCGCCCATCTTG–3′
M154L FWD	5′–AAGAGGGGCTGGTTGCGCCGCAAC–3′
M154L REV	5′–GCAACCAGCCCCTCTTGCGGGGCAAG–3′
A233V FWD	5′–CGCGTCAGTGCGCGCGTTTGGTG–3′
A233V REV	5′–ACGCGCGCACTGACGCGGCGTAG–3′

Supplemental Table 2.8: Sequences of the primers used to create the overexpression constructs and the FLAG-tagged MBL genes. The forward primers for the overexpression constructs were used to remove the signal peptide of the MBL genes to allow for cytoplasmic expression. The FLAG reverse primers were used to remove the stop codon from the MBL genes to allow the insertion of the C-terminal FLAG-tag. The primers created for NDM-1 could also be used for NDM-4, NDM-5, NDM-6 and NDM-7 since all of these NDM genes share identical sequences at the binding site for the forward and reverse primers. The restriction enzyme recognition sites are underlined in the primer sequence.

Primer Name	Sequence of Primer
NDM-1 FWD	5′–TACACGTGGTCTCCAGGTATGGGTGAAATCCGCCCGAC–3′
NDM-1 REV	5′–TACCCTAAGCTTTCAGCGCAGCTTGTCGGC–3′
VIM-2 FWD	5′–ATTAACATATGGTAGATTCTAGCGGTGAGTATCCGACAGT–3′
VIM-2 REV	5′–TATATGCTAGCCTACTCAACGACTGAGCGATTTGTGTG–3′
IMP-7 FWD	5′–TATATGCTAGCATGGAGGCTTTGCCAGATTTAAAAATTG–3′
IMP-7 REV	5′–TTATTCTCGAGTTAGTTACTTGGTTTTGATAGCTTTTTACT–3′
AIM-1 FWD	5′–TATAGACATATGTCCGATGCACCAGCGAGTCGTG–3′
AIM-1 REV	5′–TATAGACTCGAGTCAAGGGCGCGCACCAGATG–3′
NDM-1 FLAG FWD	5′–GATGACGACAAGTGAAAGCTTGCGGCCGCA–3′
NDM-1 FLAG REV	5′–GTCTTTGTAGTCGCGCAGCTTGTCGGCCAT–3′
VIM-2 FLAG FWD	5′–GATGACGACAAGTAACTCGAGCACCACCAC–3′
VIM-2 FLAG REV	5′–GTCTTTGTAGTCCTCAACGACTGAGCGATT–3′
IMP-7 FLAG FWD	5′–GATGACGACAAGTAACTCGAGCACCACCAC–3′
IMP-7 FLAG REV	5′–GTCTTTGTAGTCGTTACTTGGTTTTGATAG–3′

Supplemental Table 2.9: Retention time, collision energies and parent-daughter ion transitions for AMA and the different β-lactam antibiotics.

β-Lactam Antibiotic	Retention Time (min)	Parent $[M+H]^+$	Daughter $[M+H]^+$	Collision Energy (eV)
Bn-AMA [a]	2.85	412.1351	192.0655	24
Meropenem	2.82	384.1581	68.0511	40
Doripenem	2.27	421.1213	274.0671	20
Imipenem	1.09	300.1028	98.0068	40
Ertapenem	3.21	476.1498	432.1594	10
Cefotaxime	3.30	456.0657	125.0064	40
Ampicillin	3.11	350.1173	106.0827	10

[a] For AMA detection, samples were derivatized with benzoyl chloride to produce N-benzoyl AMA.

CHAPTER 3: Exploring the efficacy of AMA/meropenem combination therapy with and without avibactam against bacterial strains producing multiple β-lactamases

3.1 PREFACE

I performed all the experiments described in this chapter. None of this research has been published in any form.

3.2 ABSTRACT

The effectiveness of β-lactam antibiotics is being increasingly threatened by resistant bacteria that harbour hydrolytic β-lactamase enzymes. Depending on the class of β-lactamase present, β-lactam hydrolysis can occur through one of two distinct general molecular mechanisms. Metallo-β-lactamases (MBLs) require active site Zn^{2+} ions, while serine-β-lactamases (SBLs) deploy a catalytic serine residue. The result in both cases is drug inactivation via the opening of the β-lactam warhead of the antibiotic. MBLs confer resistance to most β-lactams and are insensitive to SBL inhibitors, including recently approved diazabicyclooctanes such as avibactam; consequently, these enzymes represent a growing threat to public health. Aspergillomarasmine A (AMA), a fungal natural product, can rescue the activity of the β-lactam antibiotic meropenem against MBL-expressing bacterial strains. However, the effectiveness of this β-lactam/β-lactamase inhibitor combination against bacteria producing multiple β-lactamases remains unknown. We systematically investigated the efficacy of AMA/meropenem combination therapy with and without avibactam against 10 *Escherichia coli*, and 10 *Klebsiella pneumoniae* laboratory strains tandemly expressing single MBL and SBL enzymes. Cell-based assays demonstrated that laboratory strains producing NDM-1 and KPC-2 were resistant to the AMA/meropenem combination but became drug-sensitive upon adding avibactam. We also probed these combinations against a panel of 30 clinical isolates expressing multiple β-lactamases. *E. coli*, *Enterobacter cloacae* and *K. pneumoniae* clinical isolates were more susceptible to AMA, avibactam and meropenem than *Pseudomonas aeruginosa* and *Acinetobacter baumannii* isolates. Overall, the results

suggested that a triple combination of AMA/avibactam/meropenem would be effective for empirical treatment of infections caused by multiple β-lactamase-producing bacteria, especially those from the order Enterobacterales.

3.3 INTRODUCTION

With the widespread misuse and overuse of antibiotics, bacterial resistance mechanisms readily spread among pathogens [1,2]. Consequently, many bacteria now demonstrate resistance to multiple antibiotics [3,4]. These multidrug-resistant (MDR) pathogens threaten the effectiveness of antibiotics, such as β-lactams, resulting in one of the biggest threats to public health in the 21st century [5]. Consequently, there is an urgent need to preserve the activity of existing antibiotics to circumvent the threat posed by MDR bacteria.

The predominant resistance mechanism to β-lactams is enzymatic inactivation by enzymes known as β-lactamases. These enzymes are divided into four classes based on their sequence identity and mechanism of action. β-Lactamases utilize either an active site serine residue (class A, C, and D serine-β-lactamases) or active site Zn^{2+} ions (class B metallo-β-lactamases) to inactivate β-lactams by hydrolyzing the β-lactam warhead essential to their activity [1,6]. An increasing number of bacteria contain multiple β-lactamases from different classes [7,8]. Therefore, combination therapy, which employs two or more antibiotics and/or resistance inhibitors to target these β-lactamase-producing bacteria, is gaining popularity in the recovery of the activity of β-lactam antibiotics. A significant advantage of this approach is synergy, where the combined effect of two or more antibiotics and/or inhibitors is greater than the sum of their individual activities

[4,9]. Given the rise of MDR strains and the growing diversity of β-lactamases, the discovery of a combination therapy that targets bacteria producing β-lactamases from all four classes would be the most advantageous.

Several serine-β-lactamase (SBL) inhibitors have been developed for clinical use (e.g., avibactam, vaborbactam, clavulanic acid) in fixed-dose combinations with various β-lactams [10,11]. However, metallo-β-lactamases (MBLs) remain a clinical challenge due to their insensitivity to approved SBL inhibitors and their ability to hydrolyze most β-lactam antibiotics [12,13]. Aspergillomarasmine A (AMA) is a natural product synthesized by *Aspergillus versicolor* that inhibits clinically relevant MBLs, including NDM-1 and VIM-2 [14]. Although exhibiting no antimicrobial activity itself, AMA restores the activity of the β-lactam meropenem against Enterobacteriaceae, *Acinetobacter*, and *Pseudomonas* isolates, producing either NDM-1 or VIM-2 [14]. Furthermore, we recently demonstrated that the inhibitory potency of AMA was enhanced when paired with carbapenems such as meropenem [15].

While AMA offers a means to mitigate the presence of MBLs, given the growing number of MDR isolates expressing both MBLs and SBLs, the addition of an SBL inhibitor provides a strategy to expand the effectiveness of an AMA/meropenem combination therapy. This study used isogenic *Escherichia coli* and *Klebsiella pneumoniae* laboratory strains expressing individual MBL and SBL genes together with MDR clinical isolates to evaluate the AMA/meropenem pairing efficacy. The inhibitory potency of different AMA/β-lactam combinations was also explored in the presence of avibactam, which can inhibit several SBL enzymes [16]. The resulting data provide a

road map to study the effect of combining MBL and SBL inhibitors in treating infections caused by bacteria producing multiple β-lactamases.

3.4 RESULTS

3.4.1 Construction of tandem β-lactamase gene expression plasmids

We previously determined that AMA can rescue meropenem activity in MBL-producing bacteria [14,15]. However, the efficiency of an AMA/meropenem combination against bacterial strains producing multiple β-lactamases remains unknown. To investigate this activity, one MBL (NDM-1) and one SBL (KPC-2) were cloned into the low-copy number plasmid pGDP2 in tandem, creating NDM-1/KPC-2 and KPC-2/NDM-1 ordered constructs [17]. These plasmids contained a P_{Lac} promoter upstream of both genes (Supplemental Figure 3.1). Once transformed into *E. coli* BW25113, minimum inhibitory concentration (MIC) assays for different β-lactam antibiotics were conducted to investigate gene expression.

Under individual promoter control, the NDM-1/KPC-2 and KPC-2/NDM-1 constructs had identical meropenem, piperacillin, cefepime and cefaclor MIC values and similar doripenem and cefotaxime MIC values (Supplemental Table 3.1). These results are consistent with the observation that these two β-lactamase enzymes confer resistance to these antibiotics (Supplemental Table 3.2). To determine if the genes were being expressed equally in the constructs, we evaluated the MIC for aztreonam, which is known to be susceptible to KPC-2 but not NDM-1 (Supplemental Table 3.2). The NDM-1/KPC-2 and KPC-2/NDM-1 constructs demonstrated respective aztreonam MIC values of 128 μg/mL and 256 μg/mL, indicating similar KPC expression (Supplemental Table 3.1).

Table 3.1: Concentration of AMA needed to restore the activity of different β-lactam antibiotics to their susceptibility breakpoint concentration against *E. coli* BW25113 strains producing one MBL and one SBL.[a] Genes from class A are shown in blue, while genes from class B, class C, and class D are depicted in black, pink, and green. All assays were conducted in duplicate. This table shows the results from replicate 1.

β-Lactamase		[AMA] at the susceptibility breakpoint of the antibiotics in different combinations (μg/mL) [b, c]								
Gene 1	**Gene 2**	**AMA/ MEM**	**AVI/ MEM**	**AMA/AVI/ MEM**	**AMA/AVI/ DOR**	**AMA/AVI/ PIP**	**AMA/AVI/ AMP**	**AMA/AVI/ CTX**	**AMA/AVI/ FEP**	**AMA/AVI/ CEC**
NDM-1	KPC-2	> 32	16	8	8	16	> 32	32	16	> 32
KPC-2	NDM-1	> 32	16	8	8	16	> 32	32	16	> 32
NDM-1	CTX-M-15	8	16	8	8	16	> 32	32	16	> 32
CTX-M-15	NDM-1	16	16	8	8	16	> 32	32	16	> 32
NDM-1	CMY-2	16	16	8	8	16	> 32	32	16	> 32
CMY-2	NDM-1	16	16	8	8	16	> 32	32	16	> 32
NDM-1	OXA-23	16	16	16	16	32	> 32	32	16	> 32
OXA-23	NDM-1	16	16	16	16	32	> 32	32	16	> 32
NDM-1	OXA-48	16	16	8	16	16	> 32	32	16	> 32
OXA-48	NDM-1	16	16	8	16	16	> 32	32	16	> 32

Abbreviations: AMA aspergillomarasmine A, AVI avibactam, MEM meropenem, DOR doripenem, PIP piperacillin, AMP ampicillin, CTX cefotaxime, FEP cefepime, CEC cefaclor.

[a] Both β-lactamase genes were cloned into pGDP2 with individual promoters.

[b] The EUCAST susceptibility breakpoint concentrations for MEM, DOR, PIP, AMP, CTX, FEP and CEC are 2, 1, 8, 8, 1, 1 and 1 μg/mL.

[c] AVI was maintained at 4 μg/mL, except during the AVI/MEM combination.

3.4.2 Inhibition of multiple β-lactamases by the AMA/meropenem combination is dependent on β-lactamase class and carbapenemase activity

We previously demonstrated that the MBL inhibitory potency of AMA varied with the β-lactam partner and that the optimal antibiotic was a carbapenem such as meropenem [15]. To follow up on this finding, we sought to determine the efficacy of an AMA/meropenem combination against 10 *E. coli* BW25113 and 10 *K. pneumoniae* ATCC 33495 strains producing one MBL and one SBL. These included common β-lactamases from each class, such as KPC-2 and CTX-M-15 (class A), NDM-1 (class B), CMY-2 (class C), and OXA-48 (class D) [18–22]. In addition, certain strains were designed to produce OXA-23, which is among the most frequently isolated carbapenem-hydrolyzing class D β-lactamase and a predominant cause of carbapenem resistance in *A. baumannii* isolates worldwide [23].

Most *E. coli* and *K. pneumoniae* strains required an AMA concentration of 8–16 μg/mL to restore the activity of meropenem to its susceptibility breakpoint (Tables 3.1, 3.2 and Supplemental Tables 3.3, 3.4). The NDM-1/KPC-2 and KPC-2/NDM-1 constructs demonstrated the highest resistance level, requiring a concentration of AMA of > 32 μg/mL to restore susceptibility to meropenem (Tables 3.1, 3.2 and Supplemental Tables 3.3, 3.4), consistent with the carbapenemase activity of KPC-2 (Supplemental Table 3.2). Furthermore, OXA-23 and OXA-48 showed little to no activity against meropenem and doripenem when produced by *E. coli* BW25113 (Supplemental Table 3.2) and had only modest resistance in *K. pneumoniae* (Supplemental Table 3.5). Singkham-in et al. have reported that carbapenem susceptibility varied between different

K. pneumoniae isolates in a strain-specific manner partially related to gene expression levels [24]. Overall, the results demonstrated that strains expressing SBL carbapenemases (e.g., KPC-2) are resistant to the AMA/meropenem combination and may also require the presence of an SBL inhibitor (e.g., avibactam) to alleviate β-lactam resistance.

Table 3.2: Concentration of AMA needed to restore the activity of meropenem to its susceptibility breakpoint concentration against *K. pneumoniae* ATCC 33495 strains producing one MBL and one SBL.[a] Genes from class A are shown in blue, while genes from class B, class C, and class D are depicted in black, pink, and green. All assays were conducted in duplicate. This table shows the results from replicate 1.

β-Lactamase		**[AMA] at 2 µg/mL of MEM in different combinations (µg/mL)** [b, c]		
Gene 1	**Gene 2**	**AMA/ MEM**	**AVI/ MEM**	**AMA/AVI/ MEM**
NDM-1	KPC-2	> 64	> 64	8
KPC-2	NDM-1	> 64	> 64	8
NDM-1	CTX-M-15	16	> 64	16
CTX-M-15	NDM-1	16	> 64	16
NDM-1	CMY-2	8	> 64	8
CMY-2	NDM-1	8	> 64	8
NDM-1	OXA-23	16	> 64	16
OXA-23	NDM-1	16	> 64	16
NDM-1	OXA-48	8	> 64	16
OXA-48	NDM-1	16	> 64	16

Abbreviations: AMA aspergillomarasmine A, AVI avibactam, MEM meropenem.

[a] Both β-lactamase genes were cloned into pGDP2 with individual promoters.

[b] 2 µg/mL is the EUCAST susceptibility breakpoint concentration for MEM.

[c] AVI was maintained at 4 µg/mL, except during the AVI/MEM combination.

3.4.3 β-Lactamase inhibitors showed a greater inhibitory potency when combined with a carbapenem antibiotic

To determine the optimal AMA/avibactam/β-lactam combination, we partnered AMA and avibactam with two carbapenems (meropenem, doripenem), two penams (piperacillin, ampicillin), and three cephems (cefotaxime, cefepime, cefaclor). The inhibitory potency of these combinations was evaluated against 10 laboratory *E. coli* strains producing one MBL and one SBL. The results demonstrated that most *E. coli* strains required 8 µg/mL of AMA and 4 µg/mL of avibactam to restore susceptibility to both meropenem and doripenem (Table 3.1 and Supplemental Table 3.3). For strains producing either NDM-1/KPC-2 or KPC-2/NDM-1, this is an improvement over the AMA/meropenem combination, where resistance to meropenem was observed even at 32 µg/mL of AMA. Furthermore, most strains generally become resensitized to piperacillin and cefepime at 16 µg/mL of AMA and 4 µg/mL of avibactam (Table 3.1 and Supplemental Table 3.3). However, > 32 µg/mL of AMA and 4 µg/mL of avibactam were necessary to restore susceptibility to ampicillin and cefaclor (Table 3.1 and Supplemental Table 3.3). The wild-type *E. coli* BW25113 strain encodes a chromosomal cephalosporinase (AmpC). Therefore, these results are consistent with carbapenems, piperacillin, cefepime and cefotaxime being poor substrates for AmpC while ampicillin and older cephalosporins are susceptible to hydrolysis by this β-lactamase [25]. Overall, the results indicated that AMA and avibactam achieved the greatest inhibitory potency when combined with a carbapenem antibiotic such as meropenem.

Table 3.3: Concentration of AMA needed to restore the activity of meropenem to its susceptibility breakpoint concentration in combination with and without avibactam against clinical strains producing multiple β-lactamases. Genes from class A are shown in blue, while genes from class B, class C, and class D are depicted in black, pink, and green. All assays were conducted in duplicate. This table shows the results from replicate 1.

Strain	β-Lactamases			[AMA] at 2 µg/mL of MEM (µg/mL) [a, b]		
				AMA/ MEM	AVI/ MEM	AMA/AVI/ MEM
Acinetobacter baumannii B1NG08a	NDM-1	OXA-23	OXA-69	> 64	> 64	> 64
Citrobacter freundii GN978	TEM-1 NDM-1 OXA-1	CTX-M-15 CMY-6	CMY-46 CMY-18	8	> 64	8
Enterobacter cloacae 36749	NDM-1 ACT-25	TEM-171	OXA-1	8	16	8
Enterobacter cloacae 47219	ACT-17 LAP-2	NDM-1 TEM-1	OXA-1	8	32	16
Enterobacter cloacae 86502	ACT-17 OXA-1	TEM-1 VIM-1	CTX-M-15	8	32	16
Enterobacter cloacae 397260	ACT-17	VIM-1		8	32	8
Enterobacter cloacae GN574	TEM-1 OXA-1	NDM-1 ACT-17	CTX-M-15	16	> 64	16
Enterobacter cloacae GN579	CTX-M-15 ACT-25	TEM-1 OXA-1	NDM-1	16	32	8
Enterobacter cloacae GN687	NDM-1 TEM-1	OXA-9 ACT-25	CTX-M-15	16	> 64	16
Escherichia coli 130392-1	TEM-1 CMY-83	NDM-5	CMY-42	32	32	32
Escherichia coli 376762	NDM-5 TEM-1	CTX-M-15 AmpC	OXA-1 AmpC1	32	8	32
Escherichia coli 376948	AmpC1 AmpC	NDM-5	TEM-1	32	8	> 64
Escherichia coli 387039	NDM-5 AmpC1	OXA-181 CMY-2	AmpC OXA-1	> 64	64	64
Escherichia coli GN610	CTX-M-15 NDM-1 OXA-1	TEM-166 CMY-6	OXA-2 AmpC	> 64	16	16
Escherichia coli GN688	CTX-M-15 OXA-1	TEM-1 AmpC	NDM-1	16	8	8

Table 3.3: Continued.

Strain	β-Lactamases			[AMA] at 2 µg/mL of MEM (µg/mL) [a, b]		
				AMA/ MEM	AVI/ MEM	AMA/AVI/ MEM
Klebsiella oxytoca GN942	NDM-1 OXA-9	CTX-M-15 OXY-2-8	TEM-1	8	32	8
Klebsiella pneumoniae 86500	SHV-11 NDM-5	CTX-M-15 OXA-1	OXA-232 TEM-1	> 64	> 64	64
Klebsiella pneumoniae 110027	CTX-M-14 OXA-48 OXA-9	NDM-1 SHV-1	CTX-M-15 TEM-1	> 64	> 64	16
Klebsiella pneumoniae 130392-2	DHA-1 OXA-232 OXA-9	SHV-27 CTX-M-15 CMY-42	NDM-1 TEM-183	16	64	16
Klebsiella pneumoniae 420322	SHV-1 CTX-M-15	OXA-181 OXA-1	NDM-5 TEM-1	> 64	> 64	64
Klebsiella pneumoniae GN529	TEM-1 SHV-144	NDM-1 OXA-1	CTX-M-15 SHV-66	8	> 64	8
Klebsiella pneumoniae GN629	SHV-11 DHA-7	CTX-M-15 OXA-1	NDM-1	16	> 64	16
Klebsiella pneumoniae N11-0306	CTX-M-15 OXA-1	SHV-11 DHA-7	NDM-1	16	> 64	16
Klebsiella pneumoniae N11-2218	NDM-1 SHV-83	CTX-M-15 SHV-144	CMY-6 SHV-11	8	> 64	8
Morganella morganii GN575	CTX-M-15	NDM-1	DHA-1	8	> 64	8
Providencia rettgeri GN570	NDM-1 CMY-6	VEB-1a OXA-1	TEM-1	64	> 64	16
Providencia stuartii GN576	CMY-2	NDM-1		8	> 64	8
Pseudomonas aeruginosa 411090	NDM-1 PDC-3	VEB-9 OXA-50	OXA-10	> 64	> 64	> 64
Pseudomonas aeruginosa H1010805	VIM-2			> 64	> 64	> 64
Pseudomonas aeruginosa H1010812	IMP-7	PDC-7	OXA-485	> 64	> 64	> 64

Abbreviations: AMA aspergillomarasmine A, AVI avibactam, MEM meropenem.

[a] 2 µg/mL is the EUCAST susceptibility breakpoint concentration for MEM.

[b] AVI was maintained at 4 µg/mL, except during the AVI/MEM combination.

3.4.4 The efficacy of the AMA/avibactam/meropenem combination depends on the class of β-lactamase and the bacterial order

The meropenem concentration chosen to evaluate the effectiveness of AMA and avibactam was 2 μg/mL because this concentration represents the European Committee on Antimicrobial Susceptibility Testing (EUCAST) susceptibility breakpoint of meropenem [26]. These AMA/avibactam/meropenem potentiation assays were then evaluated against 10 *K. pneumoniae* ATCC 33495 strains producing one MBL and one SBL. Similar to the results against *E. coli*, all *K. pneumoniae* strains were resensitized to meropenem at 8–16 μg/mL of AMA and 4 μg/mL of avibactam (Table 3.2 and Supplemental Table 3.4). However, more variability in the effectiveness of the AMA/avibactam/meropenem combination was observed when tested against 30 MDR clinical strains.

Several clinical strains became susceptible to meropenem at 8–16 μg/mL of AMA and 4 μg/mL of avibactam (Table 3.3 and Supplemental Table 3.6). The results were similar whether these strains produced seven different β-lactamases (CTX-M-15, TEM-166, OXA-2, NDM-1, CMY-6, AmpC, OXA-1) such as *E. coli* GN610 or just two β-lactamases (ACT-17, VIM-1) such as *E. cloacae* 397260. If no β-lactamases were being expressed, the AMA/avibactam/meropenem combination was not expected to have any effect on the antibiotic susceptibility of these clinical strains. In addition, the results demonstrated that the addition of avibactam to the AMA/meropenem combination generally increased inhibitory potency against strains producing multiple class D OXA β-lactamases but had minimal effect on strains producing β-lactamases solely from classes A–C. Furthermore, AMA/avibactam/meropenem was less effective against *P. aeruginosa*

isolates, requiring concentrations greater than 64 µg/mL of AMA and 4 µg/mL of avibactam to restore meropenem susceptibility, even if only VIM-2 was being produced (e.g., *P. aeruginosa* H1010812). In addition, *A. baumannii* B1NG08a showed a high level of resistance to the AMA/avibactam/meropenem combination (Table 3.3 and Supplemental Table 3.6) due to the production of OXA-23, a carbapenem-hydrolyzing class D β-lactamase, which is insensitive to AMA and avibactam [14,27]. Additional findings demonstrated that the efficacy of the AMA/avibactam/meropenem combination was not necessarily related to the initial degree of avibactam resistance for the strains. For example, *E. coli* GN688 and *P. rettgeri* GN570 conferred avibactam MIC values of 16 µg/mL and 1024 µg/mL. Yet, both strains were resensitized to meropenem with 16 µg/mL of AMA and 4 µg/mL of avibactam (Table 3.3 and Supplemental Tables 3.6, 3.7). Overall, the results indicated that the AMA/avibactam/meropenem combination was effective against Enterobacterales producing β-lactamases from classes A–D but lacked activity against *Pseudomonas* and *Acinetobacter* isolates.

3.5 DISCUSSION

While AMA has previously been shown to restore the activity of β-lactam antibiotics against MBL-expressing bacteria [14,15], many bacterial strains produce multiple β-lactamases from different classes [7,8]. Therefore, tandem β-lactamase pGDP2 expression vectors were constructed to explore the inhibitory potency of the AMA/avibactam/β-lactam antibiotic combinations against 10 *E. coli* and 10 *K. pneumoniae* laboratory strains producing one MBL (NDM-1) and one SBL (KPC-2, CTX-M-15, CMY-2, OXA-23, or OXA-48) enzyme.

Generating plasmids with a promoter upstream of both β-lactamase genes resulted in similar antibiograms, regardless of the position of the genes in the constructs (Supplemental Table 3.1). These results are consistent with previous studies which demonstrated that adding a second promoter allowed equal expression of two genes in the same plasmid [28]. The effectiveness of AMA and avibactam in combination with β-lactam antibiotics from three subclasses (penam, cephem, carbapenem) could then be determined against bacterial strains containing these plasmids. Consistent with our previous study, AMA and avibactam demonstrated the most significant inhibitory potency when paired with a carbapenem antibiotic such as meropenem or doripenem (Table 3.1 and Supplemental Table 3.3), possibly due to β-lactam antibiotics having varying affinities for their targets, the penicillin-binding proteins (PBPs) [15]. For example, carbapenems (e.g., meropenem and doripenem) are potent inhibitors of essential PBPs such as PBP2, which is important for bacterial cell shape and elongation [29,30]. Comparatively, ampicillin's bactericidal activity results from the inhibition of several non-essential PBPs [30].

Consistent with the mode of action of AMA, the AMA/meropenem combination demonstrated no activity in inhibiting SBL carbapenemases (e.g., KPC-2) in *E. coli* and *K. pneumoniae* laboratory strains [14]. However, in the presence of AMA and avibactam, the activity of meropenem was restored against all laboratory strains producing multiple β-lactamases (Tables 3.1, 3.2 and Supplemental Tables 3.3, 3.4). These results indicated that combining an MBL inhibitor and an SBL inhibitor can restore β-lactam susceptibility against bacterial strains producing multiple β-lactamases. In addition, the inhibitory

potency of the AMA/avibactam/meropenem combination did not appear to be pathogen-dependent for two representative Enterobacteriaceae laboratory strains.

The inhibitory potency of AMA, avibactam and meropenem was also explored against 30 MDR clinical isolates. Both the AMA/meropenem and AMA/avibactam/meropenem combinations were shown to be most effective against Enterobacterales isolates producing SBLs from classes A and C as well as NDM-1 (Table 3.3 and Supplemental Table 3.6). However, the AMA/meropenem combination was less effective against clinical isolates producing multiple class D OXA β-lactamases or NDM variants (e.g., NDM-5). Still, meropenem susceptibility generally increased upon adding avibactam to the combination. These results are consistent with previous studies demonstrating that AMA is a rapid and potent MBL inhibitor [14] while avibactam effectively inhibits class A, C, and some class D enzymes [27].

The AMA/meropenem and AMA/avibactam/meropenem combinations demonstrated little activity against *A. baumannii* and *P. aeruginosa* isolates regardless of their β-lactamase content (Table 3.3 and Supplemental Table 3.6). This observed resistance could reflect the notable level of intrinsic and acquired antibiotic resistance mechanisms in *P. aeruginosa* [31]. Furthermore, previous studies have shown that avibactam has little to no activity against carbapenem-hydrolyzing class D β-lactamases such as OXA-23, OXA-24/40, OXA-51, OXA-58 and OXA-143 [27,32], which are typically produced by *A. baumannii* [22,23]. Therefore, different SBL inhibitors may be required to alleviate *A. baumannii* and *P. aeruginosa* resistance. For example, both durlobactam and

taniborbactam have shown potent activity in clinical trials against MDR *Acinetobacter* spp. and carbapenem-resistant *P. aeruginosa*, respectively [27].

Overall, these results demonstrate that an AMA/avibactam/meropenem combination may have value in infections caused by Enterobacteriaceae producing class A, B and C β-lactamase enzymes. As MDR isolates are increasingly found to express many β-lactamases, higher-order combinations of antibiotics with β-lactamase inhibitors should be considered for further development to ensure adequate coverage of resistance mechanisms.

3.6 MATERIALS AND METHODS

3.6.1 Construction of pGDP2 vectors containing a promoter for each β-lactamase gene

The sequences of the β-lactamase genes were obtained from the Comprehensive Antibiotic Resistance Database (CARD) [33]. The pGDP2 plasmids containing a single β-lactamase gene were constructed as described previously [15]. These plasmids were then used as the foundation for cloning the second β-lactamase gene into the pGDP2 vectors. The construction of the pGDP2:NDM-1/KPC-2 (Supplemental Figure 3.1) began with the polymerase chain reaction (PCR) amplification of $bla_{\text{NDM-1}}$ from the pGDP2:NDM-1 plasmid using 5′–GCC AGC CTA GCC GGG AGA TCT–3′ as a forward primer and 5′–CCG TTG AGC ACC GCC GCC GCA GAA GGC CAT CCT GAC GGA TGG–3′ as the reverse primer. To facilitate gene expression in downstream experiments, the primers were designed to amplify the P_{Lac} promoter, the sequence of $bla_{\text{NDM-1}}$, and the rrnB T2 terminator from the template plasmid. In addition, the forward primer and the

reverse primer were engineered to amplify approximately 20 nucleotides upstream and downstream, respectively, of the BglII recognition site of the pGDP2 vector. Gibson assembly was then employed to insert the purified *bla*$_{NDM-1}$ DNA into a BglII digested pGDP2:KPC-2 plasmid following the guidelines specified by the manufacturer [34].

Following XbaI digestion, to quickly verify the insertion of the second gene, the purified plasmid was then transformed into chemically competent *E. coli* BW25113 or *K. pneumoniae* ATCC 33495 cells. Transformation into *K. pneumoniae* cells was conducted using the freeze-thaw transformation procedure described in reference [35]. The sequence of the plasmid was verified by Sanger sequencing. All other pGDP2 vectors containing two β-lactamase genes and two promoters were constructed as described above but using their respective β-lactamase genes.

3.6.2 Cell-based antimicrobial assays

All cell-based assays were conducted in 96-well round base micro test plates (Sarstedt, Nümbrecht, Germany) based on the protocol described in references [15,36]. Most compounds employed in these assays were dissolved in water. However, AMA was diluted in water containing ≤ 5% (v/v) ammonium hydroxide (NH_4OH), avibactam was dissolved in dimethyl sulfoxide (DMSO), and cefaclor was diluted in water containing 1 M hydrochloric acid (HCl). If water was used as a solvent, compounds were filter-sterilized before use.

For all the cell-based assays, a bacterial inoculum was prepared from the bacterial cells of interest using colonies picked from overnight plates whose optical density at 625 nm (OD_{625}) was adjusted to 0.08–0.10. Once the optimal OD_{625} was reached, a 200-fold

dilution of the inoculum in cation-adjusted Mueller Hinton II broth (CAMHB) was conducted before adding it to the micro test plate for a final assay volume of 100 µL.

For minimum inhibitory concentration (MIC) assays, ten two-fold dilutions of the β-lactam antibiotics or β-lactamase inhibitors (3.9–2000 ng/mL, 0.5–256 µg/mL or 8–4096 µg/mL) were added along the x-axis of the plate. Two columns were reserved for controls; one served as a growth control as it contained only bacterial inoculum, while the other was a sterility control containing only CAMHB. The MIC value was determined as the lowest concentration of β-lactam antibiotic or β-lactam inhibitor showing no bacterial growth.

Two-dimensional checkerboard assays were performed using AMA and meropenem or avibactam and meropenem. Briefly, two-fold dilutions of AMA (2–32 µg/mL for *E. coli* BW25113 strains and 0.5–64 µg/mL for all other strains) or avibactam (1–16 µg/mL for *E. coli* BW25113 strains and 0.5–64 µg/mL for all other strains) were added along the x-axis. Two-fold dilutions of meropenem (1–16 µg/mL for *E. coli* BW25113 strains and 0.5–64 µg/mL for all other strains) were then added along the y-axis of the plate. Four columns were reserved for controls; one contained two-fold dilutions of AMA or avibactam, one possessed two-fold dilutions of meropenem to verify MIC values, and the last two contained the bacterial inoculum and CAMHB to serve as growth and sterility controls. The efficacy of the combination was scored based on the minimum concentration of AMA or avibactam required to restore meropenem growth inhibition. According to the European Committee on Antimicrobial Susceptibility Testing (EUCAST), the susceptibility breakpoint concentration for meropenem is 2 µg/mL [26].

Potentiation assays were conducted with AMA, avibactam, and a β-lactam antibiotic. In brief, two-fold dilutions of AMA (2–32 µg/mL for *E. coli* BW25113 strains and 0.5–64 µg/mL for all other strains) were added along the x-axis of a plate while two-fold dilutions of avibactam (1–16 µg/mL for *E. coli* BW25113 strains and 0.5–64 µg/mL for all other strains) were added along the y-axis of the plate. The β-lactam antibiotic was added to both plate axes at its EUCAST susceptibility breakpoint concentration [26]. The susceptibility breakpoint concentrations for meropenem, doripenem, piperacillin, ampicillin, cefotaxime, cefepime and cefaclor were 2, 1, 8, 8, 1, 1 and 1 µg/mL, respectively. Four columns of the plates were reserved for controls; three contained two-fold dilutions of either AMA, avibactam, or the β-lactam antibiotic to verify MIC values, while one alternatively contained the bacterial inoculum and CAMHB to serve as growth and sterility controls. The efficacy of the combination was scored based on the concentration of AMA required to restore the activity of the different β-lactam antibiotics to their respective EUCAST susceptibility breakpoint concentration at 4 µg/mL of avibactam [26].

After a 16–20 h static incubation at 37°C, bioassay plates containing *E. coli* BW25113 were shaken for 5 min to resuspend the bacterial cells. However, bioassay plates containing all other strains were resuspended manually using a pipette to minimize the formation of aerosols. The bioassay plates were read spectrophotometrically at a wavelength of 600 nm using a BioTek Synergy H1 plate reader (BioTek, Winooski, VT). All cell-based assays were performed in duplicate.

3.6.3 Genomic DNA extraction

LB medium was inoculated with the appropriate clinical strain. The inoculated medium was incubated at 37°C in a shaking incubator for 16–20 h. Cells were harvested by centrifugation (10,000 × *g*, 3 min, room temperature) using a Fisher Scientific accuSpin Micro 17 microcentrifuge (Thermo Fisher Scientific, Waltham, MA). Cell pellets were resuspended in a combination of 180 µL of genomic digestion buffer [25 mM Tris-HCl, 2.5 mM EDTA, 1% (w/v) SDS, pH 8.0] and 20 µL of proteinase K (final concentration of 1–5 mg/mL). The resuspended cells were incubated at 55°C for 2 h with occasional mixing. The samples were supplemented with 20 µL of RNase A (final concentration of 1 mg/mL) and placed in a 37°C static incubator for 2 h. Following incubation, 200 µL of genomic lysis/binding buffer [30 mM Tris-HCl, 30 mM EDTA, 800 mM guanidine thiocyanate, 5% (v/v) Triton X-100, 5% (v/v) Tween 20, pH 8.0] was added, and the samples were mixed until a homogenous solution was obtained. A volume of 500 µL of phenol:chloroform:isoamyl alcohol (25:24:1) was then used to separate unwanted proteins and cellular debris from the genomic DNA. Following centrifugation (17,000 × *g*, 5 min, room temperature), the genomic DNA, located in the top aqueous layer, was removed, and placed in a new microcentrifuge tube. The phenol:chloroform:isoamyl alcohol extraction was repeated until there was no longer any white precipitate between the organic and aqueous phases. The genomic DNA was then supplemented with a 0.1 volume of 3 M sodium acetate (pH 5.2) and one volume of cold 2-propanol. The tube was then gently inverted until a precipitate could be seen. Following centrifugation (12,000 × *g*, 10 min, 4°C), the supernatant was removed, while ensuring that the precipitated DNA

remained undisturbed. The pellet was then washed with 1 mL of cold 70% (v/v) ethanol. The supernatant was removed after centrifugation (12,000 × *g*, 10 min, 4°C). This ethanol wash was repeated twice. The pellet was then allowed to air dry prior to being resuspended in 50 µL of Tris-EDTA buffer. The purity of the genomic DNA was analyzed using a NanoDrop Spectrophotometer (Thermo Fisher Scientific) and a 1.0% (w/v) agarose gel. The genomes of the clinical strains were then sequenced by Illumina sequencing. Following sequencing, the genomes of the clinical strains were assembled, and resistance genes were identified by analyzing the genome assemblies using the Resistance Gene Identifier from the CARD, where only perfect and strict hits were retained [33].

3.7 ACKNOWLEDGEMENTS

This research was funded by a Canadian Institutes of Health Research grant (FRN-148463) and a Canada Research Chair in Antibiotic Biochemistry (to Gerard D. Wright).

We thank Hamilton Health Sciences, Barbara Willey (Mount Sinai Hospital), Dr. Johann Pitout (University of Calgary), Dr. Michael Mulvey (Public Health Agency of Canada) and Dr. Roberto Melano (Public Health Ontario) for the clinical strains. We also thank Allison Guitor for preparing libraries and assembling genomes for the sequenced clinical strains.

3.8 REFERENCES

1. King, D.T., Sobhanifar, S., and Strynadka, N.C.J. (2016) One ring to rule them all: Current trends in combating bacterial resistance to the β-lactams. *Protein Sci.*, **25**: 787–803.

2. Blair, J.M.A., Webber, M.A., Baylay, A.J., Ogbolu, D.O., and Piddock, L.J.V. (2015) Molecular mechanisms of antibiotic resistance. *Nat. Rev. Microbiol.*, **13**: 42–51.

3. Shaw, E., Rombauts, A., Tubau, F., et al. (2018) Clinical outcomes after combination treatment with ceftazidime/avibactam and aztreonam for NDM-1/OXA-48/CTX-M-15-producing *Klebsiella pneumoniae* infection. *J. Antimicrob. Chemother.*, **73**: 1104–1106.

4. Gonzales, P.R., Pesesky, M.W., Bouley, R., et al. (2015) Synergistic, collaterally sensitive β-lactam combinations suppress resistance in MRSA. *Nat. Chem. Biol.*, **11**: 855–864.

5. Nikaido, H. (2009) Multidrug resistance in bacteria. *Annu. Rev. Biochem.*, **78**: 119–146.

6. Bebrone, C. (2007) Metallo-β-lactamases (classification, activity, genetic organization, structure, zinc coordination) and their superfamily. *Biochem. Pharmacol.*, **74**: 1686–1701.

7. Rawat, D. and Nair, D. (2010) Extended-spectrum β-lactamases in Gram Negative Bacteria. *J. Glob. Infect. Dis.*, **2**: 263–274.

8. Mhlongo, N., Essack, S., and Govinden, U. (2015) NDM-1, novel TEM-205, novel TEM-213 and other extended-spectrum β-lactamases co-expressed in isolates from cystic fibrosis patients from South Africa. *South. African J. Infect. Dis.*, **30**: 103–107.

9. Tamma, P.D., Cosgrove, S.E., and Maragakis, L.L. (2012) Combination Therapy for Treatment of Infections with Gram-Negative Bacteria. *Clin. Microbiol. Rev.*, **25**: 450–470.

10. Palzkill, T. (2013) Metallo-β-lactamase structure and function. *Ann. N. Y. Acad. Sci.*, **1277**: 91–104.

11. Bush, K. and Bradford, P.A. (2019) Interplay between β-lactamases and new β-lactamase inhibitors. *Nat. Rev. Microbiol.*, **17**: 295–306.

12. Rotondo, C.M. and Wright, G.D. (2017) Inhibitors of metallo-β-lactamases. *Curr.*

Opin. Microbiol., **39**: 96–105.

13. Tehrani, K.H.M.E. and Martin, N.I. (2018) β-lactam/β-lactamase inhibitor combinations: an update. *Med. Chem. Comm.*, **9**: 1439–1456.

14. King, A.M., Reid-Yu, S.A., Wang, W., et al. (2014) Aspergillomarasmine A overcomes metallo-β-lactamase antibiotic resistance. *Nature*, **510**: 503–506.

15. Rotondo, C.M., Sychantha, D., Koteva, K., and Wright, G.D. (2020) Suppression of *β*-Lactam Resistance by Aspergillomarasmine A Is Influenced by both the Metallo-*β*-Lactamase Target and the Antibiotic Partner. *Antimicrob. Agents Chemother.*, **64**: e01386-19.

16. Ehmann, D.E., Jahić, H., Ross, P.L., et al. (2013) Kinetics of Avibactam Inhibition against Class A, C, and D β-Lactamases. *J. Biol. Chem.*, **288**: 27960–27971.

17. Cox, G., Sieron, A., King, A.M., De Pascale, G., Pawlowski, A.C., Koteva, K., and Wright, G.D. (2017) A Common Platform for Antibiotic Dereplication and Adjuvant Discovery. *Cell Chem. Biol.*, **24**: 98–109.

18. Mehta, S.C., Rice, K., and Palzkill, T. (2015) Natural Variants of the KPC-2 Carbapenemase have Evolved Increased Catalytic Efficiency for Ceftazidime Hydrolysis at the Cost of Enzyme Stability. *PLoS Pathog.*, **11**: 1–20.

19. Poirel, L., Nordmann, P., Ducroz, S., Boulouis, H.J., Arné, P., and Millemann, Y. (2013) Extended-spectrum β-lactamase CTX-M-15-producing *Klebsiella pneumoniae* of sequence type ST274 in companion animals. *Antimicrob. Agents Chemother.*, **57**: 2372–2375.

20. Dortet, L., Poirel, L., and Nordmann, P. (2014) Worldwide Dissemination of the NDM-Type Carbapenemases in Gram-Negative Bacteria. *Biomed Res. Int.*, **2014**.

21. Guo, Y.F., Zhang, W.H., Ren, S.Q., Yang, L., Lü, D.H., Zeng, Z.L., Liu, Y.H., and Jiang, H.X. (2014) IncA/C plasmid-mediated spread of CMY-2 in multidrug-resistant *Escherichia coli* from food animals in China. *PLoS One*, **9**.

22. Poirel, L., Potron, A., and Nordmann, P. (2012) OXA-48-like carbapenemases: the phantom menace. *J. Antimicrob. Chemother.*, **67**: 1597–1606.

23. Antunes, N.T., Lamoureaux, T.L., Toth, M., Stewart, N.K., Frase, H., and Vakulenko, S.B. (2014) Class D β-Lactamases: Are They All Carbapenemases? *Antimicrob. Agents Chemother.*, **58**: 2119–2125.

24. Singkham-In, U., Muhummudaree, N., and Chatsuwan, T. (2021) In Vitro Synergism of Azithromycin Combination with Antibiotics against OXA-48-producing *Klebsiella pneumoniae* Clinical Isolates. *Antibiotics*, **10**: 1551.

25. Jacoby, G.A. (2009) AmpC β-Lactamases. *Clin. Microbiol. Rev.*, **22**: 161–182.

26. The European Committee on Antimicrobial Susceptibility Testing. (2022) Breakpoint tables for interpretation of MICs and zone diameters, Version 12.0. [Online]. Retrieved June 2022 from: https://www.eucast.org/clinical_breakpoints/.

27. Lence, E. and González-Bello, C. (2021) Bicyclic Boronate *β*-Lactamase Inhibitors: The Present Hope against Deadly Bacterial Pathogens. *Adv. Ther.*, **4**: 2000246.

28. Kim, K.-J., Kim, H.-E., Lee, K.-H., Han, W., Yi, M.-J., Jeong, J., and Oh, B.-H. (2004) Two-promoter vector is highly efficient for overproduction of protein complexes. *Protein Sci.*, **13**: 1698–1703.

29. Legaree, B.A., Daniels, K., Weadge, J.T., Cockburn, D., and Clarke, A.J. (2007) Function of penicillin-binding protein 2 in viability and morphology of *Pseudomonas aeruginosa*. *J. Antimicrob. Chemother.*, **59**: 411–424.

30. Kocaoglu, O. and Carlson, E.E. (2015) Profiling of β-Lactam Selectivity for Penicillin-Binding Proteins in *Escherichia coli* Strain DC2. *Antimicrob. Agents Chemother.*, **59**: 2785–2790.

31. Pang, Z., Raudonis, R., Glick, B.R., Lin, T.J., and Cheng, Z. (2019) Antibiotic resistance in *Pseudomonas aeruginosa*: mechanisms and alternative therapeutic strategies. *Biotechnol. Adv.*, **37**: 177–192.

32. Lahiri, S.D., Mangani, S., Jahić, H., et al. (2015) Molecular Basis of Selective Inhibition and Slow Reversibility of Avibactam against Class D Carbapenemases: A Structure-Guided Study of OXA-24 and OXA-48. *ACS Chem. Biol.*, **10**: 591–600.

33. Alcock, B.P., Raphenya, A.R., Lau, T.T.Y., et al. (2020) CARD 2020: Antibiotic resistome surveillance with the comprehensive antibiotic resistance database. *Nucleic Acids Res.*, **48**: D517–D525.

34. New England BioLabs. (2012) Gibson Assembly Protocol (E5510). [Online]. Retrieved February 2022 from: https://international.neb.com/protocols/2012/12/11/gibson-assembly-protocol-e5510.

35. Merrick, M.J., Gibbins, J.R., and Postgate, J.R. (1987) A Rapid and Efficient Method for Plasmid Transformation of *Klebsiella pneumoniae* and *Escherichia coli*. *Microbiology*, **133**: 2053–2057.

36. Clinical and Laboratory Standards Institute. (2012) Methods for Dilution Antimicrobial Susceptibility Tests for Bacteria That Grow Aerobically ; Approved

Standard—Ninth Edition. Wayne, PA: CLSI. M07-A9.

3.9 SUPPLEMENTAL MATERIAL

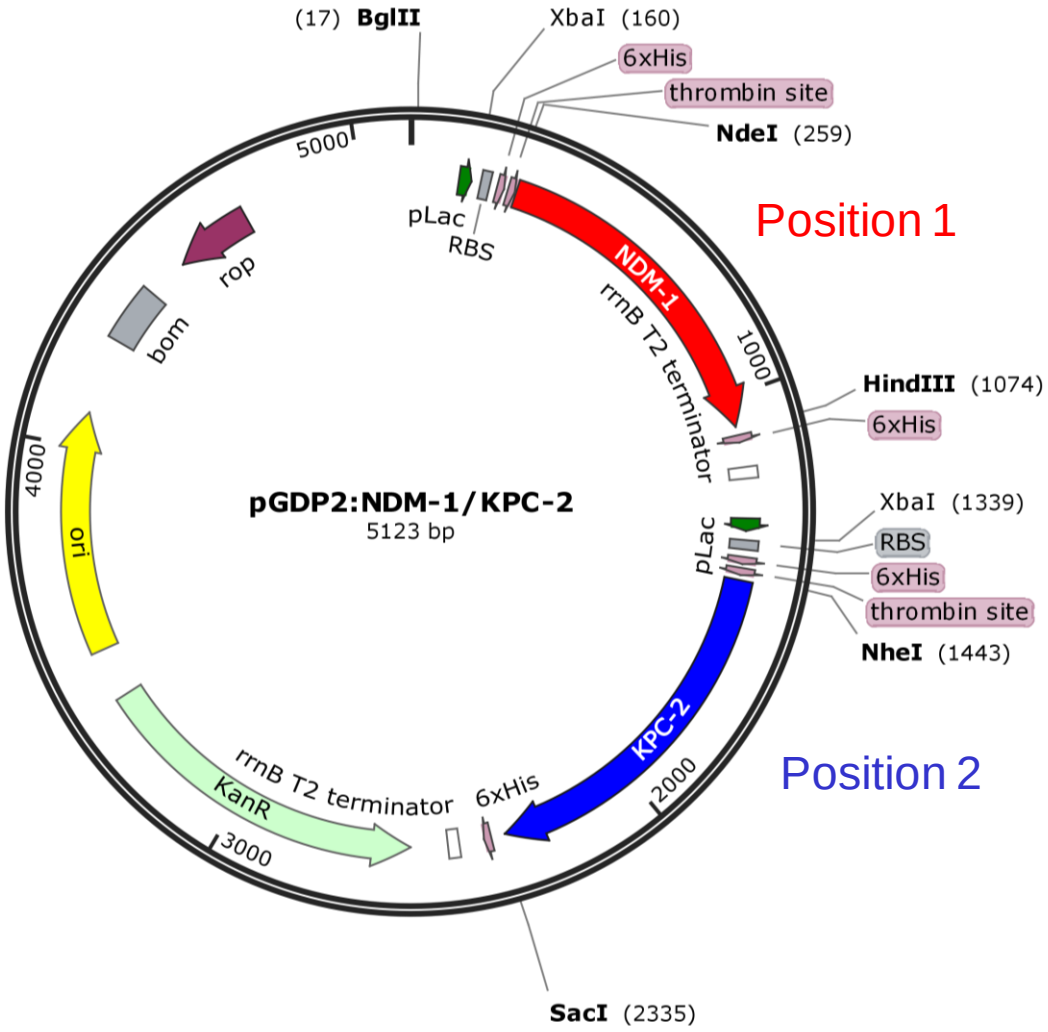

Supplemental Figure 3.1: Plasmid map for the NDM-1/KPC-2 construct under individual promoter control. The positions of the β-lactamase genes in the plasmid are depicted in red and blue. The restriction sites used to clone the genes within the plasmid are also portrayed. Plasmid map was created and annotated using SnapGene Viewer (Dotmatics, Boston, MA).

Supplemental Table 3.1: Minimum inhibitory concentration (MIC) values of *E. coli* BW25113 strains producing one MBL and one SBL when tested against various β-lactam antibiotics.[a] Genes from class A are shown in blue, while genes from class B, class C, and class D are depicted in black, pink, and green. All assays were conducted in duplicate.

β-Lactamase		MIC values (μg/mL)								
Gene 1	**Gene 2**	**ATM**	**AVI**	**MEM**	**DOR**	**PIP**	**AMP**	**CTX**	**FEP**	**CEC**
NDM-1	KPC-2	128	16	64	32	2048	> 4096	256	64	512
KPC-2	NDM-1	256	16	64	64	2048	> 4096	256–512	64	512
NDM-1	CTX-M-15	128	16	64	32	4096	> 4096	4096	1024–2048	1024
CTX-M-15	NDM-1	256	16	64	64	4096	> 4096	2048–4096	1024	1024
NDM-1	CMY-2	32	8	64	32	512	> 4096	256	32	512–1024
CMY-2	NDM-1	64	8	64	64	512–1024	> 4096	256	64	512
NDM-1	OXA-23	0.25	16–32	128	64	1024	> 4096	256–512	128	512
OXA-23	NDM-1	0.13	16	64	32–64	512	> 4096	256	64	512
NDM-1	OXA-48	0.13	8	64	32	512	> 4096	256	32	512
OXA-48	NDM-1	0.13	8	64	32	512	> 4096	256	32	512

Abbreviations: ATM aztreonam, AVI avibactam, MEM meropenem, DOR doripenem, PIP piperacillin, AMP ampicillin, CTX cefotaxime, FEP cefepime, CEC cefaclor.

[a] Both β-lactamase genes were cloned into pGDP2 with individual promoters.

Supplemental Table 3.2: Minimum inhibitory concentration (MIC) values of *E. coli* BW25113 strains producing a single β-lactamase gene when tested against various β-lactam antibiotics.[a] Genes from class A are shown in blue, while genes from class B, class C, and class D are depicted in black, pink, and green. *E. coli* BW25113 transformed with empty pGDP2 plasmid was used as a control. All assays were conducted in duplicate.

β-Lactamase	MIC values (µg/mL)								
	ATM	**AVI**	**MEM**	**DOR**	**PIP**	**AMP**	**CTX**	**FEP**	**CEC**
None	0.13	8–16	0.06	0.03	2–4	8	0.06	0.06–0.013	4
NDM-1	0.13	16	32–64	32	256	> 4096	256	32	256
KPC-2	128	16–32	8	4	512	4096	128–256	8	1024
CTX-M-15	128	16	0.06	0.06	1024	> 4096	512	64	512
CMY-2	32	16–32	0.06	0.06	32–64	512	2	0.25–0.50	512
OXA-23	0.25	16	0.25	0.06	128	1024	0.06	0.13–0.25	32
OXA-48	0.13	16	1	0.06	64–128	4096	512	0.13	64

Abbreviations: ATM aztreonam, AVI avibactam, MEM meropenem, DOR doripenem, PIP piperacillin, AMP ampicillin, CTX cefotaxime, FEP cefepime, CEC cefaclor

[a] All the β-lactamase genes were cloned into the pGDP2 vector.

Supplemental Table 3.3: Concentration of AMA needed to restore the activity of different β-lactam antibiotics to their susceptibility breakpoint concentration against *E. coli* BW25113 strains producing one MBL and one SBL.[a] Genes from class A are shown in blue, while genes from class B, class C, and class D are depicted in black, pink, and green. All assays were conducted in duplicate. This table shows the results from replicate 2.

β-Lactamase		[AMA] at the susceptibility breakpoint of the antibiotics in different combinations (μg/mL) [b, c]								
Gene 1	**Gene 2**	**AMA/ MEM**	**AVI/ MEM**	**AMA/AVI/ MEM**	**AMA/AVI/ DOR**	**AMA/AVI/ PIP**	**AMA/AVI/ AMP**	**AMA/AVI/ CTX**	**AMA/AVI/ FEP**	**AMA/AVI/ CEC**
NDM-1	KPC-2	> 32	16	8	8	16	> 32	32	16	> 32
KPC-2	NDM-1	> 32	16	8	8	16	> 32	32	16	> 32
NDM-1	CTX-M-15	8	16	8	8	16	> 32	32	16	> 32
CTX-M-15	NDM-1	16	16	8	8	16	> 32	32	16	> 32
NDM-1	CMY-2	16	16	8	8	16	> 32	32	16	> 32
CMY-2	NDM-1	16	16	8	8	16	> 32	32	16	> 32
NDM-1	OXA-23	16	16	16	16	32	> 32	32	16	> 32
OXA-23	NDM-1	16	16	16	16	32	> 32	32	16	> 32
NDM-1	OXA-48	16	16	8	16	16	> 32	32	16	> 32
OXA-48	NDM-1	16	16	8	16	16	> 32	32	16	> 32

Abbreviations: AMA aspergillomarasmine A, AVI avibactam, MEM meropenem, DOR doripenem, PIP piperacillin, AMP ampicillin, CTX cefotaxime, FEP cefepime, CEC cefaclor.

[a] Both β-lactamase genes were cloned into pGDP2 with individual promoters.

[b] The EUCAST susceptibility breakpoint concentrations for MEM, DOR, PIP, AMP, CTX, FEP and CEC are 2, 1, 8, 8, 1, 1 and 1 μg/mL.

[c] AVI was maintained at 4 μg/mL, except during the AVI/MEM combination.

Supplemental Table 3.4: Concentration of AMA needed to restore the activity of meropenem to its susceptibility breakpoint concentration against *K. pneumoniae* ATCC 33495 strains producing one MBL and one SBL.[a] Genes from class A are shown in blue, while genes from class B, class C, and class D are depicted in black, pink, and green. All assays were conducted in duplicate. This table shows the results from replicate 2.

β-Lactamase		[AMA] at 2 µg/mL of MEM in different combinations (µg/mL) [b, c]		
Gene 1	**Gene 2**	**AMA/ MEM**	**AVI/ MEM**	**AMA/AVI/ MEM**
NDM-1	KPC-2	> 64	> 64	8
KPC-2	NDM-1	> 64	> 64	8
NDM-1	CTX-M-15	16	> 64	16
CTX-M-15	NDM-1	16	> 64	16
NDM-1	CMY-2	8	> 64	8
CMY-2	NDM-1	8	> 64	8
NDM-1	OXA-23	16	> 64	16
OXA-23	NDM-1	16	> 64	16
NDM-1	OXA-48	16	> 64	16
OXA-48	NDM-1	16	> 64	16

Abbreviations: AMA aspergillomarasmine A, AVI avibactam, MEM meropenem.

[a] Both β-lactamase genes were cloned into pGDP2 with individual promoters.

[b] 2 µg/mL is the EUCAST susceptibility breakpoint concentration for MEM.

[c] AVI was maintained at 4 µg/mL, except during the AVI/MEM combination.

Supplemental Table 3.5: Minimum inhibitory concentration (MIC) values of *K. pneumoniae* ATCC 33495 producing a single β-lactamase gene when tested against various β-lactam antibiotics.[a] Genes from class A are shown in blue, while genes from class B, and D are depicted in black, and green. *K. pneumoniae* ATCC 33495 transformed with empty pGDP2 plasmid was used as a control. All assays were conducted in duplicate.

β-Lactamase	MIC values (µg/mL)								
	ATM	**AVI**	**MEM**	**DOR**	**PIP**	**AMP**	**CTX**	**FEP**	**CEC**
None	0.06	32	0.06	0.06	8	64	0.06	0.06	0.50–1
NDM-1	0.06	512–1024	128	256–512	512	> 4096	256	32	1024
CTX-M-15	64–128	1024	0.06	0.13	2048	> 4096	4096	32	> 4096
OXA-23	0.06–0.13	256	0.25	256	256	2048	0.06–0.13	0.13	128
OXA-48	0.06	256	0.25	64	128–256	1024–2048	0.50	0.06–0.13	128

Abbreviations: ATM aztreonam, AVI avibactam, MEM meropenem, DOR doripenem, PIP piperacillin, AMP ampicillin, CTX cefotaxime, FEP cefepime, CEC cefaclor.

[a] All the β-lactamase genes were cloned into the pGDP2 vector.

Supplemental Table 3.6: Concentration of AMA needed to restore the activity of meropenem to its susceptibility breakpoint concentration in combination with and without avibactam against clinical strains producing multiple β-lactamases. Genes from class A are shown in blue, while genes from class B, class C, and class D are depicted in black, pink, and green. All assays were conducted in duplicate. This table shows the results from replicate 2.

Strain	β-Lactamases			[AMA] at 2 µg/mL of MEM (µg/mL) [a, b]		
				AMA/ MEM	AVI/ MEM	AMA/AVI/ MEM
Acinetobacter baumannii B1NG08a	NDM-1	OXA-23	OXA-69	> 64	> 64	> 64
Citrobacter freundii GN978	TEM-1 NDM-1 OXA-1	CTX-M-15 CMY-6	CMY-46 CMY-18	8	> 64	8
Enterobacter cloacae 36749	NDM-1 ACT-25	TEM-171	OXA-1	8	16	8
Enterobacter cloacae 47219	ACT-17 LAP-2	NDM-1 TEM-1	OXA-1	8	32	16
Enterobacter cloacae 86502	ACT-17 OXA-1	TEM-1 VIM-1	CTX-M-15	8	32	16
Enterobacter cloacae 397260	ACT-17	VIM-1		8	32	8
Enterobacter cloacae GN574	TEM-1 OXA-1	NDM-1 ACT-17	CTX-M-15	16	> 64	16
Enterobacter cloacae GN579	CTX-M-15 ACT-25	TEM-1 OXA-1	NDM-1	16	32	8
Enterobacter cloacae GN687	NDM-1 TEM-1	OXA-9 ACT-25	CTX-M-15	16	> 64	16
Escherichia coli 130392-1	TEM-1 CMY-83	NDM-5	CMY-42	32	32	32
Escherichia coli 376762	NDM-5 TEM-1	CTX-M-15 AmpC	OXA-1 AmpC1	32	8	16
Escherichia coli 376948	AmpC1 AmpC	NDM-5	TEM-1	32	4	> 64
Escherichia coli 387039	NDM-5 AmpC1	OXA-181 CMY-2	AmpC OXA-1	> 64	64	64
Escherichia coli GN610	CTX-M-15 NDM-1 OXA-1	TEM-166 CMY-6	OXA-2 AmpC	> 64	16	16
Escherichia coli GN688	CTX-M-15 OXA-1	TEM-1 AmpC	NDM-1	16	8	8

Supplemental Table 3.6: Continued.

Strain	β-Lactamases			[AMA] at 2 µg/mL of MEM (µg/mL) [a, b]		
				AMA/ MEM	AVI/ MEM	AMA/AVI/ MEM
Klebsiella oxytoca GN942	NDM-1 OXA-9	CTX-M-15 OXY-2-8	TEM-1	8	32	8
Klebsiella pneumoniae 86500	SHV-11 NDM-5	CTX-M-15 OXA-1	OXA-232 TEM-1	> 64	> 64	64
Klebsiella pneumoniae 110027	CTX-M-14 OXA-48 OXA-9	NDM-1 SHV-1	CTX-M-15 TEM-1	> 64	> 64	16
Klebsiella pneumoniae 130392-2	DHA-1 OXA-232 OXA-9	SHV-27 CTX-M-15 CMY-42	NDM-1 TEM-183	16	64	16
Klebsiella pneumoniae 420322	SHV-1 CTX-M-15	OXA-181 OXA-1	NDM-5 TEM-1	> 64	> 64	64
Klebsiella pneumoniae GN529	TEM-1 SHV-144	NDM-1 OXA-1	CTX-M-15 SHV-66	8	> 64	8
Klebsiella pneumoniae GN629	SHV-11 DHA-7	CTX-M-15 OXA-1	NDM-1	16	> 64	16
Klebsiella pneumoniae N11-0306	CTX-M-15 OXA-1	SHV-11 DHA-7	NDM-1	16	> 64	16
Klebsiella pneumoniae N11-2218	NDM-1 SHV-83	CTX-M-15 SHV-144	CMY-6 SHV-11	8	> 64	8
Morganella morganii GN575	CTX-M-15	NDM-1	DHA-1	8	> 64	8
Providencia rettgeri GN570	NDM-1 CMY-6	VEB-1a OXA-1	TEM-1	> 64	> 64	16
Providencia stuartii GN576	CMY-2	NDM-1		8	> 64	8
Pseudomonas aeruginosa 411090	NDM-1 PDC-3	VEB-9 OXA-50	OXA-10	> 64	> 64	> 64
Pseudomonas aeruginosa H1010805	VIM-2			> 64	> 64	> 64
Pseudomonas aeruginosa H1010812	IMP-7	PDC-7	OXA-485	> 64	> 64	> 64

Abbreviations: AMA aspergillomarasmine A, AVI avibactam, MEM meropenem.

[a] 2 µg/mL is the EUCAST susceptibility breakpoint concentration for MEM.

[b] AVI was maintained at 4 µg/mL, except during the AVI/MEM combination.

Supplemental Table 3.7: Minimum inhibitory concentration (MIC) values of clinical strains. All assays were conducted in duplicate.

Strain	MIC values (μg/mL)	
	MEM	**AVI**
Acinetobacter baumannii B1NG08a	256	> 4096
Citrobacter freundii GN978	32	64
Enterobacter cloacae 36749	8–16	16
Enterobacter cloacae 47219	64	32
Enterobacter cloacae 86502	128	32
Enterobacter cloacae 397260	16	64–128
Enterobacter cloacae GN574	128–256	128
Enterobacter cloacae GN579	32	32
Enterobacter cloacae GN687	128	64
Escherichia coli 130392-1	128	32–64
Escherichia coli 376762	128	128
Escherichia coli 376948	256	16
Escherichia coli 387039	256	64
Escherichia coli GN610	512	16
Escherichia coli GN688	128	16
Klebsiella oxytoca GN942	128	64
Klebsiella pneumoniae 86500	512	128–256
Klebsiella pneumoniae 110027	1024	256–512
Klebsiella pneumoniae 130392-2	128	256–512
Klebsiella pneumoniae 420322	512	> 4096
Klebsiella pneumoniae GN529	128–256	256–512
Klebsiella pneumoniae GN629	64–128	512
Klebsiella pneumoniae N11-0306	64–128	256
Klebsiella pneumoniae N11-2218	128	256–512
Morganella morganii GN575	16–32	> 4096
Providencia rettgeri GN570	128	1024
Providencia stuartii GN576	64	> 4096
Pseudomonas aeruginosa 411090	2048	> 4096
Pseudomonas aeruginosa H1010805	256	4096
Pseudomonas aeruginosa H1010812	1024–2048	> 4096

Abbreviations: MEM meropenem, AVI avibactam.

CHAPTER 4: Expanding the antibiotic resistance platform to *Acinetobacter* and *Pseudomonas* species

4.1 PREFACE

None of this research has been published in any form.

4.2 AUTHOR CONTRIBUTIONS

C.M.R., M.D.S. and G.D.W. designed the experiments discussed in this chapter. C.M.R. constructed the pROTO/pROKA vector series as well as conducted cloning of resistance genes and bacterial transformations. C.M.R. and M.K. prepared competent cells and performed the cell-based assays. C.M.R. and M.D.S. wrote the manuscript whereas M.K. and G.D.W. revised the manuscript.

4.3 ABSTRACT

Rising rates of antibiotic resistance are jeopardizing our ability to treat bacterial infections. One promising strategy for overcoming resistance is to employ antibiotic adjuvants, which rescue the efficacy of existing antibiotics by inhibiting specific resistance enzymes or enhancing their antibiotic partner's activity. For example, antibiotic adjuvants such as aspergillomarasmine A (AMA) and avibactam restore the activity of the β-lactam meropenem against β-lactamase-producing bacteria. Tools such as the antibiotic resistance platform (ARP) can facilitate the discovery and characterization of antibiotic adjuvants. The ARP consists of a cell-based array of resistance genes expressed in an identical genetic background. However, the plasmid chassis used to construct the ARP contains a pMB1 origin of replication, limiting this platform to Enterobacterales such as *Escherichia coli*. To expand the host range of the ARP to priority pathogens within the Pseudomonadales, such as *Acinetobacter baumannii* and *Pseudomonas aeruginosa*, we constructed ARP plasmids containing additional origins of replication. These new *Escherichia-Acinetobacter* and *Escherichia-Pseudomonas* shuttle vectors, pROTO1–4 and pROKA1–4, respectively, can efficiently replicate and express antibiotic resistance genes in diverse Enterobacterales and Pseudomonadales. Using pROTO, we generated a series of tandem β-lactamase-expressing *A. baumannii*. We demonstrate that a combination of AMA/avibactam re-sensitizes *A. baumannii* to meropenem even when it simultaneously produces multiple classes of β-lactamases, a common obstacle in the clinic. Overall, as any gene from the ARP can be sub-cloned into these new vectors, the

pROTO and pROKA plasmids can advance the discovery and characterization of new antibiotic adjuvants effective against *A. baumannii* and *P. aeruginosa*.

4.4 INTRODUCTION

In 2017, the World Health Organization published a list of priority pathogens that posed the greatest threat to human health, with *Acinetobacter baumannii* and *Pseudomonas aeruginosa* among the most critical [1,2]. These pathogens are common causes of nosocomial infections, including bacteremia, ventilator-associated pneumonia, urinary tract infections, and sepsis [3–7]. In the past, these hospital-acquired infections were manageable with β-lactam antibiotics such as carbapenems. However, the emergence of multidrug-resistant and carbapenem-resistant *A. baumannii* and *P. aeruginosa* is threatening the effectiveness of these antibiotics [4,7]. Although *A. baumannii* and *P. aeruginosa* can employ several mechanisms to negate the effect of antibiotics, resistance to β-lactams is primarily achieved through enzymatic inactivation by β-lactamases [8,9]. In addition to these enzymes, both species possess a highly impermeable cell envelope which prevents the entry of many antibiotic classes [4,10]. These factors make *A. baumannii* and *P. aeruginosa* infections challenging to treat with our current antibiotic repertoire. Therefore, new antibiotics and antimicrobial strategies are needed to overcome *A. baumannii* and *P. aeruginosa* resistance.

One promising strategy for combatting bacterial antibiotic resistance is to develop antibiotic adjuvants. Antibiotic adjuvants are compounds that can inhibit specific bacterial resistance enzymes or enhance the activity of existing antibiotics [11]. Several antibiotic adjuvants are currently in clinical use, including clavulanic acid, which inhibits

several β-lactamase enzymes and subsequently re-sensitizes bacteria to β-lactams [11,12]. Pairing amoxicillin with clavulanic acid generated Augmentin, the first β-lactam/β-lactamase inhibitor combination, which has seen widespread clinical success [11]. However, many bacterial strains can evade inhibition by Augmentin through overproduction of the susceptible β-lactamase or co-expression with a resistant β-lactamase [13]. This spurred the development of β-lactamase inhibitors active against a broader spectrum of β-lactamases such as tazobactam, avibactam, vaborbactam, and relebactam [14]. Unfortunately, no β-lactam/β-lactamase inhibitor combination on the market can inhibit strains expressing metallo-β-lactamases (MBLs), such as the plasmid-borne NDM-1, although some promising MBL inhibitors are currently in development [15–17]. We previously demonstrated that a fungal natural product, aspergillomarasmine A (AMA), can rescue the activity of the β-lactam antibiotic meropenem against bacterial strains producing either NDM-1 or VIM-2, two clinically relevant MBL enzymes [18]. AMA was discovered through a high-throughput screen of natural product extracts, which re-sensitized *Escherichia coli* harbouring NDM-1 to meropenem [18]. In principle, this same approach applies to any other resistance enzyme. To facilitate the discovery of novel adjuvants and reverse antibiotic resistance, we created the antibiotic resistance platform [18,19].

The antibiotic resistance platform (ARP) consists of a library of *E. coli* expressing individual resistance genes from a series of stable, low-copy number plasmids (the pGDP series, pGDP1–4) [19,20]. For convenient cloning, all pGDP vectors use a common cloning site (MCS) modelled after the widely used pET vectors. Two 6×His motifs flank

the MCS allowing for the addition of N- or C- terminal 6×His-tags to facilitate protein purification/detection [19]. These vectors are available with two different selection markers, kanamycin or ampicillin, so that any resistance enzyme can be expressed without cross-resistance from the selectable marker [19]. Users can also choose two constitutive promoters offering high or low expression levels, P_{Bla} and P_{Lac}. pGDP1–4 correspond to all combinations of selectable markers and promoters: pGDP1 (kanamycin-resistant, strong promoter), pGDP2 (kanamycin-resistant, weak promoter), pGDP3 (ampicillin-resistant, strong promoter), pGDP4 (ampicillin-resistant, weak promoter). Lastly, the pGDP series carry the ubiquitous pMB1 origin of replication for plasmid maintenance in *E. coli* [19,21].

Currently, the ARP contains over 100 functionally verified resistance genes that target 18 classes of antibiotics [20], and has also shown repeated success in identifying antibiotic adjuvants. For instance, Cox *et al.* identified 27 molecules capable of enhancing gentamicin activity against ANT(2″)-Ia-expressing *E. coli,* including several promising hits with inhibition constants in the low μM range [19]. Gallique *et al.* also used the ARP to show that cranberry-derived proanthocyanidins potentiated β-lactam activity against β-lactamase-producing *E. coli* [22]. However, one drawback to the ARP is that it is only functional in *E. coli* [19,21], limiting our ability to characterize the activity of adjuvants in different bacterial species.

In comparison to *E. coli*, priority pathogens such as *A. baumannii* and *P. aeruginosa* have comparatively fewer tools for genetic manipulation and heterologous expression of resistance genes [23,24]. Adjuvants are therefore often evaluated against panels of

clinical isolates, which can possess multiple independent resistance mechanisms and any number of genetic polymorphisms. For instance, many clinical strains have acquired plasmids containing numerous resistance genes, often functionally redundant, such as multiple extended-spectrum β-lactamases [25–28]. These factors make it difficult to ascertain the relative contributions of any given gene to the organism's antibiogram and complicate the investigation of adjuvants which target specific resistance enzyme(s) such as AMA. The limited host range of the ARP prevents the discovery of narrow-spectrum adjuvants by precluding high-throughput screening directly in *A. baumannii* or *P. aeruginosa*.

To overcome the aforementioned pitfalls of the ARP, we expanded its host range to *A. baumannii* and *P. aeruginosa* by adding a second origin of replication to the pGDP plasmid chassis. These new *Escherichia-Acinetobacter* and *Escherichia-Pseudomonas* shuttle vectors, designated pROTO and pROKA, can be used to further study antibiotic resistance genes, and antibiotic adjuvants in *A. baumannii* and *P. aeruginosa*. In this work, we also demonstrate the utility of these vectors by establishing that a combination of AMA, avibactam, and meropenem can inhibit *A. baumannii* producing multiple classes of β-lactamase simultaneously. Antibiotic adjuvants can be a successful strategy in tackling antibiotic-resistant pathogens, and the expansion of the ARP described here can remove barriers in adjuvant research.

4.5 RESULTS

4.5.1 General construction of the pROTO and pROKA vectors

As constructed, the ARP plasmids (pGDP series) lack the machinery to replicate in *A. baumannii* and *P. aeruginosa*. Because a pan-Pseudomonadales plasmid replication system hasn't been characterized, it was necessary to build separate vectors for *A. baumannii* and *P. aeruginosa*. To construct an ARP-compatible *E. coli-A. baumannii* shuttle vector, we added ori1266 from pFLP2 to pGDP1–4 to create pROTO1–4 (Figure 4.1). For plasmid propagation in both *E. coli* and *P. aeruginosa*, the pRO1600 oriV and replication protein from pMS402 were inserted into pGDP1–4 to generate pROKA1–4 (Figure 4.2). These additional origins of replication were added at restriction recognition sites that would prevent interference with the stability of the existing functional elements of the pGDP plasmids such as the MCS or the pMB1 ori.

Furthermore, pROKA1–2 required substitution of the kanamycin selectable marker gene *aph(3')-Ia* for the gentamicin selectable marker gene *ant(2'')-Ia*. This step was necessary because many *P. aeruginosa,* including the common laboratory strain PAO1, are intrinsically resistant to kanamycin due to a chromosomally-encoded aminoglycoside phosphotransferase [29], making selection on kanamycin impossible. *P. aeruginosa* is also intrinsically resistant to ampicillin through the action of its inducible AmpC β-lactamase [30,31]. However, it was not necessary to replace the ampicillin selectable marker gene $bla_{\text{TEM-1}}$ because this gene also confers high levels of resistance to carbenicillin, which is not a substrate for AmpC and has previously been employed for *P. aeruginosa* selection [32,33].

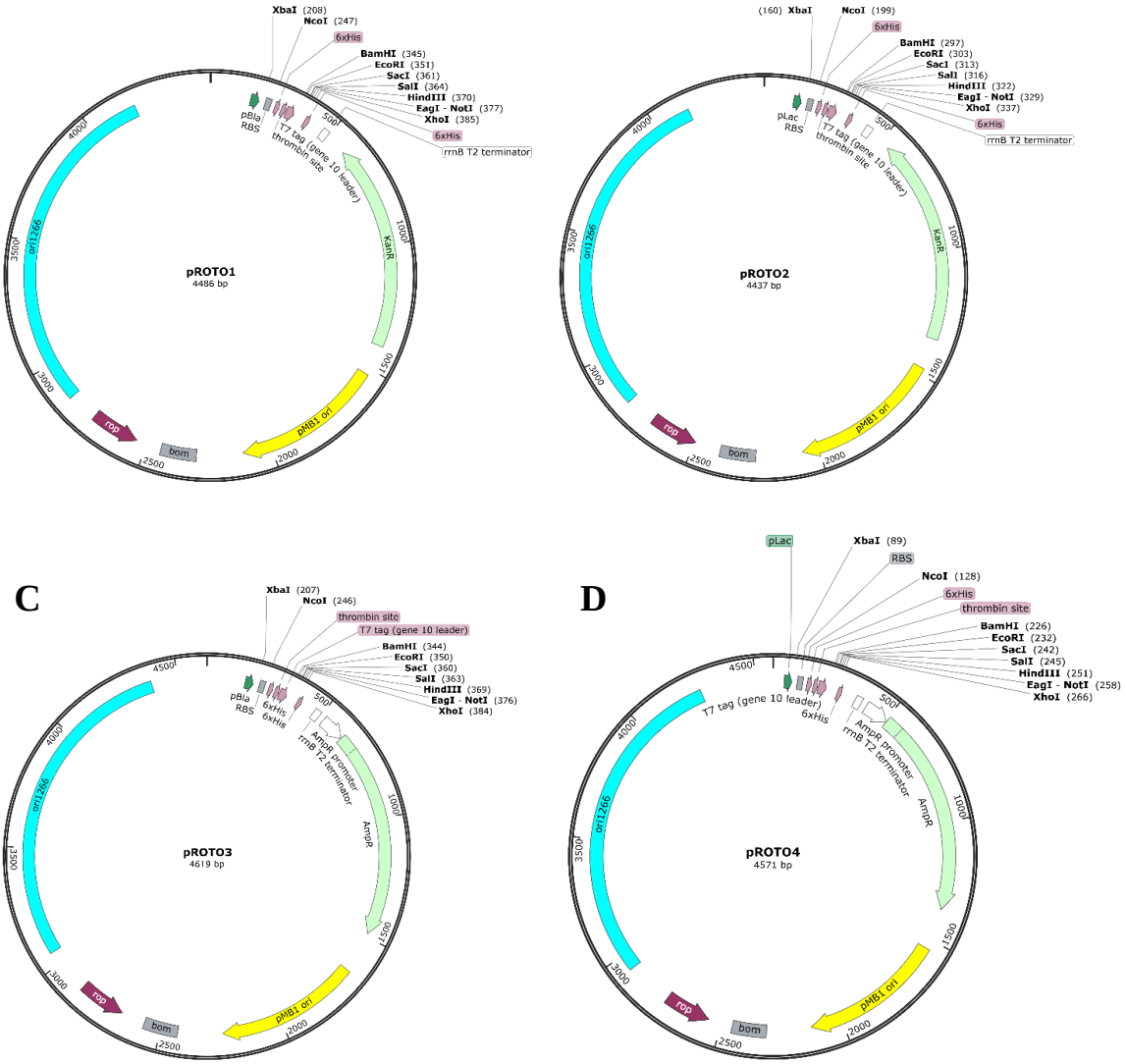

Figure 4.1: Detailed pROTO plasmid maps. The restriction enzymes forming the multiple cloning site (MCS) are shown for each plasmid: (A) pROTO1, (B) pROTO2, (C) pROTO3, (D) pROTO4. Plasmid maps were created and annotated using SnapGene Viewer (Dotmatics, Boston, MA).

As pROTO and pROKA employed the pGDP series of ARP plasmids as backbones, these new *Escherichia-Acinetobacter* and *Escherichia-Pseudomonas* shuttle vectors retain the same functionality and nomenclature as the originals. For instance, pGDP1, pROTO1, and pROKA1 all have the P_{Bla} promoter for high-level, constitutive expression,

and the aminoglycoside selectable marker (kanamycin/gentamicin). In addition, the backwards compatibility afforded by the universal pGDP backbone ensures that any of the 100 genes in the ARP can be easily sub-cloned into these vectors and transferred to diverse *Acinetobacter* spp. or *Pseudomonas* spp.

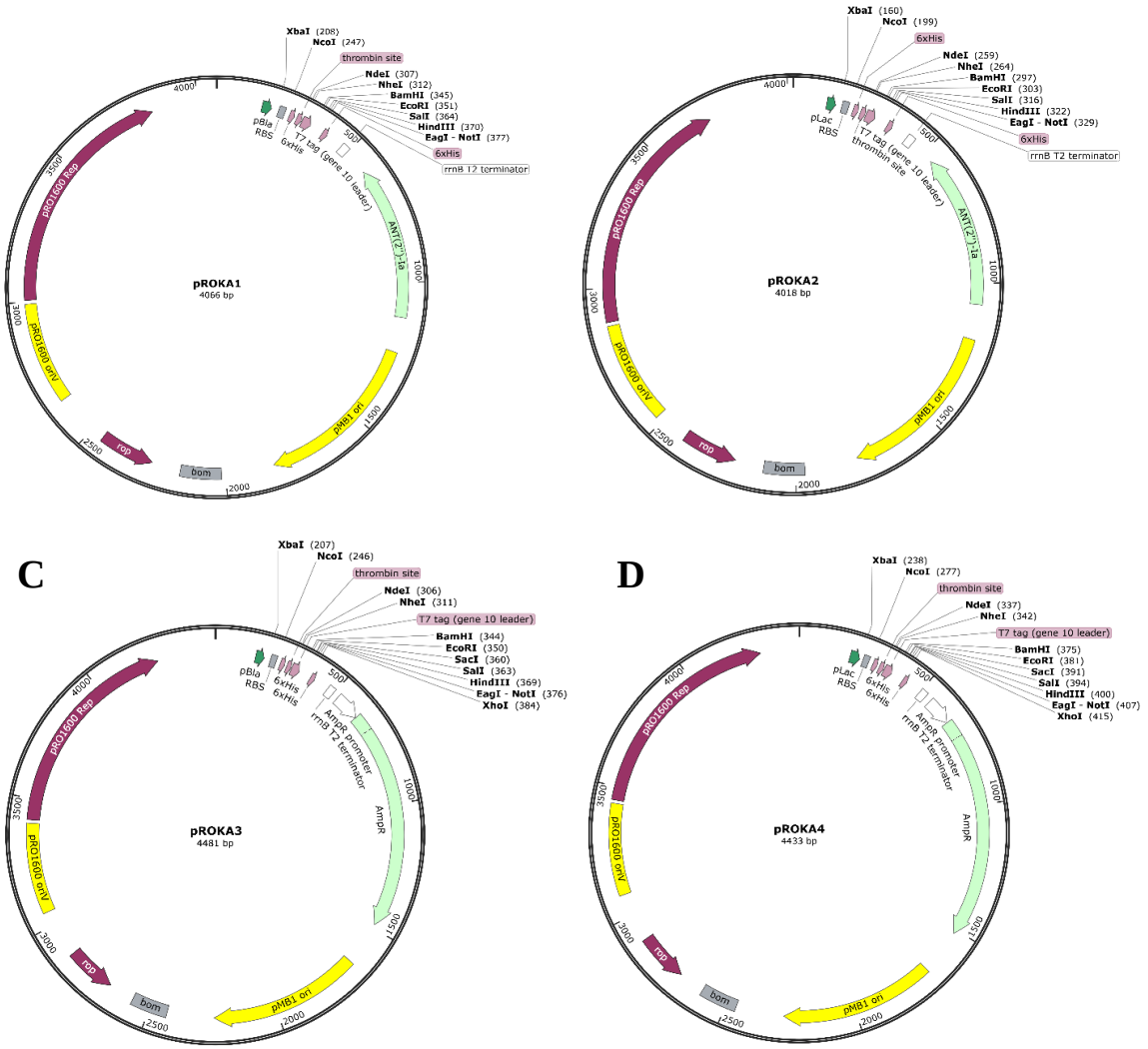

Figure 4.2: Detailed pROKA plasmid maps. The restriction enzymes forming the multiple cloning site (MCS) are shown for each plasmid: (A) pROKA1, (B) pROKA2, (C) pROKA3, (D) pROKA4. Plasmid maps were created and annotated using SnapGene Viewer (Dotmatics, Boston, MA).

4.5.2 Plasmid stability and host range

We next examined the ability of pROTO1–4 and pROKA1–4 to replicate in different Gram-negative hosts, including *E. coli* BW25113, *A. baumannii* ATCC 17978, *A. baumannii* ATCC 19606, *P. aeruginosa* PAO1 and *P. aeruginosa* PA14. Additionally, since the pMB1 ori found on the pGDP backbone is present in plasmids isolated outside *Escherichia* spp., we tested the ability of the pROTO and pROKA series to replicate in other Enterobacterales, such as *Klebsiella pneumoniae* ATCC 33495 and *Enterobacter aerogenes* ATCC 13048. These bacteria are common laboratory/reference strains routinely used in testing and research [34–37]. All strains we tested were reliably transformed with our panel of expanded ARP plasmids. Robust selection of transformants across most species was possible at 50 µg/mL of kanamycin (pROTO1–2), 20 µg/mL of gentamicin (pROKA1–2), and 250 µg/mL of carbenicillin (pROKA3–4). Selection of pROTO3–4 was conducted using 100 µg/mL of ampicillin (*E. coli*, *A. baumannii* ATCC 17978) or 250 µg/mL of carbenicillin (*A. baumannii* ATCC 19606, *E. aerogenes*). In addition, for *K. pneumoniae*, selection of pROTO/pROKA series 3 and 4 containing either *ant(2″)-Ia* or *aac(6′)-Ib10* was more efficient using kanamycin (50 µg/mL). We observed no difference in baseline antibiotic susceptibility with these plasmids other than the expected changes from the resistance cassette (Figures 4.1, 4.2). These results demonstrate that the modifications we made to expand the host range of the ARP to *A. baumannii* and *P. aeruginosa* were successful. We also note that the original pGDP series can replicate stably in *K. pneumoniae* and *E. aerogenes*, meaning the ARP can function directly in these pathogens. Together, pGDP, pROTO, and pROKA cover all the Gram-

negative members of the ESKAPE pathogen panel (*K. pneumoniae*, *A. baumannii*, *P. aeruginosa*, *Enterobacter* spp.) [38]. Future studies will quantify the stability of the plasmid in the absence of selection, the relative fitness of the plasmid through competition with plasmid-free strains, and determine the plasmid copy number in both *A. baumannii* and *P. aeruginosa.*

4.5.3 pROTO and pROKA validation

The ARP and the pROTO/pROKA series serve as a standardized platform for the heterologous expression of antibiotic resistance genes. Our newly constructed vectors must reliably perform this task across *E. coli*, *A. baumannii*, and *P. aeruginosa* hosts. Therefore, we chose two β-lactamases (*bla*$_{\text{NDM-1}}$ and *bla*$_{\text{CTX-M-15}}$) and two aminoglycoside modifying enzymes [*ant(2'')-Ia* and *aac(6')-Ib10*] for expression in the appropriate pROTO and pROKA vectors (avoiding cross-resistance with the selectable marker). We used these constructs to validate all the key functions of our plasmids in *A. baumannii* and *P. aeruginosa*, namely the expression of cargo genes, the difference between the stronger promoter (P_{Bla}, pROTO/pROKA series 1 and 3) and weaker promoter (P_{Lac}, pROTO/pROKA series 2 and 4), and the function of the N- and C-terminal 6×His-tags. The aforementioned genes were chosen because of their well-documented resistance phenotypes and broad distribution among Gram-negative pathogens such as *A. baumannii, Citrobacter freundii, E. cloacae, E. coli, K. pneumoniae, Providencia stuartii, P. aeruginosa, Salmonella enterica*, and *Serratia marcescens* [39].

Table 4.1: Minimum inhibitory concentration (MIC) values of different antibiotics against *E. coli* and *A. baumannii* strains producing plasmids from the pROTO series. All MIC assays were conducted in duplicate.

Bacteria/Plasmid/Gene		MIC values (μg/mL)					
		MEM	**CTX**	**PIP/AMP [a]**	**KAN**	**GEN**	**TOB**
***E. coli* BW25113 wild-type**							
pROTO1	None	0.031	0.063	2	4096	ND	ND
	NDM-1	32	256	512	2048	ND	ND
	CTX-M-15	0.031	4096	1024–2048	4096	ND	ND
pROTO2	None	0.031	0.063	2	2048–4096	ND	ND
	NDM-1	32	128	128–256	2048–4096	ND	ND
	CTX-M-15	0.031	256	256	4096	ND	ND
pROTO3	None	ND	ND	> 4096	2–4	0.50	0.25
	ANT(2″)-Ia	ND	ND	> 4096	512	256	256–512
	ACC(6′)-Ib10	ND	ND	> 4096	256	16	32–64
pROTO4	None	ND	ND	> 4096	2	0.50	0.25
	ANT(2″)-Ia	ND	ND	> 4096	256	64–128	128
	ACC(6′)-Ib10	ND	ND	> 4096	512	8	64
***A. baumannii* ATCC 17978**							
pROTO1	None	0.25	8	16	2048	ND	ND
	NDM-1	64	128	512–1024	2048	ND	ND
	CTX-M-15	0.25	512–1024	512	2048	ND	ND
pROTO2	None	0.25	16	16	2048	ND	ND
	NDM-1	32	64	256	1024	ND	ND
	CTX-M-15	0.50	512–1024	256	1024–2048	ND	ND
pROTO3	None	ND	ND	> 4096	4	4	1
	ANT(2″)-Ia	ND	ND	> 4096	256–512	2048	256
	ACC(6′)-Ib10	ND	ND	> 4096	256	64	32–64
pROTO4	None	ND	ND	> 4096	4–8	4	1
	ANT(2″)-Ia	ND	ND	> 4096	256	512–1024	128
	ACC(6′)-Ib10	ND	ND	> 4096	256	8	64
***A. baumannii* ATCC 19606**							
pROTO1	None	1	64	32–64	4096	ND	ND
	NDM-1	128–256	2048	256–512	2048	ND	ND
	CTX-M-15	1	2048	1024	2048	ND	ND
pROTO2	None	1	64	32	2048	ND	ND
	NDM-1	64	1024	128	2048	ND	ND
	CTX-M-15	1	1024	256–512	2048	ND	ND
pROTO3	None	ND	ND	4096	16	32	4
	ANT(2″)-Ia	ND	ND	4096	2048	> 4096	2048–4096
	ACC(6′)-Ib10	ND	ND	> 4096	512	256–512	256
pROTO4	None	ND	ND	4096	16	32	4
	ANT(2″)-Ia	ND	ND	4096	512	> 4096	512–1024
	ACC(6′)-Ib10	ND	ND	4096	1024	256	256

Abbreviations: MEM meropenem, CTX cefotaxime, PIP piperacillin, AMP ampicillin, KAN kanamycin, GEN gentamicin, TOB tobramycin, ND not determined.

[a] PIP was used for MIC assays against pROTO1–2 while AMP was used for MIC assays against pROTO3–4.

Table 4.2: Minimum inhibitory concentration (MIC) values of different antibiotics against *E. coli* and *P. aeruginosa* strains producing plasmids from the pROKA series. All MIC assays were conducted in duplicate.

Bacteria/Plasmid/Gene		MIC values (μg/mL)					
		MEM	**CTX**	**PIP/CAR [a]**	**KAN**	**GEN**	**TOB**
***E. coli* BW25113 wild-type**							
pROKA1	None	0.031	0.063	2	ND	128	ND
	NDM-1	16	512	2048	ND	256	ND
	CTX-M-15	0.063	> 4096	4096	ND	256	ND
pROKA2	None	0.031	0.063	2	ND	128–256	ND
	NDM-1	32	256–512	256–512	ND	256	ND
	CTX-M-15	0.031	1024	1024	ND	256	ND
pROKA3	None	ND	ND	> 4096	2	0.50	1
	ANT(2″)-Ia	ND	ND	> 4096	1024	512–1024	512–1024
	ACC(6′)-Ib10	ND	ND	> 4096	512	8–16	16–32
pROKA4	None	ND	ND	> 4096	2	0.50	0.50
	ANT(2″)-Ia	ND	ND	> 4096	256	256	128
	ACC(6′)-Ib10	ND	ND	> 4096	512	16–32	32
***P. aeruginosa* PAO1**							
pROKA1	None	2	16	2	ND	1024	ND
	NDM-1	512	> 4096	128	ND	1024–2048	ND
	CTX-M-15	2	512	128	ND	1024–2048	ND
pROKA2	None	2	4	1–2	ND	2048	ND
	NDM-1	> 4096	> 4096	1024	ND	1024–2048	ND
	CTX-M-15	4	> 4096	2048	ND	1024	ND
pROKA3	None	ND	ND	4096	128	0.50–1	0.50–1
	ANT(2″)-Ia	ND	ND	> 4096	128	128–256	64
	ACC(6′)-Ib10	ND	ND	2048–4096	128	8	16
pROKA4	None	ND	ND	> 4096	64	1–2	1
	ANT(2″)-Ia	ND	ND	> 4096	2048	2048	512
	ACC(6′)-Ib10	ND	ND	> 4096	1024	16	128
***P. aeruginosa* PA14**							
pROKA1	None	0.50–1	32	4–8	ND	4096	ND
	NDM-1	128	> 4096	128	ND	> 4096	ND
	CTX-M-15	0.50	1024	128–256	ND	2048–4096	ND
pROKA2	None	0.50–1	16	4	ND	> 4096	ND
	NDM-1	1024	> 4096	512	ND	> 4096	ND
	CTX-M-15	2	> 4096	2048	ND	> 4096	ND
pROKA3	None	ND	ND	4096	64	2	1
	ANT(2″)-Ia	ND	ND	> 4096	256	256–512	64–128
	ACC(6′)-Ib10	ND	ND	4096	64–128	8	32
pROKA4	None	ND	ND	> 4096	64	1	1
	ANT(2″)-Ia	ND	ND	> 4096	2048	4096	1024
	ACC(6′)-Ib10	ND	ND	> 4096	1024	32	256

Abbreviations: MEM meropenem, CTX cefotaxime, PIP piperacillin, AMP ampicillin, KAN kanamycin, GEN gentamicin, TOB tobramycin, ND not determined.

[a] PIP was used for MIC assays against pROKA1–2 while CAR was used for MIC assays against pROKA3–4.

We extensively validated the function of these constructs through antibiotic susceptibility testing across multiple strains of *E. coli*, *A. baumannii*, and *P. aeruginosa* (Tables 4.1, 4.2). The correct antibiotic resistance phenotypes were recapitulated across all genes and hosts. For example, NDM-1 expressing constructs confer resistance to three of the general β-lactam subclasses: carbapenems (meropenem), penicillins/penams (piperacillin) and cephalosporins/cephems (cefotaxime). Conversely, CTX-M-15 cannot hydrolyze carbapenems such as meropenem [40], and therefore conferred resistance to only piperacillin and cefotaxime (Tables 4.1, 4.2). In the case of ANT(2″)-Ia and AAC(6′)-Ib10, both enzymes confer robust resistance to kanamycin and tobramycin, but AAC(6′)-Ib10 conferred significantly less resistance to gentamicin (Tables 4.1, 4.2). This enzyme is well known to possess weak activity against gentamicin [41]. The fold-change in resistance conferred by our constructs is generally consistent (in most cases within two to eight-fold) among strains (i.e., PAO1 and PA14) and among different species (Tables 4.1, 4.2 and Supplemental Tables 4.1, 4.2). For instance, pROTO1:NDM-1 and pROKA1:NDM-1 increase the meropenem MIC by 128–256 in *A. baumannii* ATCC 17978, ATCC 19606 and *P. aeruginosa* PAO1, PA14, and by 256–512-fold in *E. coli* BW25113 wild-type. Exceptions to this can be at least in part explained by differences in intrinsic resistance (i.e., a higher initial MIC, as can be seen for *A. baumannii* ATCC 19606 and cefotaxime, piperacillin resistance). Consistent with our original pGDP series [19], genes expressed from P_{Bla} (pROTO/pROKA series 1 and 3) generally conferred two-fold to four-fold higher resistance than P_{Lac} controlled constructs (pROTO/pROKA series 2 and 4), offering users some control over the expression/resistance level. In summary,

we have comprehensively validated the function of the pROTO and pROKA series across six different microbial hosts with four independent antibiotic resistance genes. These data show that pROTO and pROKA are robust and reliable tools for the study of antimicrobial resistance.

To simplify protein purification and detection, we included 6×His motifs upstream and downstream of the MCS in pROTO and pROKA. To confirm that N- and C-tagged proteins are produced using our vectors, we constructed tagged versions of NDM-1, CTX-M-15, ANT(2″)-Ia and AAC(6′)-Ib10. Because β-lactamases contain N-terminal signal sequences that are removed during their localization to the periplasm [40], any N-terminal 6×His-tag would be cleaved. As a result, it was only possible to generate C-terminally tagged β-lactamases. Both pROTO and pROKA plasmids expressing C-terminally tagged NDM-1 or CTX-M-15 confer resistance to the expected antibiotics (piperacillin, cefotaxime, and in the case of NDM-1 meropenem), indicating that they are indeed expressed. However, in all cases, they exhibited a two-fold to four-fold increase in susceptibility relative to their untagged counterparts (Tables 4.1, 4.2 and Supplemental Tables 4.3, 4.4). We attribute this to a protein-specific effect of the 6×His-tag on β-lactamases, as C-terminally tagged pROTO and pROKA plasmids expressing either ANT(2″)-Ia or AAC(6′)-Ib10 demonstrated similar gentamicin, kanamycin, and tobramycin MIC values as their N-terminally tagged counterparts (Tables 4.1, 4.2 and Supplemental Tables 4.3, 4.4). Despite their usefulness, affinity tags are widely understood to have pleiotropic effects on protein function [42]. Nevertheless, these results suggest that the 6×His-tags are correctly translated and can be used to monitor protein

expression. Future experiments will confirm the production of each 6×His-tagged protein in various Gram-negative hosts via Western blotting.

4.5.4 Determination of the susceptibility of tandem β-lactamase gene expression shuttle vectors

Bacterial infections caused by multidrug-resistant and carbapenem-resistant *A. baumannii* are often difficult to treat due to the production of multiple β-lactamases [43]. β-lactamases either employ active site Zn^{2+} (metallo-β-lactamase; MBL) or serine (serine-β-lactamase; SBL) to hydrolyze β-lactam antibiotics [44,45]. Antibiotic adjuvants with the capacity to inhibit these β-lactamase enzymes represent a promising strategy for overcoming *A. baumannii* resistance. We hypothesized that the combination of a classic, broad-spectrum SBL inhibitor such as avibactam [46], and the MBL inhibitor AMA should be able to inhibit the activity of almost any combination of β-lactamases. To test this hypothesis, we built pROTO plasmids capable of expressing one MBL (NDM-1) and one SBL (KPC-2, CTX-M-15, CMY-2, or OXA-48) from independent promoters and transformed them into *A. baumannii* ATCC 17978. To avoid any possible artifacts introduced by the relative positions of the β-lactamases, we constructed each combination in both orientations (i.e., MBL upstream of SBL vs. SBL upstream of MBL). We attempted to re-sensitize these strains to the β-lactam antibiotic meropenem by using a combination of avibactam and AMA. The efficiency of the β-lactam/β-lactamase inhibitor combinations was then evaluated based on the minimum concentration of AMA needed to restore meropenem MIC to its European Committee on Antimicrobial Susceptibility

Testing (EUCAST) breakpoint of 2 µg/mL while maintaining the concentration of avibactam at 4 µg/mL [47].

A. baumannii expressing either NDM-1/KPC-2 or KPC-2/NDM-1 remain resistant to meropenem in the absence of avibactam even at an AMA concentration of 64 µg/mL (Table 3 and Supplemental Table 6). This is because KPC-2 possesses carbapenemase activity, and as an SBL it is not affected by AMA [18,48]. These *A. baumannii* strains also possess high-level resistance to meropenem when only avibactam is employed as a β-lactamase inhibitor, as this does not inhibit MBLs [46]. However, meropenem activity is restored upon adding both AMA (8–16 µg/mL) and avibactam (4 µg/mL) (Table 4.3 and Supplemental Table 4.6). *A. baumannii* strains expressing NDM-1/CMY-2 or CMY-2/NDM-1 required an AMA concentration of 8 µg/mL to rescue meropenem activity both in the absence and the presence of avibactam (Table 4.3 and Supplemental Table 4.6). Comparable results were observed upon introducing the remainder of the constructs into the *A. baumannii* strains. These results are consistent with NDM-1 being inhibited by AMA [18], while CTX-M-15 and CMY-2 are susceptible to meropenem due to a lack of carbapenemase activity [40,49]. While OXA-48 seems to demonstrate meropenem susceptibility, this β-lactamase has previously been shown to possess significant carbapenemase activity in *K. pneumoniae* [50]. Therefore, OXA-48 may need to be codon-optimized to obtain optimal carbapenemase activity. In addition, OXA-48 could be substituted for an OXA enzyme which is predominantly found in *A. baumannii* such as OXA-23, OXA-24/40, OXA-51, OXA-58 or OXA-143 [51]. Overall, these results indicate that antibiotic adjuvants such as AMA and avibactam can re-sensitize *A.*

baumannii to existing antibiotics such as meropenem, even in strains producing multiple common β-lactamases [52–56].

Table 4.3: Concentration of AMA needed to restore the activity of meropenem to its susceptibility breakpoint concentration against *A. baumannii* ATCC 17978 strains producing two β-lactamases.[a] All assays were conducted in duplicate. This table shows the results from replicate 1.

β-Lactamase		**[AMA] at 2 µg/mL of MEM in different combinations (µg/mL)** [b, c]		
Gene 1	**Gene 2**	**AMA/ MEM**	**AVI/ MEM**	**AMA/AVI/ MEM**
NDM-1	KPC-2	> 64	64	16
KPC-2	NDM-1	> 64	64	8
NDM-1	CTX-M-15	16	32	16
CTX-M-15	NDM-1	8	32	16
NDM-1	CMY-2	8	16	8
CMY-2	NDM-1	16	16	8
NDM-1	OXA-48	8	16	16
OXA-48	NDM-1	8	16	16

Abbreviations: AMA aspergillomarasmine A, AVI avibactam, MEM meropenem.
[a] Both β-lactamase genes were cloned into pROTO2 with individual promoters.
[b] 2 µg/mL is the EUCAST susceptibility breakpoint concentration for MEM.
[c] AVI was maintained at 4 µg/mL, except during the AVI/MEM combination.

4.6 DISCUSSION

Multidrug-resistant and carbapenem-resistant *A. baumannii* and *P. aeruginosa* are among the most critical priority pathogens, according to the World Health Organization [1,2]. The discovery of antibiotic adjuvants, especially those capable of inhibiting β-lactamase enzymes, provides an alternative therapeutic strategy for suppressing the resistance of these pathogens [11]. As the ARP is a valuable tool for the study of antibiotic resistance and adjuvant discovery in Enterobacterales such as *E. coli*, we sought to broaden the host

range of this platform by creating a series of pGDP-derived vectors capable of propagating in *A. baumannii* and *P. aeruginosa*. These plasmids were constructed by inserting origins of replication known to function in *Acinetobacter* (ori1266 from pFLP2) and *Pseudomonas* (pRO1600 oriV from pMS402) into the pGDP vector series used in the ARP. In total, four *Escherichia-Acinetobacter* and four *Escherichia-Pseudomonas* shuttle vectors containing different promoters (P_{Bla} for pROTO/pROKA series 1 and 3, and P_{Lac} for pROTO/pROKA series 2 and 4) and selectable markers (*aph(3')-Ia* for pROTO1–2, *ant(2'')-Ia* for pROKA1–2, and bla_{TEM-1} pROTO/pROKA series 3 and 4) were generated (Figures 4.1, 4.2).

We extensively tested pROTO and pROKA using four antibiotic resistance genes commonly found in Gram-negative bacteria. We used antibiotic susceptibility testing to confirm that bla_{NDM-1}, $bla_{CTX-M-15}$, *ant(2″)-Ia*, and *aac(6′)-Ib10* were expressed and functional in the pROTO and pROKA shuttle vectors (Tables 4.1, 4.2 and Supplemental Tables 4.1, 4.2, 4.3, 4.4). Our vectors successfully replicated the known resistance phenotypes associated with these four genes in *E. coli,* two strains of *A. baumannii,* and two strains of *P. aeruginosa* (Tables 4.1, 4.2). Our results show that increased resistance is conferred in *A. baumannii* ATCC 19606 compared to *A. baumannii* ATCC 17978 across all pROTO constructs due to higher innate resistance (Table 4.1). This finding is corroborated by previous reports suggesting that ATCC 19606 has stronger efflux pump activity than ATCC 17978 [57]. On the other hand, pROKA constructs gave similar antibiograms between both *P. aeruginosa* strains (Table 4.2).

Key features of the original ARP are retained in the pROTO and pROKA series, such as variable expression levels through the choice of two promoters (Tables 4.1, 4.2 and Supplemental Tables 4.1, 4.2) and the availability of both N- and C-terminal 6×His-tags to monitor expression (Supplemental Tables 4.3, 4.4). The ability to choose between high and low levels of expression allows users to mitigate the overexpression of toxic proteins or to produce more protein for purification. In the case of antibiotic resistance genes, the MIC can also be raised or lowered to better approximate resistance levels seen in clinical isolates or improve performance in a high-throughput screen. Most importantly, because the pROTO and pROKA series share a common MCS with the pGDP series, the entire catalogue of over 100 resistance genes contained in the ARP can effectively be shuttled into *A. baumannii* and/or *P. aeruginosa*. The standardized nature of this system will simplify the study of antibiotic resistance mechanisms in a wider range of pathogens. We anticipate that this vector series may also be generally useful for the study of *A. baumannii* and *P. aeruginosa* biology, beyond the study of antibiotic resistance.

The development of the pROTO and pROKA series will allow users to screen for novel antibiotic adjuvants directly in Pseudomonadales, using the same methodology we detailed previously for *E. coli*. Both *A. baumannii* and *P. aeruginosa* possess several efflux pumps and formidable outer membrane permeability barriers [4,10]. Screening directly in these strains prevents wasted time on adjuvants that are susceptible to active efflux or cannot enter these cells, and enables the discovery of narrow-spectrum adjuvants. Problematic resistance genes in *A. baumannii* and *P. aeruginosa* already found in the ARP represent good candidates for future adjuvant screening. For *A. baumannii*,

these genes include *bla*$_{\text{NDM-1}}$, *bla*$_{\text{TEM-1}}$, *bla*$_{\text{VEB-1}}$, *bla*$_{\text{IMP-1}}$, *bla*$_{\text{KPC-2}}$, *rmtB, ant(2″)-Ia, aac(3)-Ia, armA, aph(4)-Ia, aac(6′)-Ib, aac(6′)-Ib-cr, aph(3′)-Ia, aph(3′)-VIa, tet(A), tet(M), tet(X), qnrA1, erm(C),* and *mph(A)* since β-lactam, aminoglycoside, tetracycline, quinolone, and macrolide resistance are increasingly prevalent in this pathogen due to the presence of these resistance genes [58]. Therapeutics which could reverse this resistance would undoubtedly aid in the fight against *A. baumannii*.

Finally, we used the pROTO series to study the efficacy of a dual adjuvant therapy against multiple β-lactamase producing *A. baumannii*. Bacteria that produce multiple classes of β-lactamases can resist essentially all β-lactam antibiotics, making them a significant threat to public health [8,9]. We constructed tandem β-lactamase expressing pROTO constructs to systematically explore the inhibitory potency of an AMA/ avibactam/meropenem combination on *A. baumannii* strains expressing multiple β-lactamase enzymes. We show that an AMA/avibactam/meropenem combination is effective against *A. baumannii* strains producing both an MBL and an SBL, especially if these enzymes have carbapenemase activity such as NDM-1 and KPC-2 (Table 4.3 and Supplemental Table 4.6). These results demonstrate that antibiotic adjuvants, specifically those inhibiting MBL activity, can be employed to rescue the activity of β-lactam antibiotics against carbapenem-resistant *A. baumannii*.

The pROTO and pROKA shuttle vectors described here will be useful tools to broadly study *A. baumannii* and *P. aeruginosa* both in terms of antibiotic resistance (e.g., expression of resistance genes, investigation of antibiotic adjuvants) and infection (e.g., virulence, biofilm formation).

4.7 MATERIALS AND METHODS

4.7.1 Detailed construction of the pROTO vectors

The pROTO shuttle vectors (Figure 4.1) were assembled by combining PCR amplicons with the pGDP plasmids from the ARP [19]. Briefly, pROTO1 was constructed by ligating two DNA fragments originating from: (i) the pGDP1 plasmid, which provided the pMB1 origin of replication for plasmid maintenance in *E. coli* [19,21]; and (ii) the pFLP2 plasmid, which encompassed ori1266 to permit plasmid replication in *Acinetobacter* spp. [59,60]. The 3149-bp fragment corresponding to the entire sequence of the pGDP1 plasmid was obtained by Psp1406I (AclI) digestion. The digested pGDP1 fragment not only supplied the pMB1 ori, but also contained a the constitutive P_{Bla} promoter, the 6×His motifs, the MCS, and the *aph(3')-Ia* gene for kanamycin resistance [19]. The 1384-bp fragment containing ori1266 was obtained through PCR amplification of pFLP2 using the EASV-AclI-FWD and EASV-AclI-REV primers (Supplemental Table 4.7). Both fragments were ligated using Gibson Assembly and transformed into *E. coli* TOP10 cells. Selection of pROTO1 was conducted on Luria-Bertani (LB) agar supplemented with 50 µg/mL of kanamycin.

To generate *Escherichia-Acinetobacter* shuttle vectors capable of varying gene expression levels, the pGDP1 fragment was replaced with Psp1406I digested pGDP2. Following ligation with ori1266, the resulting plasmid, named pROTO2, contained the weaker P_{Lac} promoter. Furthermore, aiming to express a broader range of antibiotic resistance genes, the *Escherichia-Acinetobacter* shuttle vectors were assembled using Eco47III (AfeI) digested pGDP3 or pGDP4 instead of the pGDP2 fragment. The 3,281-bp

or 3,163-bp fragment corresponding to the entirety of the pGDP3 or pGDP4 plasmids, respectively, were ligated with an ori1266 amplicon acquired through PCR of the pFLP2 plasmid using the EASV-AfeI-FWD and EASV-AfeI-REV primers (Supplemental Table 4.7). The resulting plasmids, named pROTO3 and pROTO4, contained a *bla*$_{\text{TEM-1}}$ gene to allow for selection on ampicillin or carbenicillin. Once constructed, all plasmid sequences were verified by Sanger sequencing.

4.7.2 Detailed construction of the pROKA vectors

The pROKA shuttle vectors (Figure 4.2) were constructed by joining various PCR amplicons with the pGDP plasmids. Briefly, pROKA1 was generated following the ligation of three DNA fragments stemming from: (i) the pGDP1 plasmid; (ii) the pMS402 plasmid, which contained the pRO1600 oriV and pRO1600 replication protein required for plasmid maintenance in *Pseudomonas* spp. [61,62]; and (iii) the *ant(2'')-Ia* gene for gentamicin resistance. The 3,149-bp fragment corresponding to the entire sequence of the pGDP1 plasmid was obtained by Eco47III digestion. The 1,241-bp fragment containing pRO1600 was acquired by PCR amplification of pMS402 using the EPSV-AfeI-FWD and EPSV-AfeI-REV primers (Supplemental Table 4.7). Ligation of both fragments was achieved through Gibson Assembly before transformation into *E. coli* TOP10 cells. Selection was conducted on LB agar supplemented with 50 µg/mL of kanamycin. Colony PCR was used to identify positive colonies. Following isolation and purification of plasmid DNA from the colonies, high-fidelity PCR was conducted using the KAN-Out-FWD and KAN-Out-REV primers (Supplemental Table 4.7) to remove the kanamycin selectable marker from the plasmid. Gibson Assembly was then employed to combine the

resulting plasmid amplicon with the *ant(2'')-Ia* gene. The 576-bp fragment containing the *ant(2'')-Ia* gene was obtained by PCR with the EPSV+ANT-FWD and EPSV+ANT-REV primers (Supplemental Table 4.7), using the pGDP3:ANT(2")-Ia plasmid from the ARP as a template. Following ligation, pROKA1 was transformed into *E. coli* TOP10 cells before conducting plasmid selection on LB agar supplemented with 20 µg/mL of gentamicin.

To construct *Escherichia-Pseudomonas* shuttle vectors capable of varying gene expression levels, the pGDP1 fragment was substituted for Psp1406I digested pGDP2. The 3,101-bp fragment corresponding to the entirety of the pGDP2 plasmid was ligated with a pRO1600 amplicon obtained through the PCR of the pMS402 plasmid using the EPSV-AclI-FWD and EPSV-AclI-REV primers (Supplemental Table 4.7). Following insertion of the gentamicin selectable marker as described above, the resulting plasmid, named pROKA2, contained the weaker P_{Lac} promoter. Furthermore, to study a broader range of antibiotic resistance genes, the *Escherichia-Pseudomonas* shuttle vectors were assembled using Eco47III digested pGDP3 or pGDP4 instead of the pGDP1 fragment. Following ligation with pRO1600, the resulting plasmids were named pROKA3 and pROKA4. Once constructed, all plasmid sequences were verified by Sanger sequencing.

4.7.3 Culture Media

Bacterial strains employed in this study were grown in LB broth or on LB agar plates at a temperature of 37°C. Kanamycin, gentamicin, ampicillin and carbenicillin were added when plasmid selection was required. A concentration of kanamycin of 50 µg/mL was utilized for all strains containing the pROTO1 and pROTO2 plasmids while 20 µg/mL of

gentamicin was to culture all strains containing the pROKA1 and pROKA2 plasmids. The ampicillin concentration for *E. coli* strains and *A. baumannii* ATCC 17978 containing the pROTO3 and pROTO4 plasmids was 100 µg/mL. A carbenicillin concentration of 250 µg/mL was employed for *E. coli* and *P. aeruginosa* strains containing the pROKA3 and pROKA4 plasmids. This same concentration of carbenicillin was added for *A. baumannii* ATCC 19606 strains containing the pROTO3 and pROTO4 plasmids as well as *E. aerogenes* strains containing the pROTO3, pROTO4, pROKA3 and pROKA4 plasmids. Finally, a concentration of 50 µg/mL of kanamycin was used in the selection of *K. pneumoniae* strains containing the pROTO3, pROTO4, pROKA3 and pROKA4 plasmids. However, if the empty plasmids were being transformed into *K. pneumoniae* ATCC 33495, 100 µg/mL of ampicillin was employed as a selection marker.

4.7.4 DNA manipulations

The β-lactamases and aminoglycoside modifying enzymes subsequently cloned into the pROTO/pROKA shuttle vectors were obtained from the ARP [19]. Each gene bared the same sequence as found in the Comprehensive Antibiotic Resistance Database [39]. The genes were amplified from the ARP plasmids using the Thermo Scientific Phusion High-Fidelity DNA Polymerase and the primers shown in Supplemental Table 4.8, which were purchased from Integrated DNA Technologies (IDT; Coralville, Iowa). The appropriate FastDigest enzymes (Thermo Fisher Scientific, Waltham, MA) were employed to digest the PCR fragment prior to their ligation into the shuttle vectors using T4 DNA Ligase (Thermo Fisher Scientific). All gene sequences were verified by Sanger sequencing.

4.7.5 Preparation of *E. coli* chemically competent cells

A volume of 100 mL of PSI broth (0.5 g of bacto yeast extract; 2.0 g of bacto tryptone; 0.5 g of $MgSO_4$; pH 7.6) was inoculated with 1 mL from an overnight culture of *E. coli* BW25113 wild-type or *E. coli* BW25113 Δ*bamB*Δ*tolC*. Cultures were incubated at 37°C with shaking (250 rpm) until the optical density at 550 nm (OD_{550}) reached 0.48 and then placed on ice for 15 min. Cells were harvested by centrifugation (5,000 × *g*; 5 min; 4°C) prior to being resuspended in 40 mL of TfbI [0.59 g of 30 mM CH_3CO_2K, 2.42 g of 100 mM RbCl, 0.22 g of 10 mM $CaCl_2$, 2.00 g of 50 mM $MnCl_2$, 30 mL of 15% (v/v) glycerol, pH 5.8 per 200 mL]. Cells were then placed on ice for 15 min and then once again harvested by centrifugation (5,000 × *g*; 5 min; 4°C). Following removal of the supernatant, cells were resuspended in 4 mL of TfbII [0.21 g of 10 mM MOPS, 0.12 g of 10 mM RbCl, 0.83 g of 75 mM $CaCl_2$, 15 mL of 15% (v/v) glycerol, pH 6.5 per 100 mL]. Cells were then chilled for 15 min before being separated into 50–200 µL aliquots and stored at –80°C until required.

4.7.6 Preparation of *E. aerogenes* and *A. baumannii* electrocompetent cells

A volume of 100 mL of LB media was inoculated with 1 mL from an overnight culture of *E. aerogenes* ATCC 13048, *A. baumannii* ATCC 17978 or *A. baumannii* ATCC 19606. The inoculated media were inoculated at 37°C with shaking (250 rpm) until the OD_{595} reached 0.50–0.60. Cells were harvested by centrifugation (5,000 rpm; 10 min; 4°C) and then resuspended in 5 mL of cold water. This centrifugation and resuspension step was repeated once. Cultures were once again centrifuged (5,000 rpm; 10 min; 4°C) prior to being resuspended in 5 mL of 10% (v/v) glycerol. Cells then underwent one final

centrifugation (5,000 rpm; 10 min, 4°C) before resuspension in 1 mL of 10% (v/v) glycerol and separation into 50–100 µL aliquots, which were stored at –80°C for further use.

4.7.7 Preparation of *K. pneumoniae* electrocompetent cells

A volume of 200 mL of LB media was inoculated with 20 mL from an overnight culture of *K. pneumoniae* ATCC 33495. The inoculated media were inoculated at 37°C with shaking (250 rpm) until the OD_{550} reached 0.50–0.53. Once the desired OD was reached, $MgCl_2$ and $MgSO_4$ were added at a final concentration of 10 mM each. Following incubation (10 min, 37°C, 250 rpm), cultures were transferred to a water bath at 42°C for 3 min with gentle shaking to ensure uniform heat distribution. Cultures were once again incubated with shaking for 20 min at 37°C before being placed in an ice bath for 20 min. Cells were then harvested by centrifugation (3,500 rpm; 10 min; 4°C) and resuspended in 20 mL of cold 10% (v/v) glycerol. This centrifugation and resuspension step was repeated once. Cells then underwent one final centrifugation (3,500 rpm; 10 min; 4°C) before being resuspended in 2 mL of cold 10% (v/v) glycerol. Aliquots containing 50–100 µL of cells were prepared and stored at –80°C until required.

4.7.8 Preparation of *P. aeruginosa* electrocompetent cells

P. aeruginosa electrocompetent cells were prepared based on the microcentrifuge protocol described in reference [63]. Briefly, a volume of 6 mL of LB media was inoculated with a *P. aeruginosa* PAO1 or *P. aeruginosa* PA14 colony and kept in a shaking incubator (37°C, 250 rpm) overnight. The cells were harvested by centrifugation (16,000 × *g*; 2 min) in four microcentrifuge tubes. The pellets were washed three times

with 1 mL of 300 mM sucrose. The four pellets were then resuspended in 25 µL of 300 mM sucrose, combined, and stored at –80°C for further use.

4.7.9 Chemical transformation

Chemically competent cells were thawed on ice. Typically for *E. coli*, a volume of 49.5 µL of cells was mixed with 0.5 µL of DNA. The mixtures were incubated on ice for 30 min. Cells were then placed in a heat block at 42°C for 1 min before being placed on ice for 5 min. Following the addition of 200 µL of LB, the cultures were incubated at 37°C with shaking (250 rpm) for 1 h. A volume of 100 µL was plated on LB agar plates containing the appropriate antibiotic.

4.7.10 Electroporation transformation

Electrocompetent cells were thawed on ice. Typically for *K. pneumoniae*, *A. baumannii* and *E. aerogenes*, a volume of 49.5 µL of cells was mixed with 0.5 µL of DNA. However, in the case of *P. aeruginosa*, a volume of 27 µL of cells was mixed with 3 µL of DNA. The mixtures were incubated on ice for 1 min. Cells were then placed in a 1 mm electroporation cuvette and shaken down before pulsed using a Gene Pulser set to 25 µF and 2.5 kV for a time constant of 4–5 msec. A volume of 1 mL of LB was added to the cuvettes immediately following their removal from the Gene Pulser and the entire solution was well mixed. Cultures were then incubated at 37°C with shaking (250 rpm) for 1 h. A volume of 200 µL was plated on LB agar plates containing the appropriate antibiotic. Prior to plating, a 1/10 or 1/100 dilution was performed for the *K. pneumoniae* and *P. aeruginosa* cultures while a two-fold to five-fold increase in concentration was

conducted for the *E. aerogenes* and *A. baumannii* cultures to ensure the acquisition of single colonies on the transformation plates.

4.7.11 Cell-based assays

All cell-based assays were conducted in 96-well round base microtest plates (Sarstedt, Nümbrecht, Germany). In addition, all assays were performed in a final volume of 100 µL. To begin, meropenem and avibactam were dissolved in dimethyl sulfoxide (DMSO) while AMA was diluted in water containing ≤ 5% (v/v) ammonium hydroxide (NH_4OH). All other β-lactam and aminoglycoside antibiotics were dissolved in water. Filter sterilization was used to ensure the sterility of compounds where water was used as a solvent.

MIC assays were conducted based on the protocol described in reference [64] and began with the preparation of ten two-fold dilutions of the compounds, which were subsequently pipetted into columns 1 to 10 of the microtest plate. Overnight petri dishes containing the bacterial cells of interest were then employed in the preparation of a bacterial inoculum with an OD_{625} of 0.08–0.10. The bacterial inoculum was then added to columns 1 to 11 of the microtest plate following a 200-fold dilution using cation-adjusted Mueller Hinton II broth (CAMHB; BD, Sparks, MD). Column 11 served as a growth control as it contained no antibiotic. As a sterility control, the CAMHB used in the dilution of the bacterial inoculum was added to column 12. Following overnight incubation, the MIC value was reported as the lowest concentration of β-lactam or aminoglycoside antibiotic showing no bacterial growth.

Two-dimensional checkerboard assay were conducted using a similar protocol as previously described in reference [65]. Briefly, eight two-fold dilutions of the first compound (0.5–64 µg/mL) were pipetted along the x-axis of the microtest plate while eight two-fold dilutions of the second compound (0.5–64 µg/mL) were added along the y-axis of the microtest plate. For β-lactam potentiation assays, the third compound, which was typically meropenem, was added along both axes of the microtest plate at its EUCAST susceptibility breakpoint concentration of 2 µg/mL [47]. The bacterial inoculum, prepared as described above, was also added to both axes of the microtest plate. The last four columns of the microtest plate served as growth, sterility, and MIC value verification controls. Therefore, these columns contained either the bacterial inoculum, CAMHB or eight two-fold dilutions of the compounds.

Once completed, all microtest plates were placed in a static incubator for 20 h at 37°C. Following incubation, microtest plates containing *E. coli* were shaken for five minutes to resuspend bacterial colonies. However, *K. pneumoniae, E. aerogenes, A. baumannii* and *P. aeruginosa* cells were resuspended manually using a pipette to minimize the formation of aerosols. Once the cells were resuspended, the plates were read spectrophotometrically at a wavelength of 600 nm using a BioTek Synergy H1 plate reader (BioTek, Winooski, VT). All cell-based assays were conducted in duplicate.

4.7.12 Construction of tandem β-lactamase expression vectors

The pGDP2 plasmids expressing a single β-lactamase gene were constructed as described previously [65]. These plasmids were then used as the foundation for cloning in the second β-lactamase gene. The construction of the pGDP2:NDM-1/KPC-2 began with the

PCR amplification of NDM-1 from the pGDP2:NDM-1 plasmid using the pGDP2-BglII-FWD and pGDP2-BglII-REV primers (Supplemental Table 4.9). These primers were designed to amplify the regions of approximately 20 nucleotides upstream and downstream of the BglII recognition site. As a result of this primer design, Gibson assembly was employed to insert the purified NDM-1 DNA into a BglII digested pGDP2:KPC-2 plasmid. Psp1406I digestion was then conducted to obtain a 5,123-bp fragment corresponding to the entire sequence of pGDP2:NDM-1/KPC-2. This fragment was then ligated with an ori1266 amplicon acquired through PCR of the pFLP2 plasmid using the EASV-AclI-FWD and EASV-AclI-REV primers (Supplemental Table 4.1). The pROTO2 plasmids expressing KPC-2/NDM-1, NDM-1/CMY-2, CMY-2/NDM-1, and NDM-1/OXA-48 were constructed as described above.

The construction of the pROTO2 plasmid expressing OXA-48/NDM-1 began with the NcoI/XhoI digestion of pGDP2:NDM-1 (constructed as described in reference [65]) and empty pROTO2 (constructed as described above). These two DNA fragments were then ligated using T4 DNA ligase. The resulting pROTO2:NDM-1 plasmid was subjected to PCR amplification using the pROTO2-BglII-FWD and pROTO2-BglII-REV primers (Supplemental Table 4.9). Using Gibson Assembly, this 5,192-bp amplicon was then ligated to an OXA-48 amplicon acquired through PCR of pGDP2:OXA-48 (constructed as described in reference [65]) with the pGDP2-NcoI-FWD and pGDP2-XhoI-REV primers (Supplemental Table 4.9). The pROTO2 plasmids expressing NDM-1/CTX-M-15 and CTX-M-15/NDM-1 were constructed as described above.

All plasmid sequences were verified by Sanger sequencing prior to their transformation into electrocompetent *A. baumannii* ATCC 17978 cells.

4.8 ACKNOWLEDGEMENTS

This research was funded by a Canadian Institutes of Health Research grant (FRN-148463). We also thank Dr. Ayush Kumar (University of Manitoba) and Dr. Lori Burrow (McMaster University) for respectively gifting us with the pFLP2 and pMS402 plasmids required for this research.

4.9 REFERENCES

1. Carmeli, Y., Harbarth, S., Kahlmeter, G., Kluytmans, J., Mendelson, M., Pulcini, C., Singh, N., and Theuretzbacher, U. (2017) Global priority list of antibiotic-resistant bacteria to guide research, discovery, and development of new antibiotics. WHO (World Health Organization).

2. WHO (World Health Organization) News. (2017) WHO publishes list of bacteria for which new antibiotics are urgently needed. [Online]. Retrieved June 2022 from: https://www.who.int/news/item/27-02-2017-who-publishes-list-of-bacteria-for-which-new-antibiotics-are-urgently-needed.

3. Peleg, A.Y., Seifert, H., and Paterson, D.L. (2008) *Acinetobacter baumannii*: Emergence of a Successful Pathogen. *Clin. Microbiol. Rev.*, **21**: 538–582.

4. Maragakis, L.L. and Perl, T.M. (2008) *Acinetobacter baumannii*: Epidemiology, Antimicrobial Resistance, and Treatment Options. *Clin. Infect. Dis.*, **46**: 1254–1263.

5. Ruffin, M. and Brochiero, E. (2019) Repair Process Impairment by *Pseudomonas aeruginosa* in Epithelial Tissues: Major Features and Potential Therapeutic Avenues. *Front. Cell. Infect. Microbiol.*, **9**: 182.

6. Diggle, S.P. and Whiteley, M. (2020) Microbe profile: *Pseudomonas aeruginosa*: opportunistic pathogen and lab rat. *Microbiology*, **166**: 30–33.

7. Morin, C.D., Déziel, E., Gauthier, J., Levesque, R.C., and Lau, G.W. (2021) An Organ System-Based Synopsis of *Pseudomonas aeruginosa* Virulence. *Virulence*, **12**: 1469–1507.

8. Leungtongkam, U., Thummeepak, R., Tasanapak, K., and Sitthisak, S. (2018) Acquisition and transfer of antibiotic resistance genes in association with conjugative plasmid or class 1 integrons of *Acinetobacter baumannii*. *PLoS One*, **13**: e0208468.

9. Pang, Z., Raudonis, R., Glick, B.R., Lin, T.J., and Cheng, Z. (2019) Antibiotic resistance in *Pseudomonas aeruginosa*: mechanisms and alternative therapeutic strategies. *Biotechnol. Adv.*, **37**: 177–192.

10. Kievit, T. De., Parkins, M., Gillis, R., Srikumar, R., Ceri, H., Poole, K., Iglewski, B., and Storey, D. (2001) Multidrug efflux pumps: expression patterns and contribution to antibiotic resistance in *Pseudomonas aeruginosa* biofilms. *Antimicrob. Agents Chemother.*, **45**: 1761–1770.

11. Wright, G.D. (2016) Antibiotic Adjuvants: Rescuing Antibiotics from Resistance.

Trends Microbiol., **24**: 862–871.

12. Reading, C. and Cole, M. (1977) Clavulanic Acid: a Beta-Lactamase-Inhibiting Beta-Lactam from *Streptomyces clavuligerus*. *Antimicrob. Agents Chemother.*, **11**: 852–857.

13. Di Conza, J.A., Badaracco, A., Ayala, J., Rodriguez, C., Famiglietti, Á., and Gutkind, G.O. (2014) β-lactamases produced by amoxicillin-clavulanate-resistant enterobacteria isolated in Buenos Aires, Argentina: A new *bla*$_{TEM}$ gene. *Rev. Argentina Micrología*, **46**: 210–217.

14. Yusuf, E., Bax, H.I., Verkaik, N.J., and van Westreenen, M. (2021) An Update on Eight "New" Antibiotics against Multidrug-Resistant Gram-Negative Bacteria. *J. Clin. Med.*, **10**: 1068.

15. Rotondo, C.M. and Wright, G.D. (2017) Inhibitors of metallo-β-lactamases. *Curr. Opin. Microbiol.*, **39**: 96–105.

16. Tehrani, K.H.M.E. and Martin, N.I. (2018) β-lactam/β-lactamase inhibitor combinations: an update. *Med. Chem. Comm.*, **9**: 1439–1456.

17. Tooke, C.L., Hinchliffe, P., Bragginton, E.C., Colenso, C.K., Hirvonen, V.H.A., Takebayashi, Y., and Spencer, J. (2019) β-Lactamases and β-Lactamase Inhibitors in the 21st Century. *J. Mol. Biol.*, **431**: 3472–3500.

18. King, A.M., Reid-Yu, S.A., Wang, W., et al. (2014) Aspergillomarasmine A overcomes metallo-β-lactamase antibiotic resistance. *Nature*, **510**: 503–506.

19. Cox, G., Sieron, A., King, A.M., De Pascale, G., Pawlowski, A.C., Koteva, K., and Wright, G.D. (2017) A Common Platform for Antibiotic Dereplication and Adjuvant Discovery. *Cell Chem. Biol.*, **24**: 98–109.

20. Zubyk, H.L., Cox, G., and Wright, G.D. (2019) Antibiotic Dereplication Using the Antibiotic Resistance Platform. *J. Vis. Exp.*, **2019**: e60536.

21. Sutcliffe, J.G. (1979) Complete Nucleotide Sequence of the *Escherichia coli* Plasmid pBR322. *Cold Spring Harb Symp Quant Biol*, **43**: 77–90.

22. Gallique, M., Wei, K., Maisuria, V.B., Okshevsky, M., Mckay, G., Nguyen, D., and Tufenkji, N. (2021) Cranberry-Derived Proanthocyanidins Potentiate β-Lactam Antibiotics against Resistant Bacteria. *Appl. Environ. Microbiol.*, **87**: e00127-21.

23. Biswas, I. (2015) Genetic tools for manipulating Acinetobacter baumannii genome: An overview. *J. Med. Microbiol.*, **64**: 657–669.

24. Schweizer, H.P. and de Lorenzo, V. (2004) Molecular Tools for Genetic Analysis

of Pseudomonads. Ramos, J.L., editor. *Pseudomonas*. Boston, MA: Springer. pp. 317–350.

25. Biedenbach, D.J., Kazmierczak, K., Bouchillon, S.K., Sahm, D.F., and Bradford, P.A. (2015) *In Vitro* Activity of Aztreonam-Avibactam against a Global Collection of Gram-Negative Pathogens from 2012 and 2013. *Antimicrob Agents Chemother*, **59**: 4239–4248.

26. Mhlongo, N., Essack, S., and Govinden, U. (2015) NDM-1, novel TEM-205, novel TEM-213 and other extended-spectrum β-lactamases co-expressed in isolates from cystic fibrosis patients from South Africa. *South. African J. Infect. Dis.*, **30**: 103–107.

27. Suzuki, Y., Ida, M., Kubota, H., et al. (2019) Multiple β-Lactam Resistance Gene-Carrying Plasmid Harbored by *Klebsiella quasipneumoniae* Isolated from Urban Sewage in Japan. *mSphere*, **4**: e00391-19.

28. Li, Q., Chang, W., Zhang, H., Hu, D., and Wang, X. (2019) The Role of Plasmids in the Multiple Antibiotic Resistance Transfer in ESBLs-Producing *Escherichia coli* Isolated From Wastewater Treatment Plants Qing. *Front. Microbiol.*, **10**: 633.

29. Okii, M., Iyobe, S., and Mitsuhashi, S. (1983) Mapping of The Gene Specifying Aminoglycoside 3′-Phosphotransferase II on the *Pseudomonas aeruginosa* Chromosome. *J. Bacteriol.*, **155**: 643–649.

30. Sabath, L.D., Jago, M., and Abraham, E.P. (1965) Cephalosporinase and Penicillinase Activities of a β-Lactamase from *Pseudomonas pyocyanea*. *Biochem. J.*, **96**: 739–752.

31. Berrazeg, M., Jeannot, K., Ntsogo Enguéné, V.Y., Broutin, I., Loeffert, S., Fournier, D., and Plésiat, P. (2015) Mutations in β-Lactamase AmpC Increase Resistance of *Pseudomonas aeruginosa* Isolates to Antipseudomonal Cephalosporins. *Antimicrob. Agents Chemother.*, **59**: 6248–6255.

32. Choi, K.H. and Schweizer, H.P. (2005) An improved method for rapid generation of unmarked *Pseudomonas aeruginosa* deletion mutants. *BMC Microbiol.*, **5**: 30.

33. Wang, T., Du, X., Ji, L., et al. (2021) *Pseudomonas aeruginosa* T6SS-mediated molybdate transport contributes to bacterial competition during anaerobiosis. *Cell Rep.*, **35**: 108957.

34. Grenier, F., Matteau, D., Baby, V., and Rodrigue, S. (2014) Complete Genome Sequence of *Escherichia coli* BW25113. *Genome Announc.*, **2**: e01038-14.

35. Kröger, C., MacKenzie, K.D., Alshabib, E.Y., et al. (2018) The primary

transcriptome, small RNAs and regulation of antimicrobial resistance in *Acinetobacter baumannii* ATCC 17978. *Nucleic Acids Res.*, **46**: 9684–9698.

36. Hamidian, M., Blasco, L., Tillman, L.N., To, J., Tomas, M., and Myers, G.S.A. (2020) Analysis of Complete Genome Sequence of *Acinetobacter baumannii* Strain ATCC 19606 Reveals Novel Mobile Genetic Elements and Novel Prophage. *Microorganisms*, **8**: 1851.

37. LaBauve, A.E. and Wargo, M.J. (2012) Growth and Laboratory Maintenance of *Pseudomonas aeruginosa*. *Curr. Protoc. Microbiol.*, **Chapter 6**: Unit–6E.1.

38. Zohra, T., Numan, M., Ikram, A., et al. (2021) Cracking the Challenge of Antimicrobial Drug Resistance with CRISPR/Cas9, Nanotechnology and Other Strategies in ESKAPE Pathogens. *Microorganisms*, **9**: 954.

39. Alcock, B.P., Raphenya, A.R., Lau, T.T.Y., et al. (2020) CARD 2020: Antibiotic resistome surveillance with the comprehensive antibiotic resistance database. *Nucleic Acids Res.*, **48**: D517–D525.

40. Poirel, L., de la Rosa, J.M.O., Richard, A., Aires-de-Sousa, M., and Nordmann, P. (2019) CTX-M-33 is a CTX-M-15 Derivative Conferring Reduced Susceptibility to Carbapenems. *Antimicrob. Agents Chemother.*, **63**: e01515-19.

41. Ramirez, M.S. and Tolmasky, M.E. (2010) Aminoglycoside Modifying Enzymes. *Drug Resist Updat*, **13**: 151–171.

42. Sabaty, M., Grosse, S., Adryanczyk, G., Boiry, S., Biaso, F., Arnoux, P., and Pignol, D. (2013) Detrimental effect of the 6 His C-terminal tag on YedY enzymatic activity and influence of the TAT signal sequence on YedY synthesis. *BMC Biochem.*, **14**: 28.

43. Manchanda, V., Sinha, S., and Singh, N. (2010) Multidrug Resistant *Acinetobacter*. *J. Glob. Infect. Dis.*, **2**: 291–304.

44. King, D.T., Sobhanifar, S., and Strynadka, N.C.J. (2016) One ring to rule them all: Current trends in combating bacterial resistance to the β-lactams. *Protein Sci.*, **25**: 787–803.

45. Bebrone, C. (2007) Metallo-β-lactamases (classification, activity, genetic organization, structure, zinc coordination) and their superfamily. *Biochem. Pharmacol.*, **74**: 1686–1701.

46. Lence, E. and González-Bello, C. (2021) Bicyclic Boronate *β*-Lactamase Inhibitors: The Present Hope against Deadly Bacterial Pathogens. *Adv. Ther.*, **4**: 2000246.

47. The European Committee on Antimicrobial Susceptibility Testing. (2022) Breakpoint tables for interpretation of MICs and zone diameters, Version 12.0. [Online]. Retrieved June 2022 from: https://www.eucast.org/clinical_breakpoints/.

48. Ke, W., Bethel, C.R., Thomson, J.M., Bonomo, R.A., and van den Akker, F. (2007) Crystal structure of KPC-2: insights into carbapenemase activity in Class A β-lactamases Wei. *Biochemistry*, **46**: 5732–5740.

49. Goessens, W.H.F., van Der Bij, A.K., van Boxtel, R., Pitout, J.D.D., van Ulsen, P., Melles, D.C., and Tommassen, J. (2013) Antibiotic Trapping by Plasmid-Encoded CMY-2 β-Lactamase Combined with Reduced Outer Membrane Permeability as a Mechanism of Carbapenem Resistance in *Escherichia coli*. *Antimicrob. Agents Chemother.*, **57**: 3941–3949.

50. Singkham-In, U., Muhummudaree, N., and Chatsuwan, T. (2021) In Vitro Synergism of Azithromycin Combination with Antibiotics against OXA-48-producing *Klebsiella pneumoniae* Clinical Isolates. *Antibiotics*, **10**: 1551.

51. Antunes, N.T., Lamoureaux, T.L., Toth, M., Stewart, N.K., Frase, H., and Vakulenko, S.B. (2014) Class D β-Lactamases: Are They All Carbapenemases? *Antimicrob. Agents Chemother.*, **58**: 2119–2125.

52. Mehta, S.C., Rice, K., and Palzkill, T. (2015) Natural Variants of the KPC-2 Carbapenemase have Evolved Increased Catalytic Efficiency for Ceftazidime Hydrolysis at the Cost of Enzyme Stability. *PLoS Pathog.*, **11**: 1–20.

53. Poirel, L., Nordmann, P., Ducroz, S., Boulouis, H.J., Arné, P., and Millemann, Y. (2013) Extended-spectrum β-lactamase CTX-M-15-producing *Klebsiella pneumoniae* of sequence type ST274 in companion animals. *Antimicrob. Agents Chemother.*, **57**: 2372–2375.

54. Dortet, L., Poirel, L., and Nordmann, P. (2014) Worldwide Dissemination of the NDM-Type Carbapenemases in Gram-Negative Bacteria. *Biomed Res. Int.*, **2014**.

55. Guo, Y.F., Zhang, W.H., Ren, S.Q., Yang, L., Lü, D.H., Zeng, Z.L., Liu, Y.H., and Jiang, H.X. (2014) IncA/C plasmid-mediated spread of CMY-2 in multidrug-resistant *Escherichia coli* from food animals in China. *PLoS One*, **9**.

56. Poirel, L., Potron, A., and Nordmann, P. (2012) OXA-48-like carbapenemases: the phantom menace. *J. Antimicrob. Chemother.*, **67**: 1597–1606.

57. Lucaßen, K., Gerson, S., Xanthopoulou, K., Wille, J., Wille, T., Seifert, H., and Higgins, P.G. (2021) Comparison of the *Acinetobacter baumannii* Reference Strains ATCC 17978 and ATCC 19606 in Antimicrobial Resistance Mediated by the AdeABC Efflux Pump. *Antimicrob. Agents Chemother.*, **65**: e00570-21.

58. Kyriakidis, I., Vasileiou, E., Pana, Z.D., and Tragiannidis, A. (2021) *Acinetobacter baumannii* Antibiotic Resistance Mechanisms. *Pathogens*, **10**: 373.

59. Ducas-Mowchun, K., De Silva, P.M., Crisostomo, L., Fernando, D.M., Chao, T.C., Pelka, P., Schweizer, H.P., and Kumar, A. (2019) Next Generation of Tn7-Based Single-Copy Insertion Elements for Use in Multi- and Pan-Drug-Resistant Strains of Acinetobacter baumannii. *Appl. Environ. Microbiol.*, **85**: e00066-19.

60. Hoang, T.T., Karkhoff-Schweizer, R.R., Kutchma, A.J., and Schweizer, H.P. (1998) A broad-host-range Flp-FRT recombination system for site-specific excision of chromosomally-located DNA sequences: application for isolation of unmarked *Pseudomonas aeruginosa* mutants. *Gene*, **212**: 77–86.

61. West, S.E.H., Schweizer, H.P., Dall, C., Sample, A.K., and Runyen-Janecky, L.J. (1994) Construction of improved *Escherichia-Pseudomonas* shuttle vectors derived from pUC18/19 and sequence of the region required for their replication in *Pseudomonas aeruginosa*. *Gene*, **128**: 81–86.

62. Olsen, R.H., DeBusscher, G., and McCombie, W.R. (1982) Development of Broad-Host-Range Vectors and Gene Banks: Self-Cloning of the *Pseudomonas aeruginosa* PAO Chromosome. *J. Bacteriol.*, **150**: 60–69.

63. Choi, K.H., Kumar, A., and Schweizer, H.P. (2006) A 10-min method for preparation of highly electrocompetent *Pseudomonas aeruginosa* cells: Application for DNA fragment transfer between chromosomes and plasmid transformation. *J. Microbiol. Methods*, **64**: 391–397.

64. Clinical and Laboratory Standards Institute. (2012) Methods for Dilution Antimicrobial Susceptibility Tests for Bacteria That Grow Aerobically ; Approved Standard—Ninth Edition. Wayne, PA: CLSI. M07-A9.

65. Rotondo, C.M., Sychantha, D., Koteva, K., and Wright, G.D. (2020) Suppression of *β*-Lactam Resistance by Aspergillomarasmine A Is Influenced by both the Metallo-*β*-Lactamase Target and the Antibiotic Partner. *Antimicrob. Agents Chemother.*, **64**: e01386-19.

4.10 SUPPLEMENTAL MATERIAL

Supplemental Table 4.1: Minimum inhibitory concentration (MIC) values of different antibiotics against *E. coli*, *K. pneumoniae*, and *E. aerogenes* producing plasmids from the pROTO series. All MIC assays were conducted in duplicate.

Bacteria/Plasmid/Gene		MIC values (μg/mL)					
		MEM	CTX	PIP/AMP [a]	KAN	GEN	TOB
E. coli* BW25113 Δ*bamB*Δ*tolC							
pROTO1	None	0.031	0.016	0.031–0.063	2048	ND	ND
	NDM-1	32	64–128	128	2048	ND	ND
	CTX-M-15	0.016–0.031	128	256	2048	ND	ND
pROTO2	None	0.031	0.008	0.031	2048	ND	ND
	NDM-1	4–8	64	32	2048	ND	ND
	CTX-M-15	0.031	32–64	64	2048	ND	ND
pROTO3	None	ND	ND	> 4096	2	0.25–0.50	0.50
	ANT(2″)-Ia	ND	ND	> 4096	512	256	256
	ACC(6′)-Ib10	ND	ND	> 4096	256	1	16
pROTO4	None	ND	ND	> 4096	2	0.25	0.50
	ANT(2″)-Ia	ND	ND	> 4096	128	64	64
	ACC(6′)-Ib10	ND	ND	4096	256	1	32
***K. pneumoniae* ATCC 33495**							
pROTO1	None	0.063	0.063	8	2048–4096	ND	ND
	NDM-1	128	256	512	2048	ND	ND
	CTX-M-15	0.031	512	4096	2048–4096	ND	ND
pROTO2	None	0.063	0.063	8	2048	ND	ND
	NDM-1	128	256	2048	2048	ND	ND
	CTX-M-15	0.031	512	1024	2048	ND	ND
pROTO3	None	ND	ND	> 4096	2	0.50	0.50
	ANT(2″)-Ia	ND	ND	> 4096	512–1024	256	256
	ACC(6′)-Ib10	ND	ND	> 4096	128	2	16
pROTO4	None	ND	ND	> 4096	2	0.50–1	1
	ANT(2″)-Ia	ND	ND	> 4096	256	64–128	128
	ACC(6′)-Ib10	ND	ND	> 4096	128–256	2	32
***E. aerogenes* ATCC 13048**							
pROTO1	None	0.063	0.25	8	2048	ND	ND
	NDM-1	128	512	1024	2048	ND	ND
	CTX-M-15	0.063	> 4096	> 4096	2048	ND	ND
pROTO2	None	0.063	0.13	4	2048	ND	ND
	NDM-1	64	256	512	2048	ND	ND
	CTX-M-15	0.063	512	1024	2048–4096	ND	ND
pROTO3	None	ND	ND	> 4096	2–4	1	1
	ANT(2″)-Ia	ND	ND	> 4096	512–1024	256	256
	ACC(6′)-Ib10	ND	ND	> 4096	64	2	16
pROTO4	None	ND	ND	> 4096	2–4	0.50	0.50
	ANT(2″)-Ia	ND	ND	> 4096	256	64	64
	ACC(6′)-Ib10	ND	ND	> 4096	256	4	32

Abbreviations: MEM meropenem, CTX cefotaxime, PIP piperacillin, AMP ampicillin, KAN kanamycin, GEN gentamicin, TOB tobramycin, ND not determined.

[a] PIP was used for MIC assays against pROTO1–2 while AMP was used for MIC assays against pROTO3–4.

Supplemental Table 4.2: Minimum inhibitory concentration (MIC) values of different antibiotics against *E. coli*, *K. pneumoniae*, and *E. aerogenes* producing plasmids from the pROKA series. All MIC assays were conducted in duplicate.

Bacteria/Plasmid/Gene		MIC values (μg/mL)					
		MEM	**CTX**	**PIP/CAR [a]**	**KAN**	**GEN**	**TOB**
E. coli* BW25113 Δ*bamB*Δ*tolC							
pROKA1	None	0.031	0.004	0.031	ND	128	ND
	NDM-1	64–128	64	256	ND	128	ND
	CTX-M-15	0.063	512	256	ND	128	ND
pROKA2	None	0.031	0.008	0.031	ND	128	ND
	NDM-1	16	64	64	ND	128	ND
	CTX-M-15	0.031	128	128	ND	128–256	ND
pROKA3	None	ND	ND	> 4096	2	0.25	0.50
	ANT(2″)-Ia	ND	ND	> 4096	512	256	128–256
	ACC(6′)-Ib10	ND	ND	> 4096	128–256	1	16–32
pROKA4	None	ND	ND	> 4096	2	0.25–0.50	0.50
	ANT(2″)-Ia	ND	ND	> 4096	256	128	128
	ACC(6′)-Ib10	ND	ND	> 4096	256	1	32
***K. pneumoniae* ATCC 33495**							
pROKA1	None	0.031	0.063–0.13	8	ND	128	ND
	NDM-1	128	256	2048	ND	128	ND
	CTX-M-15	0.063	> 4096	> 4096	ND	128	ND
pROKA2	None	0.031	0.063	16	ND	128	ND
	NDM-1	128	128	512	ND	128	ND
	CTX-M-15	0.031	512–1024	1024	ND	128	ND
pROKA3	None	ND	ND	> 4096	2–4	1	0.50
	ANT(2″)-Ia	ND	ND	> 4096	512	512	256
	ACC(6′)-Ib10	ND	ND	> 4096	128	2	16
pROKA4	None	ND	ND	> 4096	2	0.50	0.50
	ANT(2″)-Ia	ND	ND	> 4096	256	128	128
	ACC(6′)-Ib10	ND	ND	> 4096	256	4	32
***E. aerogenes* ATCC 13048**							
pROKA1	None	0.063	0.13	4	ND	128	ND
	NDM-1	128	256	2048	ND	128	ND
	CTX-M-15	0.13	> 4096	> 4096	ND	128	ND
pROKA2	None	0.063	0.25	4	ND	256	ND
	NDM-1	128	128	1024	ND	512	ND
	CTX-M-15	0.063	512	4096	ND	256	ND
pROKA3	None	ND	ND	> 4096	2	0.50	0.50–1
	ANT(2″)-Ia	ND	ND	> 4096	1024	256	256
	ACC(6′)-Ib10	ND	ND	> 4096	128	1–2	16
pROKA4	None	ND	ND	> 4096	4	0.50	0.50
	ANT(2″)-Ia	ND	ND	> 4096	256	128–256	128
	ACC(6′)-Ib10	ND	ND	> 4096	128	2	32

Abbreviations: MEM meropenem, CTX cefotaxime, PIP piperacillin, CAR carbenicillin, KAN kanamycin, GEN gentamicin, TOB tobramycin. ND determined.

[a] PIP was used for MIC assays against pROKA1–2 while CAR was used for MIC assays against pROKA3–4.

Supplemental Table 4.3: Minimum inhibitory concentration (MIC) values of different antibiotics against *E. coli*, and *A. baumannii* producing C-terminally tagged resistance genes. All MIC assays were conducted in duplicate.

Bacteria/Plasmid/Gene		MIC values (μg/mL)					
		MEM	**CTX**	**PIP/AMP [a]**	**KAN**	**GEN**	**TOB**
***E. coli* BW25113 wild-type**							
pROTO1	NDM-1_{His}	8	64–128	128–256	4096	ND	ND
	CTX-M-15_{His}	0.031	1024	512	4096	ND	ND
pROTO2	NDM-1_{His}	8	32	32–64	4096	ND	ND
	CTX-M-15_{His}	0.031	512–1024	512	4096	ND	ND
pROTO3	ANT(2″)-Ia_{Hia}	ND	ND	> 4096	1024	256	256
	ACC(6′)-$Ib10_{\mathbf{His}}$	ND	ND	> 4096	512	8–16	32
pROTO4	ANT(2″)-Ia_{Hia}	ND	ND	> 4096	128	64	128
	ACC(6′)-$Ib10_{\mathbf{His}}$	ND	ND	> 4096	256	8	32
E. coli* BW25113 Δ*bamB*Δ*tolC							
pROTO1	NDM-1_{His}	16	64	32	2048	ND	ND
	CTX-M-15_{His}	0.016	64	128	1024	ND	ND
pROTO2	NDM-1_{His}	2–4	32	4–8	2048	ND	ND
	CTX-M-15_{His}	0.031	16	64	2048	ND	ND
pROTO3	ANT(2″)-Ia_{Hia}	ND	ND	4096	512–1024	256	256
	ACC(6′)-$Ib10_{\mathbf{His}}$	ND	ND	4096	256	2	32
pROTO4	ANT(2″)-Ia_{Hia}	ND	ND	> 4096	64	32	16–32
	ACC(6′)-$Ib10_{\mathbf{His}}$	ND	ND	4096	128	1	32
***A. baumannii* ATCC 17978**							
pROTO1	NDM-1_{His}	64	64	256	2048	ND	ND
	CTX-M-15_{His}	0.50	1024	256	4096	ND	ND
pROTO2	NDM-1_{His}	16	64	128	2048	ND	ND
	CTX-M-15_{His}	0.25	256	256	4096	ND	ND
pROTO3	ANT(2″)-Ia_{Hia}	ND	ND	> 4096	256	512	128
	ACC(6′)-$Ib10_{\mathbf{His}}$	ND	ND	> 4096	256	512	64
pROTO4	ANT(2″)-Ia_{Hia}	ND	ND	> 4096	256	256–512	64–128
	ACC(6′)-$Ib10_{\mathbf{His}}$	ND	ND	4096	512	16	128
***A. baumannii* ATCC 19606**							
pROTO1	NDM-1_{His}	64	1024	128	4096	ND	ND
	CTX-M-15_{His}	2	1024	128	2048	ND	ND
pROTO2	NDM-1_{His}	32	512	64	4096	ND	ND
	CTX-M-15_{His}	1	256	128	2048	ND	ND
pROTO3	ANT(2″)-Ia_{Hia}	ND	ND	4096	1024	> 4096	2048
	ACC(6′)-$Ib10_{\mathbf{His}}$	ND	ND	4096	512	128	64–128
pROTO4	ANT(2″)-Ia_{Hia}	ND	ND	4096	512	> 4096	1024
	ACC(6′)-$Ib10_{\mathbf{His}}$	ND	ND	4096	512	128–256	512

Abbreviations: MEM meropenem, CTX cefotaxime, PIP piperacillin, AMP ampicillin, KAN kanamycin, GEN gentamicin, TOB tobramycin, ND not determined.

[a] PIP was used for MIC assays against pROTO1–2 while AMP was used for MIC assays against pROTO3–4.

Supplemental Table 4.4: Minimum inhibitory concentration (MIC) values of different antibiotics against *E. coli*, and *P. aeruginosa* producing C-terminally tagged resistance genes. All MIC assays were conducted in duplicate.

Bacteria/Plasmid/Gene		MIC values (µg/mL)					
		MEM	**CTX**	**PIP/CAR [a]**	**KAN**	**GEN**	**TOB**
***E. coli* BW25113 wild-type**							
pROKA1	NDM-1_{His}	4	256	512	ND	256	ND
	CTX-M-15_{His}	0.063	4096	2048	ND	256	ND
pROKA2	NDM-1_{His}	4	64–128	64	ND	256	ND
	CTX-M-15_{His}	0.031	512	256	ND	256	ND
pROKA3	ANT(2″)-Ia_{Hia}	ND	ND	> 4096	1024	256	256
	ACC(6′)-$Ib10_{\mathbf{His}}$	ND	ND	> 4096	512	8–16	64
pROKA4	ANT(2″)-Ia_{Hia}	ND	ND	> 4096	256	128	128
	ACC(6′)-$Ib10_{\mathbf{His}}$	ND	ND	> 4096	512–1024	16	32
E. coli* BW25113 Δ*bamB*Δ*tolC							
pROKA1	NDM-1_{His}	16–32	32	64	ND	128	ND
	CTX-M-15_{His}	0.063	128	256	ND	128	ND
pROKA2	NDM-1_{His}	4	32	16	ND	128	ND
	CTX-M-15_{His}	0.031	64	128	ND	128	ND
pROKA3	ANT(2″)-Ia_{Hia}	ND	ND	> 4096	1024	256	256
	ACC(6′)-$Ib10_{\mathbf{His}}$	ND	ND	> 4096	256	2	64
pROKA4	ANT(2″)-Ia_{Hia}	ND	ND	> 4096	256	32–64	64
	ACC(6′)-$Ib10_{\mathbf{His}}$	ND	ND	> 4096	256	2	32
***P. aeruginosa* PAO1**							
pROKA1	NDM-1_{His}	256–512	4096	64	ND	1024	ND
	CTX-M-15_{His}	2	128	64	ND	1024	ND
pROKA2	NDM-1_{His}	> 4096	> 4096	1024	ND	1024	ND
	CTX-M-15_{His}	4	> 4096	512–1024	ND	1024	ND
pROKA3	ANT(2″)-Ia_{Hia}	ND	ND	> 4096	64–128	128	32
	ACC(6′)-$Ib10_{\mathbf{His}}$	ND	ND	4096	128	8	16–32
pROKA4	ANT(2″)-Ia_{Hia}	ND	ND	> 4096	1024–2048	2048	256
	ACC(6′)-$Ib10_{\mathbf{His}}$	ND	ND	> 4096	512	16	128
***P. aeruginosa* PA14**							
pROKA1	NDM-1_{His}	128–256	2048	64	ND	> 4096	ND
	CTX-M-15_{His}	0.50–1	4096	4096	ND	4096	ND
pROKA2	NDM-1_{His}	1024	> 4096	512	ND	> 4096	ND
	CTX-M-15_{His}	2	> 4096	1024	ND	> 4096	ND
pROKA3	ANT(2″)-Ia_{Hia}	ND	ND	> 4096	128	128	32
	ACC(6′)-$Ib10_{\mathbf{His}}$	ND	ND	4096	256	8	16–32
pROKA4	ANT(2″)-Ia_{Hia}	ND	ND	> 4096	2048	> 4096	1024
	ACC(6′)-$Ib10_{\mathbf{His}}$	ND	ND	> 4096	512	16	128

Abbreviations: MEM meropenem, CTX cefotaxime, PIP piperacillin, CAR carbenicillin, KAN kanamycin, GEN gentamicin, TOB tobramycin, ND not determined.

[a] PIP was used for MIC assays against pROKA1–2 while CAR was used for MIC assays against pROKA3–4.

Supplemental Table 4.5: Minimum inhibitory concentration (MIC) values of *A. baumannii* ATCC 17978 strains producing two β-lactamases when tested against various β-lactam antibiotics.[a] All assays were conducted in duplicate.

β-Lactamase		**MIC values (μg/mL)**		
Gene 1	**Gene 2**	**ATM**	**AVI**	**MEM**
NDM-1	KPC-2	64	32	128
KPC-2	NDM-1	64	64	128
NDM-1	CTX-M-15	128	64	64
CTX-M-15	NDM-1	128	32–64	64–128
NDM-1	CMY-2	16	64–128	64
CMY-2	NDM-1	16	64	128
NDM-1	OXA-48	0.03–0.06	64	64
OXA-48	NDM-1	0.03	32–64	64

Abbreviations: ATM aztreonam, AVI avibactam, MEM meropenem.

[a] Both β-lactamase genes were cloned into pROTO2 with individual promoters.

Supplemental Table 4.6: Concentration of AMA needed to restore the activity of meropenem to its susceptibility breakpoint concentration against *A. baumannii* ATCC 17978 strains producing two β-lactamases.[a] All assays were conducted in duplicate. This table shows the results from replicate 2.

β-Lactamase		**[AMA] at 2 µg/mL of MEM in different combinations (µg/mL)** [b, c]		
Gene 1	**Gene 2**	**AMA/ MEM**	**AVI/ MEM**	**AMA/AVI/ MEM**
NDM-1	KPC-2	> 64	64	8
KPC-2	NDM-1	> 64	64	8
NDM-1	CTX-M-15	8	32	16
CTX-M-15	NDM-1	8	32	16
NDM-1	CMY-2	8	16	8
CMY-2	NDM-1	8	16	8
NDM-1	OXA-48	8	16	16
OXA-48	NDM-1	8	16	16

Abbreviations: AMA aspergillomarasmine A, AVI avibactam, MEM meropenem.

[a] Both β-lactamase genes were cloned into pROTO2 with individual promoters.

[b] 2 µg/mL is the EUCAST susceptibility breakpoint concentration for MEM.

[c] AVI was maintained at 4 µg/mL, except during the AVI/MEM combination.

Supplemental Table 4.7: Sequences of the primers used to generate the pROTO and pROKA plasmids. Start codons and stop codons are highlighted in green and red, respectively. The restriction enzyme recognition sites are underlined in the primer sequence.

Primer Name	Primer Sequence
EASV-AclI-FWD	5′–C ATG CCC GGT TAC TGG AAC GTT GAT CGT AGA AAT ATC TAT GAT TAT C –3′
EASV-AclI-REV	5′–CAT ACC GCC AGT TGT TTA CCC TCA CGG ATT TTA ACA TTT TGC GTT G–3′
EASV-AfeI-FWD	5′–CTC AGG GTC AAT GCC AGC GCT GAT CGT AGA AAT ATC TAT GAT TAT C –3′
EASV-AfeI-REV	5′–CAC CTA CAT CTG TAT TAA CGA GGA TTT TAA CAT TTT GCG TTG–3′
EPSV-AclI-FWD	5′–C ATG CCC GGT TAC TGG AAC GTT TCC GCC TCG ATA CCC TGA TTA C –3′
EPSV-AclI-REV	5′–C ATA CCG CCA GTT GTT TAC CCT CAC CTA GGC CAG ATC CAG CGG C–3′
EPSV-AfeI-FWD	5′–CTC AGG GTC AAT GCC AGC GCT TCC GCC TCG ATA CCC TGA TTA C –3′
EPSV-AfeI-REV	5′–CAC CTA CAT CTG TAT TAA CGA CTA GGC CAG ATC CAG CGG C–3′
KAN-Out-FWD	5′–GAATTAATTCATGAGCGGATACA–3′
KAN-Out-REV	5′–AACACCCCTTGTATTACTGTTTA–3′
EPSV+ANT-FWD	5′–TAT CCG CTC ATG AAT TAA TTC TTA GGC CGC ATA TCG CGA CCT G–3′
EPSV+ANT-REV	5′–AAC AGT AAT ACA AGG GGT GTT ATG GAC ACA ACG CAG GTC ACA TTG–3′

Supplemental Table 4.8: Sequences of the primers used to create the overexpression constructs and the His-tagged genes. The His reverse primers were used to remove the stop codon from the genes to allow the insertion of the C-terminal His-tag. Start codons and stop codons are highlighted in green and red, respectively. The restriction enzyme recognition sites are underlined in the primer sequence.

Primer Name	Primer Sequence
NDM-Bam-FWD	5′–TAC CCT GGA TCC ATG GAA TTG CCC AAT ATT ATG CAC C –3′
NDM-HindIII-REV	5′–TAC CCT AAG CTT TCA GCG CAG CTT GTC GGC –3′
NDM-His-REV	5′–TAC CCT AAG CTT GCG CAG CTT GTC GGC –3′
CTX-BamHI-FWD	5′–TCC CAT GGA TCC ATGGTT AAA AAA TCA CTG CGC CAG–3′
CTX-HindIII-REV	5′–TCC CAT AAG CTT TTA CAA ACC GTC GGT GAC GAT TTT AG–3′
CTX-His-REV	5′–TCC CAT AAG CTT CAA ACC GTC GGT GAC GAT TTT AG–3′
ANT-BamHI-FWD	5′–TCC TCC GGA TCC ATG GAC ACA ACG CAG GTC ACA TTG–3′
ANT-HindIII-REV	5′–TCC TCC AAG CTT TTA GGC CGC ATA TCG CGA CCT G–3′
ANT-His-REV	5′–TCC TCC AAG CTT GGC CGC ATA TCG CGA CCT G–3′
AAC-BamHI-FWD	5′–TCT TCT GGA TCC ATG TTA CGC AGC AGC AGT CGC CCT AAA ACA AAG TTAG –3′
AAC-HindIII-REV	5′–TCT TCT AAG CTT TTA GGC ATC ACT GCG TGT TCG CTC GAA TG–3′
AAC-His-REV	5′–TCT TCT AAG CTT GGC ATC ACT GCG TGT TCG CTC GAA TG –3′

Supplemental Table 4.9: Sequences of the primers used to generate the tandem β-lactamase expression vectors. Start codons and stop codons are highlighted in green and red, respectively. The restriction enzyme recognition sites are underlined in the primer sequence.

Primer Name	Primer Sequence
pGDP2-BglII-FWD	5′–GCC AGC CTA GCC GGG AGA TCT–3′
pGDP2-BglII-REV	5′–CCG TTG AGC ACC GCC GCC GCA GAA GGC CAT CCT GAC GGA TGG–3′
pROTO2-BglII-FWD	5′–CTC AGG GTC AAT GCC AGC GCT GAT CGT AGA AAT ATC TAT GAT TAT C –3′
pROTO2-BglII-REV	5′–CAC CTA CAT CTG TAT TAA CGA GGA TTT TAA CAT TTT GCG TTG–3′
pGDP2-NcoI-FWD	5′–TAT CCG CTC ATG AAT TAA TTC TTA GGC CGC ATA TCG CGA CCT G–3′
pGDP2-XhoI-FWD	5′–AAC AGT AAT ACA AGG GGT GTT ATG GAC ACA ACG CAG GTC ACA TTG–3′

CHAPTER 5: Conclusions and future directions

5.1 Summary

As the era of antibiotics seems to be coming to an end, a warning by Louis Pasteur is brought to mind "*Messieurs, c'est les microbes qui auront le dernier mot"* (Gentlemen, it is the microbes who will have the last word) [161]. Nowadays, the truth behind these words couldn't be more evident with the ever-growing number of bacteria demonstrating antibiotic resistance mechanisms and the dwindling number of antibiotics available to combat these resistant bacteria. Particularly worrisome is the ongoing emergence and dissemination of β-lactamases genes around the world as their targets, the β-lactams (e.g., penams, cephems, carbapenems), remain among the most prescribed antibiotics [25,36,37]. Efforts to preserve the effectiveness of β-lactam antibiotics have resulted in the development of various β-lactamase inhibitors for clinical use (e.g., clavulanic acid, sulbactam, tazobactam, avibactam) [76,88]. However, all these inhibitors are specific to SBL enzymes, leaving MBLs an unmet clinical challenge. The inability to design a universal MBL inhibitor is a result of the low sequence similarity and the active site diversity between members of different MBL subclasses [162,163]. Despite these challenges, several thousand MBL inhibitors have been discovered and predominantly target the conserved zinc ions essential to the activity of these enzymes [164]. Taniborbactam, a boron-containing inhibitor effective against both MBLs and SBLs, has even demonstrated positive results in phase III clinical trials [164,165]. Another candidate that received considerable attention as an MBL inhibitor was the fungal natural product AMA [147]. Therefore, the work presented in this dissertation aimed to combat the threat posed by MBL-producing bacteria by further elucidating the inhibitory potency of AMA.

5.1.1 Evaluating the inhibitory potency of AMA against a broader range of MBL enzymes and in combination with different β-lactam partners

Previous studies demonstrated that AMA could rapidly inhibit MBLs of clinical importance (NDM-1, VIM-2) and potentiate the activity of the β-lactam antibiotic meropenem against bacteria producing these metalloenzymes. However, AMA was considerably less effective against strains producing IMP-7, another clinically relevant MBL [147]. Consequently, we sought to investigate the inhibitory potency of AMA against a broader panel of MBLs from all three subclasses (B1, B2, B3). This was achieved using β-lactam antibiotics from three subclasses (penams, cephems, carbapenems) and different bacterial strains (*E. coli*, *K. pneumoniae*). Enzyme and cell-based assays revealed that the variation in the inhibitory potency of AMA resulted from the zinc dependencies of the MBL enzymes. For example, NDM-1, an enzyme from subclass B1 which demonstrated weak zinc affinity, was more susceptible to inhibition by AMA than its point mutation variants (e.g., NDM-6), and subclass B2 and B3 enzymes (CphA2, AIM-1), which have a greater affinity for zinc. In addition, suppression of β-lactam resistance by AMA was influenced by the choice of β-lactam partner. These results did not correlate with outer membrane permeability or drug efflux but may stem from the affinity of the β-lactam antibiotics for their targets, the penicillin-binding proteins. Overall, AMA exhibited the greatest inhibitory potency when paired with a carbapenem antibiotic (e.g., meropenem), which are the β-lactam antibiotics with the highest potency and broadest spectrum of activity against different bacterial strains [162].

5.1.2 Exploring the effectiveness of AMA, avibactam, and meropenem against bacterial strains producing multiple β-lactamase enzymes

While an AMA/carbapenem pairing was shown to be effective against bacteria producing a single MBL enzyme [147,162], bacterial infections worldwide are increasingly more challenging to treat due to the production of multiple β-lactamases [156,166]. We hypothesized that combining both AMA (an MBL inhibitor) and avibactam (an SBL inhibitor) would have the ability to restore the activity of meropenem (a β-lactam antibiotic) against almost any combination of β-lactamase enzymes. Therefore, the effectiveness of AMA, avibactam, and meropenem was evaluated against both laboratory strains (*E. coli*, *K. pneumoniae*) and clinical isolates producing at least one MBL and one SBL. Potentiation assays revealed that laboratory strains producing NDM-1 and an SBL carbapenemase (e.g., KPC-2) were resistant to an AMA/meropenem combination. These results were consistent with AMA's inability to inhibit serine-dependent β-lactamase enzymes [147]. Nonetheless, these laboratory strains became susceptible to the activity of meropenem upon pairing this β-lactam antibiotic with both AMA and avibactam. Furthermore, the AMA/avibactam/meropenem combination was effective against Enterobacteriaceae isolates producing class A, B, and C β-lactamase enzymes. However, this combination was less effective against clinical strains producing carbapenem-hydrolyzing class D β-lactamases due to their insensitivity to avibactam [88,167]. In addition, AMA, avibactam, and meropenem showed little inhibitory potency against β-lactamase-producing *A. baumannii* and *P. aeruginosa*, possibly due to the considerable number of antibiotic resistance mechanisms displayed by these pathogens [168,169].

5.1.3 Characterizing AMA and other antibiotic adjuvants in *A. baumannii* and *P. aeruginosa*

An increasing prevalence of carbapenem resistance in *A. baumannii* and *P. aeruginosa* is a critical threat to the treatment of many hospital-acquired infections [168,170–173]. One promising tool for re-sensitizing these pathogens to β-lactams is antibiotic adjuvants [174]. The discovery and characterization of antibiotic adjuvants in *E. coli* and other Enterobacterales is facilitated by tools such as the ARP [175,176]. However, considerably fewer tools exist for genetic manipulation and resistance gene expression in Pseudomonadales such as *A. baumannii* and *P. aeruginosa* [177,178]. Therefore, to further examine the effect of antibiotic adjuvants in different bacterial families (Enterobacteriaceae, Pseudomonadaceae, Moraxellaceae), new shuttle vectors were created to expand the host range of the ARP. These plasmids were constructed by inserting origins of replication known to function in *Acinetobacter* (ori1266 from pFLP2) and *Pseudomonas* (pRO1600 oriV from pMS402) into the pGDP vector series from the ARP. These new *Escherichia-Acinetobacter* and *Escherichia-Pseudomonas* shuttle vectors were named pROTO1–4 and pROKA1–4, respectively. Antibiotic susceptibility testing data demonstrated that the pROTO/pROKA series could replicate and express different resistance enzymes [NDM-1, CTX-M-15, ANT(2″)-Ia, and AAC(6′)-Ib10] in both Enterobacterales and Pseudomonadales. In addition, key features of the original ARP plasmids (e.g., strong/weak promoters, 6×His-tags) were retained in the pROTO and pROKA shuttle vectors to allow for variable gene expression as well as protein detection/purification. Using pROTO, we also determined that β-lactamase inhibitors

(AMA, avibactam) could restore meropenem susceptibility against *A. baumannii* strains producing multiple β-lactamases.

5.2 Future directions

The construction of the new pROTO/pROKA vector series opens the door to new potential experiments in the Wright laboratory. For example, cloning different MBL genes into these plasmids may help in cell-based screens for new inhibitors of MBL-producing *A. baumannii* and *P. aeruginosa* using the Wright Actinomycete Collection (WAC). The WAC has repeatedly identified antibiotic adjuvants such as venturicidin A, moenomycin, and AMA [147,179,180]. The targeted screen leading to the discovery of AMA was conducted with NDM-1-producing *E. coli* [147]. However, studies conducted in this dissertation demonstrated that NDM-1 had one of lowest affinities for zinc. Therefore, future cell-based screens could be performed against bacterial strains producing an MBL enzyme with a higher affinity for zinc, such as NDM-6 or IMP-7 [162]. AIM-1 could also be a metalloenzyme of great interest for screening since most studies conducted in this dissertation focused on subclass B1 enzymes. Although MBLs from subclass B3 are less common in pathogens, bacteria containing these metalloenzymes are a challenge when encountered in the clinic [181,182] and could potentially serve as reservoirs for clinically relevant β-lactam resistance in the future. Furthermore, while β-lactamase inhibitors represent an increasingly popular method to counteract β-lactam resistance in pathogens, mutations of the β-lactamase enzymes or the outer membrane porins can significantly reduce the effectiveness of any combination therapy [183]. Therefore, future experiments could include determining the bacterial frequency of spontaneous resistance towards

AMA, the MBL inhibitor, which was the focus of this dissertation. In conclusion, as MBL enzymes remain a significant public health concern, this bacterial resistance mechanism should be quickly addressed before the golden age of antibiotics is gone forever.

REFERENCES

1. Waksman, S.A. (1947) What is an antibiotic or an antibiotic substance? *Mycologia*, **39**: 565–569.

2. Clardy, J., Fischbach, M., and Currie, C. (2009) The natural history of antibiotics. *Curr. Biol.*, **19**: R437–R441.

3. Wainwright, M. (1989) Moulds in Folk Medicine. *Folklore*, **100**: 162–166.

4. Ligon, B.L. (2004) Penicillin: Its Discovery and Early Development. *Semin. Pediatr. Infect. Dis.*, **15**: 52–57.

5. Fleming, A. (1929) On the antibacterial action of cultures of a penicillium, with special reference to their use in the isolation of *B. influenzæ*. *Br. J. Exp. Pathol.*, **10**: 226–236.

6. Lobanovska, M. and Pilla, G. (2017) Penicillin's Discovery and Antibiotic Resistance: Lessons for the Future? *YALE J. Biol. Med.*, **90**: 135–145.

7. Bennett, J.W. and Chung, K.-T. (2001) Alexander Fleming and the Discovery of Penicillin. *Adv. Appl. Microbiol.*, **49**: 163–184.

8. Gaynes, R. (2017) The Discovery of Penicillin—New Insights After More Than 75 Years of Clinical Use. *Emerg. Infect. Dis.*, **23**: 849–853.

9. Lima, L.M., da Silva, B.N.M., Barbosa, G., and Barreiro, E.J. (2020) β-lactam antibiotics: An overview from a medicinal chemistry perspective. *Eur. J. Med. Chem.*, **208**: 112829.

10. Pandey, N. and Cascella, M. (2021) Beta lactam antibiotics. In: StatPearls [Internet]. Treasure Island, FL: StatPearls Publishing. Retrieved June 2022 from: https://www.ncbi.nlm.nih.gov/books/NBK545311/.

11. Fisher, J.F., Meroueh, S.O., and Mobashery, S. (2005) Bacterial Resistance to *β*-Lactam Antibiotics: Compelling Opportunism, Compelling Opportunity. *Chem. Rev.*, **105**: 395–424.

12. Papp-Wallace, K.M., Endimiani, A., Taracila, M.A., and Bonomo, R.A. (2011) Carbapenems: Past, Present, and Future. *Antimicrob. Agents Chemother.*, **55**: 4943–4960.

13. Karsisiotis, A.I., Damblon, C.F., and Roberts, G.C.K. (2014) A variety of roles for versatile zinc in metallo-β-lactamases. *Metallomics*, **6**: 1181–1197.

14. Kahan, J.S., Kahan, F.M., Goegelman, R., et al. (1979) Thienamycin, A New *β*-

Lactam Antibiotic I. Discovery, Taxonomy, Isolation And Physical Properties. *J. Antibiot. (Tokyo).*, **32**: 1–12.

15. Armstrong, T., Fenn, S.J., and Hardie, K.R. (2021) JMM Profile: Carbapenems: a broad-spectrum antibiotic. *J. Med. Microbiol.*, **70**: 001462.

16. Rodríguez, M., Méndez, C., Salas, J.A., and Blanco, G. (2010) Transcriptional organization of ThnI-regulated thienamycin biosynthetic genes in *Streptomyces cattleya*. *J. Antibiot. (Tokyo).*, **63**: 135–138.

17. Kahan, F.M., Kropp, H., Sundelof, J.G., and Birnbaum, J. (1983) Thienamycin : development of imipenem-cilastatin. *J. Antimicrob. Chemother.*, **12**: 1–35.

18. Singh, G.S. (2004) β-Lactams in the New Millennium. Part-I: Monobactams and Carbapenems. *Mini Rev. Med. Chem.*, **4**: 69–92.

19. Scheffers, D. and Pinho, M. (2005) Bacterial Cell Wall Synthesis: New Insights from Localization Studies. *Microbiol. Mol. Biol. Rev.*, **69**: 585–607.

20. Meroueh, S.O., Bencze, K.Z., Hesek, D., Lee, M., Fisher, J.F., Stemmler, T.L., and Mobashery, S. (2006) Three-dimensional structure of the bacterial cell wall peptidoglycan. *Proc. Natl. Acad. Sci. U. S. A.*, **103**: 4404–4409.

21. Sauvage, E., Kerff, F., Terrak, M., Ayala, J., and Charlier, P. (2008) The penicillin-binding proteins: structure and role in peptidoglycan biosynthesis. *FEMS Microbiol. Rev.*, **32**: 234–258.

22. Tomasz, A. (1979) The Mechanism of the Irreversible Antimicrobial Effects of Penicillins: How the Beta-Lactam Antibiotics Kill and Lyse Bacteria. *Annu. Rev. Microbiol.*, **33**: 113–137.

23. Dörr, T., Davis, B.M., and Waldor, M.K. (2015) Endopeptidase-Mediated Beta Lactam Tolerance. *PLoS Pathog.*, **11**: e1004850.

24. Cho, H., Uehara, T., and Bernhardt, T.G. (2014) Beta-Lactam Antibiotics Induce a Lethal Malfunctioning of the Bacterial Cell Wall Synthesis Machinery. *Cell*, **159**: 1300–1311.

25. King, D.T., Sobhanifar, S., and Strynadka, N.C.J. (2016) One ring to rule them all: Current trends in combating bacterial resistance to the β-lactams. *Protein Sci.*, **25**: 787–803.

26. Kumar, A. and Chordia, N. (2017) Bacterial Resistance Against Antibiotics. Arora, G., Sajid, A., and Kalia, V., editors. Drug Resistance in Bacteria, Fungi, Malaria, and Cancer. Cham, Switzerland: Springer. pp. 171–192.

27. McNulty, C., Boyle, P., Nichols, T., Clappison, P., and Davey, P. (2007) The public's attitudes to and compliance with antibiotics. *J. Antimicrob. Chemother.*, **60**: i63–i68.

28. CIHI (Canadian Institute for Health Information). (2017) lnfographic: Do you need that antibiotic? [Online]. Retrieved June 2022 from: https://www.cihi.ca/en/ infographic-do-you-need-that-antibiotic.

29. Wassmer, G.T., Kipe-Nolt, J.A., and Chayko, C.A. (2006) Why Finish Your Antibiotics? *Am. Biol. Teach.*, **68**: 476–480.

30. FDA (Food and Drug Administration). (2016) 2015 Summary Report On Antimicrobials Sold or Distributed for Use in Food-Producing Animals. Washington, DC: FDA.

31. Girou, E., Chai, S.H.T., Oppein, F., Legrand, P., Ducellier, D., Cizeau, F., and Brun-Buisson, C. (2004) Misuse of gloves: the foundation for poor compliance with hand hygiene and potential for microbial transmission? *J. Hosp. Infect.*, **57**: 162–169.

32. Hutchings, M., Truman, A., and Wilkinson, B. (2019) Antibiotics: past, present and future. *Curr. Opin. Microbiol.*, **51**: 72–80.

33. Ehlert, F. and Neu, H.C. (1987) In Vitro Activity of LY146032 (Daptomycin), a New Peptolide. *Eur. J. Clin. Microbiol.*, **6**: 84–90.

34. Ling, L.L., Schneider, T., Peoples, A.J., et al. (2015) A new antibiotic kills pathogens without detectable resistance. *Nature*, **517**: 455–459.

35. Blair, J.M.A., Webber, M.A., Baylay, A.J., Ogbolu, D.O., and Piddock, L.J.V. (2015) Molecular mechanisms of antibiotic resistance. *Nat. Rev. Microbiol.*, **13**: 42–51.

36. Bebrone, C. (2007) Metallo-β-lactamases (classification, activity, genetic organization, structure, zinc coordination) and their superfamily. *Biochem. Pharmacol.*, **74**: 1686–1701.

37. Helfand, M.S. and Bonomo, R.A. (2003) β-Lactamases: A Survey of Protein Diversity. *Curr. Drug Targets - Infect. Disord.*, **3**: 9–23.

38. Bebrone, C., Lassaux, P., Vercheval, L., Sohier, J.-S., Jehaes, A., Sauvage, E., and Galleni, M. (2010) Current Challenges in Antimicrobial Chemotherapy: Focus on β-Lactamase Inhibition. *Drugs*, **70**: 651–679.

39. Ambler, R.P. (1980) The structure of β-lactamases. *Philos. Trans. R. Soc. Lond. B. Biol. Sci.*, **289**: 321–331.

40. Singh, R., Saxena, A., and Singh, H. (2009) Identification of group specific motifs in Beta-lactamase family of proteins. *J. Biomed. Sci.*, **16**: 109.

41. Swarén, P., Maveyraud, L., Guillet, V., Masson, J.M., Mourey, L., and Samama, J.P. (1995) Electrostatic analysis of TEM1 β-lactamase: effect of substrate binding, steep potential gradients and consequences of site-directed mutations. *Structure*, **3**: 603–613.

42. Vandavasi, V.G., Langan, P.S., Weiss, K.L., Parks, J.M., Cooper, J.B., Ginell, S.L., and Coates, L. (2017) Active-Site Protonation States in an Acyl-Enzyme Intermediate of a Class A β-Lactamase with a Monobactam Substrate. *Antimicrob Agents Chemother*, **61**: e01636-16.

43. Walther-Rasmussen, J. and Høiby, N. (2007) Class A carbapenemases. *J. Antimicrob. Chemother.*, **60**: 470–482.

44. Strynadka, N.C.J., Adachi, H., Jensen, S.E., Johns, K., Sielecki, A., Betzel, C., Sutoh, K., and James, M.N.G. (1992) Molecular structure of the acyl-enzyme intermediate in *β*-lactam hydrolysis at 1.7 Å resolution. *Nature*, **359**: 700–705.

45. Hermann, J.C., Hensen, C., Ridder, L., Mulholland, A.J., and Höltje, H.D. (2005) Mechanisms of Antibiotic Resistance: QM/MM Modeling of the Acylation Reaction of a Class A *β*-Lactamase with Benzylpenicillin. *J. Am. Chem. Soc.*, **127**: 4454–4465.

46. Strynadka, N.C.J., Martin, R., Jensen, S.E., Gold, M., and Jones, J.B. (1996) Structure-based design of a potent transition state analogue for TEM-1 β-lactamase. *Nat. Struct. Biol.*, **3**: 688–695.

47. King, D.T., Sobhanifar, S., and Strynadka, N.C.J. (2014) The Mechanisms of Resistance to β-Lactam Antibiotics. Gotte, M., Berghuis, A., Matlashewski, G., Wainberg, M., and Sheppard, D., editors. Handbook of Antimicrobial Resistance. New York, NY: Springer. pp. 1–22.

48. Palzkill, T. (2018) Structural and Mechanistic Basis for Extended-Spectrum Drug-Resistance Mutations in Altering the Specificity of TEM, CTX-M, and KPC β-lactamases. *Front. Mol. Biosci.*, **5**: 1–19.

49. Bush, K. (2014) Evolution of β-Lactamases: Past, Present, and Future. Dougherty, T. and Pucci, M., editors. Antibiotic Discovery and Development. New York, NY: Springer. pp. 427–453.

50. Datta, N. and Kontomichalou, P. (1965) Penicillinase Synthesis Controlled By Infectious R Factors In Enterobacteriaceae. *Nature*, **208**: 239–241.

51. Ruiz, J. (2018) TEM. *Emerg. Infect. Dis.*, **24**: 709.

52. The Comprehensive Antibiotic Resistance Database. (2022) TEM beta-lactamase. [Online]. Retrieved June 2022 from: https://card.mcmaster.ca/ontology/36023.

53. Livermore, D.M. (1995) β-Lactamases in Laboratory and Clinical Resistance. *Clin. Microbiol. Rev.*, **8**: 557–584.

54. Cantón, R., Novais, A., Valverde, A., Machado, E., Peixe, L., Baquero, F., and Coque, T.M. (2008) Prevalence and spread of extended-spectrum β-lactamase-producing Enterobacteriaceae in Europe. *Clin. Microbiol. Infect.*, **14**: 144–153.

55. Nordmann, P., Cuzon, G., and Naas, T. (2009) The real threat of *Klebsiella pneumoniae* carbapenemase-producing bacteria. *Lancet Infect. Dis.*, **9**: 228–236.

56. Yigit, H., Queenan, A.M., Anderson, G.J., et al. (2001) Novel Carbapenem-Hydrolyzing β-Lactamase, KPC-1, from a Carbapenem-Resistant Strain of *Klebsiella pneumoniae*. *Antimicrob. Agents Chemother.*, **45**: 1151–1161.

57. The Comprehensive Antibiotic Resistance Database. (2022) KPC beta-lactamase. [Online]. Retrieved June 2022 from: https://card.mcmaster.ca/ontology/36198.

58. Schweizer, C., Bischoff, P., Bender, J., et al. (2019) Plasmid-Mediated Transmission of KPC-2 Carbapenemase in Enterobacteriaceae in Critically Ill Patients. *Front. Microbiol.*, **10**: 1–8.

59. Abraham, E.P. and Chain, E. (1940) An Enzyme from Bacteria able to Destroy Penicillin. *Nature*, **146**: 837.

60. Jacoby, G.A. (2009) AmpC β-Lactamases. *Clin. Microbiol. Rev.*, **22**: 161–182.

61. Fenollar-Ferrer, C., Frau, J., Donoso, J., and Muñoz, F. (2008) Evolution of class C β-lactamases: factors influencing their hydrolysis and recognition mechanisms. *Theor. Chem. Acc.*, **121**: 209–218.

62. Philippon, A., Arlet, G., and Jacoby, G.A. (2002) Plasmid-Determined AmpC-Type β-Lactamases. *Antimicrob. Agents Chemother.*, **46**: 1–11.

63. Doi, Y., Paterson, D.L., Egea, P., et al. (2010) Extended-spectrum and CMY-type *β*-lactamase-producing *Escherichia coli* in clinical samples and retail meat from Pittsburgh, USA and Seville, Spain. *Clin. Microbiol. Infect.*, **16**: 33–38.

64. Koga, V.L., Maluta, R.P., Da Silveira, W.D., Ribeiro, R.A., Hungria, M., Vespero, E.C., Nakazato, G., and Kobayashi, R.K.T. (2019) Characterization of CMY-2-type beta-lactamase-producing *Escherichia coli* isolated from chicken carcasses and human infection in a city of South Brazil. *BMC Microbiol.*, **19**: 1–9.

65. Walther-Rasmussen, J. and Høiby, N. (2006) OXA-type carbapenemases. *J. Antimicrob. Chemother.*, **57**: 373–383.

66. Majiduddin, F.K., Materon, I.C., and Palzkill, T.G. (2002) Molecular analysis of beta-lactamase structure and function. *Int. J. Med. Microbiol.*, **292**: 127–137.

67. Poirel, L., Naas, T., and Nordmann, P. (2010) Diversity, Epidemiology, and Genetics of Class D β-Lactamases. *Antimicrob. Agents Chemother.*, **54**: 24–38.

68. June, C.M., Vallier, B.C., Bonomo, R.A., Leonard, D.A., and Powers, R.A. (2014) Structural Origins of Oxacillinase Specificity in Class D β-Lactamases. *Antimicrob. Agents Chemother.*, **58**: 333–341.

69. Docquier, J.D., Calderone, V., De Luca, F., et al. (2009) Crystal Structure of the OXA-48 β-Lactamase Reveals Mechanistic Diversity among Class D Carbapenemases. *Chem. Biol.*, **16**: 540–547.

70. Antunes, N.T., Lamoureaux, T.L., Toth, M., Stewart, N.K., Frase, H., and Vakulenko, S.B. (2014) Class D β-Lactamases: Are They All Carbapenemases? *Antimicrob. Agents Chemother.*, **58**: 2119–2125.

71. Poirel, L., Potron, A., and Nordmann, P. (2012) OXA-48-like carbapenemases: the phantom menace. *J. Antimicrob. Chemother.*, **67**: 1597–1606.

72. Hamprecht, A., Sommer, J., Willmann, M., et al. (2019) Pathogenicity of Clinical OXA-48 Isolates and Impact of the OXA-48 IncL Plasmid on Virulence and Bacterial Fitness. *Front. Microbiol.*, **10**: 2509.

73. Carmeli, Y., Harbarth, S., Kahlmeter, G., Kluytmans, J., Mendelson, M., Pulcini, C., Singh, N., and Theuretzbacher, U. (2017) Global priority list of antibiotic-resistant bacteria to guide research, discovery, and development of new antibiotics. WHO (World Health Organization).

74. WHO (World Health Organization) News. (2017) WHO publishes list of bacteria for which new antibiotics are urgently needed. [Online]. Retrieved June 2022 from: https://www.who.int/news/item/27-02-2017-who-publishes-list-of-bacteria-for-which-new-antibiotics-are-urgently-needed.

75. Reading, C. and Cole, M. (1977) Clavulanic Acid: a Beta-Lactamase-Inhibiting Beta-Lactam from *Streptomyces clavuligerus*. *Antimicrob. Agents Chemother.*, **11**: 852–857.

76. Drawz, S.M. and Bonomo, R.A. (2010) Three decades of β-lactamase inhibitors. *Clin. Microbiol. Rev.*, **23**: 160–201.

77. Neu, H.C. (1985) Contribution of Beta-Lactamases to Bacterial Resistance and

Mechanisms To Inhibit Beta-Lactamases. *Am. J. Med.*, **79**: 2–12.

78. Chifiriuc, M.C., Holban, A.M., Curutiu, C., Ditu, L.-M., Mihaescu, G., Oprea, A.E., Grumezescu, A.M., and Lazar, V. (2016) Antibiotic Drug Delivery Systems for the Intracellular Targeting of Bacterial Pathogens. Sezer, A.D., editor. Smart Drug Delivery System. London, UK: IntechOpen. pp. 305–344.

79. Wang, D.Y., Abboud, M.I., Markoulides, M.S., Brem, J., and Schofield, C.J. (2016) The road to avibactam: The first clinically useful non-β-lactam working somewhat like a β-lactam. *Future Med. Chem.*, **8**: 1063–1084.

80. English, A.R., Retsema, J.A., Girard, A.E., Lynch, J.E., and Barth, W.E. (1978) CP-45,899, a Beta-Lactamase Inhibitor That Extends the Antibacterial Spectrum of Beta-Lactams: Initial bacteriological characterization. *Antimicrob. Agents Chemother.*, **14**: 414–419.

81. Fisher, J., Belasco, J.G., Charnas, R.L., Khosla, S., and Knowles, J.R. (1980) β-Lactamase inactivation by mechanism-based reagents. *Philos. Trans. R. Soc. Lond. B Biol. Sci.*, **289**: 309–319.

82. Akova, M. (2008) Sulbactam-containing β-lactamase inhibitor combinations. *Clin. Microbiol. Infect.*, **14**: 185–188.

83. Scholar, E. (2007) Tazobactam. Enna, S.J. and Bylund, D.B., editors. xPharm: The Comprehensive Pharmacology Reference. Amsterdam, Netherlands / Boston, MA: Elsevier. pp. 1–5.

84. Buynak, J.D. (2006) Understanding the longevity of the β-lactam antibiotics and of antibiotic/β-lactamase inhibitor combinations. *Biochem. Pharmacol.*, **71**: 930–940.

85. Coleman, K. (2011) Diazabicyclooctanes (DBOs): a potent new class of non-β-lactam β-lactamase inhibitors. *Curr. Opin. Microbiol.*, **14**: 550–555.

86. Liu, Z., Wang, Y., Walsh, T.R., et al. (2017) Plasmid-Mediated Novel *bla*$_{\text{NDM-17}}$ Gene Encoding a Carbapenemase with Enhanced Activity in a Sequence Type 48 *Escherichia coli* Strain. *Antimicrob. Agents Chemother.*, **61**: e02233-16.

87. Bonnefoy, A., Dupuis-Hamelin, C., Steier, V., et al. (2004) *In vitro* activity of AVE1330A, an innovative broad-spectrum non-β-lactam β-lactamase inhibitor. *J. Antimicrob. Chemother.*, **54**: 410–417.

88. Lence, E. and González-Bello, C. (2021) Bicyclic Boronate *β*-Lactamase Inhibitors: The Present Hope against Deadly Bacterial Pathogens. *Adv. Ther.*, **4**: 2000246.

89. Wang, X., Zhang, F., Zhao, C., et al. (2014) *In Vitro* Activities of Ceftazidime-

Avibactam and Aztreonam-Avibactam against 372 Gram-Negative Bacilli Collected in 2011 and 2012 from 11 Teaching Hospitals in China. *Antimicrob. Agents Chemother.*, **58**: 1774–1778.

90. Bush, K. and Bradford, P.A. (2019) Interplay between β-lactamases and new β-lactamase inhibitors. *Nat. Rev. Microbiol.*, **17**: 295–306.

91. Krajnc, A., Lang, P.A., Panduwawala, T.D., Brem, J., and Schofield, C.J. (2019) Will morphing boron-based inhibitors beat the β-lactamases? *Curr. Opin. Chem. Biol.*, **50**: 101–110.

92. Michaelis, A. and Becker, P. (1882) Ueber Monophenylborchlorid und einige Derivate desselben. *Ber. Dtsch. Chem. Ges.*, **15**: 180–185.

93. Dobozy, O., Mile, I., Ferencz, I., and Csányi, V. (1971) Effect of Electrolytes on the Activity and Iodine Sensitivity of Penicillinase from B. cereus. *Acta Biochim. Biophys. Acad. Sci. Hung.*, **6**: 97–105.

94. Beesley, T., Gascoyne, N., Knott-Hunziker, V., Petursson, S., Waley, S.G., Jaurint, B., and Grundströmt, T. (1983) The inhibition of class C β-lactamases by boronic acids. *Biochem. J.*, **209**: 229–233.

95. Hecker, S.J., Reddy, K.R., Totrov, M., et al. (2015) Discovery of a Cyclic Boronic Acid *β*-Lactamase Inhibitor (RPX7009) with Utility vs Class A Serine Carbapenemases. *J. Med. Chem.*, **58**: 3682–3692.

96. FDA (Food and Drug Administration). (2017) FDA approves new antibacterial drug. [Online]. Retrieved June 2022 from: https://www.fda.gov/news-events/press-announcements/fda-approves-new-antibacterial-drug.

97. Langley, G.W., Cain, R., Tyrrell, J.M., et al. (2019) Profiling interactions of vaborbactam with metallo-β-lactamases. *Bioorganic Med. Chem. Lett.*, **29**: 1981–1984.

98. Brem, J., Berkel, S.S. Van., Zollman, D., et al. (2016) Structural Basis of Metallo-β-Lactamase Inhibition by Captopril Stereoisomers. *Antimicrob. Agents Chemother.*, **60**: 142–150.

99. Rotondo, C.M. and Wright, G.D. (2017) Inhibitors of metallo-β-lactamases. *Curr. Opin. Microbiol.*, **39**: 96–105.

100. Galleni, M., Lamotte-brasseur, J., Maria, G., Spencer, J., Dideberg, O., Frère, J.-M., and Rossolini, G.M. (2001) Standard Numbering Scheme for Class B β-Lactamases. *Antimicrob. Agents Chemother.*, **45**: 660–663.

101. Pettinati, I., Brem, J., Lee, S.Y., McHugh, P.J., and Schofield, C.J. (2016) The

Chemical Biology of Human Metallo-β-Lactamase Fold Proteins. *Trends Biochem. Sci.*, **41**: 338–355.

102. Garau, G., Bebrone, C., Anne, C., Galleni, M., Frère, J.-M., and Dideberg, O. (2005) A Metallo-β-lactamase Enzyme in Action: Crystal Structures of the Monozinc Carbapenemase CphA and its Complex with Biapenem. *J. Mol. Biol.*, **345**: 785–795.

103. Crowder, M.W., Spencer, J., and Vila, A.J. (2006) Metallo-*β*-lactamases: Novel Weaponry for Antibiotic Resistance in Bacteria. *Acc. Chem. Res.*, **39**: 721–728.

104. Palzkill, T. (2013) Metallo-β-lactamase structure and function. *Ann. N. Y. Acad. Sci.*, **1277**: 91–104.

105. Page, M.I. and Badarau, A. (2008) The mechanisms of catalysis by metallo-β-lactamases. *Bioinorg. Chem. Appl.*, **2008**: 1–14.

106. Peraro, M.D., Vila, A.J., Carloni, P., and Klein, M.L. (2007) Role of zinc content on the catalytic efficiency of B1 metallo β-lactamases. *J. Am. Chem. Soc.*, **129**: 2808–2816.

107. Fonseca, F., Arthur, C.J., Bromley, E.H.C., Samyn, B., Moerman, P., Saavedra, M.J., Correia, A., and Spencer, J. (2011) Biochemical Characterization of Sfh-I, a Sbclass B2 Metallo-β-Lactamase from *Serratia fonticola* UTAD54. *Antimicrob. Agents Chemother.*, **55**: 5392–5395.

108. Villadares, M.H., Galleni, M., Frère, J.-M., et al. (1996) Overproduction and Purification of the *Aeromonas hydrophila* CphA Metallo-*β*-Lactamase Expressed in *Escherichia coli*. *Microb. Drug Resist.*, **2**: 253–256.

109. Bebrone, C., Delbrück, H., Kupper, M.B., et al. (2009) The Structure of the Dizinc Subclass B2 Metallo-β-Lactamase CphA Reveals that the Second Inhibitory Zinc Ion Binds in the Histidine Site. *Antimicrob. Agents Chemother.*, **53**: 4464–4471.

110. Mercuri, P., Bouillenne, F., Boschi, L., et al. (2001) Biochemical Characterization of the FEZ-1 Metallo-β-Lactamase of *Legionella gormanii* ATCC 33297^{T} produced in *Escherichia coli*. *Antimicrob. Agents Chemother.*, **45**: 1254–1262.

111. Ullah, J.H., Walsh, T.R., Taylor, I.A., Emery, D.C., Verma, C.S., Gamblin, S.J., and Spencer, J. (1998) The Crystal Structure of the L1 Metallo-β-lactamase from *Stenotrophomonas maltophilia* at 1.7 Å Resolution. *J. Mol. Biol.*, **284**: 125–136.

112. Horsfall, L.E., Izougarhane, Y., Lassaux, P., et al. (2011) Broad antibiotic resistance profile of the subclass B3 metallo-β-lactamase GOB-1, a di-zinc enzyme. *FEBS J.*, **278**: 1252–1263.

113. Abboud, M.I., Damblon, C., Brem, J., et al. (2016) Interaction of Avibactam with Class B Metallo-β-lactamases. *Antimicrob. Agents Chemother.*, **60**: 5655–5662.

114. Watanabe, M., Iyobe, S., Inoue, M., and Mitsuhashi, S. (1991) Transferable Imipenem Resistance in *Pseudomonas aeruginosa*. *Antimicrob. Agents Chemother.*, **35**: 147–151.

115. Meini, M.-R., Llarrull, L., and Vila, A. (2014) Evolution of Metallo-β-lactamases: Trends Revealed by Natural Diversity and *in vitro* Evolution. *Antibiotics*, **3**: 285–316.

116. Hong, D.J., Bae, I.K., Jang, I.-H., Jeong, S.H., Kang, H.-K., and Lee, K. (2015) Epidemiology and Characteristics of Metallo-β-Lactamase-Producing *Pseudomonas aeruginosa*. *Infect. Chemother.*, **47**: 81–97.

117. The Comprehensive Antibiotic Resistance Database. (2022) IMP beta-lactamase. [Online]. Retrieved June 2022 from: https://card.mcmaster.ca/ontology/36029.

118. Tada, T., Nhung, H., Miyoshi-Akiyama, T., Shimada, K., Phuong, M., and Anh, Q. (2015) IMP-51, a Novel IMP-Type Metallo-β-Lactamase with Increased Doripenem- and Meropenem-Hydrolyzing Activities, in a Carbapenem-Resistant *Pseudomonas aeruginosa* Clinical Isolate. *Antimicrob. Agents Chemother.*, **59**: 7090–7093.

119. Borgianni, L., Prandi, S., Salden, L., Santella, G., Hanson, N.D., Rossolini, G.M., and Docquier, J. (2011) Genetic Context and Biochemical Characterization of the IMP-18 Metallo-β-Lactamase Identified in a *Pseudomonas aeruginosa* Isolate from the United States. *Antimicrob. Agents Chemother.*, **55**: 140–145.

120. Yamaguchi, Y., Kuroki, T., Yasuzawa, H., et al. (2005) Probing the Role of Asp-120(81) of Metallo-*β*-lactamase (IMP-1) by Site-directed Mutagenesis, Kinetic Studies, and X-ray Crystallography. *J. Biol. Chem.*, **280**: 20824–20832.

121. García-Sáez, I., Docquier, J.-D., Rossolini, G.M., and Dideberg, O. (2008) The Three-Dimensional Structure of VIM-2, a Zn-β-lactamase from *Pseudomonas aeruginosa* in Its Reduced and Oxidised Form. *J. Mol. Biol.*, **375**: 604–611.

122. Lauretti, L., Riccio, M.L., Mazzariol, A., Cornaglia, G., Amicosante, G., Fontana, R., and Rossolini, G.M. (1999) Cloning and Characterization of bla_{VIM}, a New Integron-Borne Metallo-β-Lactamase Gene from a *Pseudomonas aeruginosa* Clinical Isolate. *Antimicrob. Agents Chemother.*, **43**: 1584–1590.

123. Walsh, T.R., Toleman, M.A., Poirel, L., and Nordmann, P. (2005) Metallo-β-Lactamases: the Quiet before the Storm? *Clin. Microbiol. Rev.*, **18**: 306–325.

124. Poirel, L., Collet, L., and Nordmann, P. (2000) Carbapenem-Hydrolyzing Metallo-β-Lactamase from a Nosocomial Isolate of *Pseudomonas aeruginosa* in France. *Emerg. Infect. Dis.*, **6**: 84–85.

125. The Comprehensive Antibiotic Resistance Database. (2022) VIM beta-lactamase. [Online]. Retrieved June 2022 from: https://card.mcmaster.ca/ontology/36030.

126. Yong, D., Toleman, M.A., Giske, C.G., Cho, H.S., Sundman, K., Lee, K., and Walsh, T.R. (2009) Characterization of a New Metallo-β-lactamase gene, *bla*$_{\text{NDM-1}}$, and a Novel Erythromycin Esterase Gene Carried on a Unique Genetic Structure in *Klebsiella pneumoniae* Sequence Type 14 from India. *Antimicrob. Agents Chemother.*, **53**: 5046–5054.

127. Johnson, A.P. and Woodford, N. (2013) Global spread of antibiotic resistance: the example of New Delhi metallo-*β*-lactamase (NDM)-mediated carbapenem resistance. *J. Med. Microbiol.*, **62**: 499–513.

128. Patel, G. and Bonomo, R.A. (2013) "Stormy waters ahead": global emergence of carbapenemases. *Front. Microbiol.*, **4**: 1–17.

129. The Comprehensive Antibiotic Resistance Database. (2022) NDM beta-lactamase. [Online]. Retrieved June 2022 from: https://card.mcmaster.ca/ontology/36196.

130. Zhang, H. and Hao, Q. (2011) Crystal structure of NDM-1 reveals a common β-lactam hydrolysis mechanism. *FASEB J.*, **25**: 2574–2582.

131. Mataseje, L.F., Peirano, G., Church, D.L., Conly, J., Mulvey, M., and Pitout, J.D. (2016) Colistin-Nonsusceptible *Pseudomonas aeruginosa* Sequence Type 654 with *bla*$_{\text{NDM-1}}$ Arrives in North America. *Antimicrob. Agents Chemother*, **60**: 1794–1800.

132. Struelens, M.J., Monnet, D.L., Magiorakos, A.P., Santos O'Connor, F., and Giesecke, J. (2010) New Delhi metallo-beta-lactamase 1-producing Enterobacteriaceae: emergence and response in Europe. *Euro Surveill.*, **15**: 1–10.

133. Kumarasamy, K.K., Toleman, M. a., Walsh, T.R., et al. (2010) Emergence of a new antibiotic resistance mechanism in India, Pakistan, and the UK: a molecular, biological, and epidemiological study. *Lancet Infect. Dis.*, **10**: 597–602.

134. Walsh, T.R., Weeks, J., Livermore, D.M., and Toleman, M.A. (2011) Dissemination of NDM-1 positive bacteria in the New Delhi environment and its implications for human health: an environmental point prevalence study. *Lancet Infect. Dis.*, **11**: 355–362.

135. Li, G.B., Abboud, M.I., Brem, J., et al. (2017) NMR-filtered virtual screening leads

to non-metal chelating metallo-β-lactamase inhibitors. *Chem. Sci.*, **8**: 928–937.

136. Cushman, D.W. and Ondetti, M.A. (1991) History of the Design of Captopril and Related Inhibitors of Angiotensin Converting Enzyme David. *Hypertension*, **17**: 589–592.

137. Opie, L.H. and Kowolik, H. (1995) The discovery of captopril: from large animals to small molecules. *Cardiovasc. Res.*, **30**: 18–25.

138. Klingler, F.M., Wichelhaus, T.A., Frank, D., et al. (2015) Approved Drugs Containing Thiols as Inhibitors of Metallo-*β*-lactamases: Strategy To Combat Multidrug-Resistant Bacteria. *J. Med. Chem.*, **58**: 3626–3630.

139. García-Sáez, I., Hopkins, J., Papamicael, C., et al. (2003) The 1.5-Å Structure of *Chryseobacterium meningosepticum* Zinc *β*-Lactamase in Complex with the Inhibitor, D-Captopril. *J. Biol. Chem.*, **278**: 23868–23873.

140. Dawn, L. and Whited, L. (2022) Dimercaprol. In: StatPearls [Internet]. Treasure Island, FL: StatPearls Publishing. Retrieved June 2022 from: https://www.ncbi.nlm.nih.gov/books/NBK549804/.

141. González, M.M., Kosmopoulou, M., Mojica, M.F., et al. (2016) Bisthiazolidines: A Substrate-Mimicking Scaffold as an Inhibitor of the NDM-1 Carbapenemase. *ACS Infect. Dis.*, **1**: 544–554.

142. Hinchliffe, P., González, M.M., Mojica, M.F., González, J.M., Castillo, V., and Saiz, C. (2016) Cross-class metallo-β-lactamase inhibition by bisthiazolidines reveals multiple binding modes. *Proc. Natl. Acad. Sci. U. S. A.*,: 1–10.

143. Tan, X., Kim, H.S., Baugh, K., et al. (2021) Therapeutic Options for Metallo-β-Lactamase Producing Enterobacterales. *Infect. Drug Resist.*, **14**: 125–142.

144. Somboro, A.M., Tiwari, D., Bester, L.A., et al. (2014) NOTA: a potent metallo-β-lactamase inhibitor. *J. Antimicrob. Chemother.*, **70**: 1594–1596.

145. Aoki, N., Ishii, Y., Tateda, K., et al. (2010) Efficacy of Calcium-EDTA as an Inhibitor for Metallo-β-Lactamase in a Mouse Model of *Pseudomonas aeruginosa* Pneumonia. *Antimicrob. Agents Chemother.*, **54**: 4582–4588.

146. Falconer, S.B., Reid-Yu, S.A., King, A.M., et al. (2016) Zinc Chelation by a Small-Molecule Adjuvant Potentiates Meropenem Activity in Vivo against NDM-1-Producing *Klebsiella pneumoniae*. *ACS Infect. Dis.*, **1**: 533–543.

147. King, A.M., Reid-Yu, S.A., Wang, W., et al. (2014) Aspergillomarasmine A overcomes metallo-β-lactamase antibiotic resistance. *Nature*, **510**: 503–506.

148. Haenni, A., Robert, M., Vetter, W., Roux, L., Barbier, M., and Lederer, E. (1965) Structure chimique des aspergillomarasmines A et B. *Helv. Chim. Acta*, **48**: 729–750.

149. Woolley, D.W. (1948) Studies on the structure of lycomarasmin. *J. Biol. Chem.*, **176**: 1291–1298.

150. Ramos, B., López, G., and Molina, A. (2015) Development of a *Fusarium oxysporum* f. sp. *melonis* functional GFP fluorescence tool to assist melon resistance breeding programmes. *Plant Pathol.*, **64**: 1349–1357.

151. Friis, P., Olsen, C.E., and Møller, B.L. (1991) Toxin production in *Pyrenophora teres*, the ascomycete causing the net-spot blotch disease of barley (*Hordeum vulgare* L.). *J. Biol. Chem.*, **266**: 13329–13335.

152. Dolgin, E. (2016) Inner Workings: Combating antibiotic resistance from the ground up. *Proc. Natl. Acad. Sci.*, **113**: 11642–11643.

153. Sychantha, D., Rotondo, C.M., Tehrani, K.H.M.E., Martin, N.I., and Wright, G.D. (2021) Aspergillomarasmine A inhibits metallo-β-lactamases by selectively sequestering Zn^{2+}. *J. Biol. Chem.*, **297**: 100918.

154. Shaw, E., Rombauts, A., Tubau, F., et al. (2018) Clinical outcomes after combination treatment with ceftazidime/avibactam and aztreonam for NDM-1/OXA-48/CTX-M-15-producing *Klebsiella pneumoniae* infection. *J. Antimicrob. Chemother.*, **73**: 1104–1106.

155. Gonzales, P.R., Pesesky, M.W., Bouley, R., et al. (2015) Synergistic, collaterally sensitive β-lactam combinations suppress resistance in MRSA. *Nat. Chem. Biol.*, **11**: 855–864.

156. Mhlongo, N., Essack, S., and Govinden, U. (2015) NDM-1, novel TEM-205, novel TEM-213 and other extended-spectrum β-lactamases co-expressed in isolates from cystic fibrosis patients from South Africa. *South. African J. Infect. Dis.*, **30**: 103–107.

157. Ahmed, A., Azim, A., Gurjar, M., and Baronia, A. (2014) Current concepts in combination antibiotic therapy for critically ill patients. *Indian J. Crit. Care Med.*, **18**: 310–314.

158. Tamma, P.D., Cosgrove, S.E., and Maragakis, L.L. (2012) Combination Therapy for Treatment of Infections with Gram-Negative Bacteria. *Clin. Microbiol. Rev.*, **25**: 450–470.

159. Mouton, J.W. (1999) Combination Therapy as a Tool to Prevent Emergence of

Bacterial Resistance. *Infection,* **27**: S24–S28.

160. Bush, K. (2015) Antibiotics: Synergistic MRSA combinations. *Nat. Chem. Biol.*, **11**: 832–833.

161. Nai, C., Magrini, B., and Offe, J. (2016) Let microorganisms do the talking, let us talk more about microorganisms. *Fungal Biol. Biotechnol.*, **3**: 5.

162. Rotondo, C.M., Sychantha, D., Koteva, K., and Wright, G.D. (2020) Suppression of *β*-Lactam Resistance by Aspergillomarasmine A Is Influenced by both the Metallo-*β*-Lactamase Target and the Antibiotic Partner. *Antimicrob. Agents Chemother.*, **64**: e01386-19.

163. Tehrani, K.H.M.E. and Martin, N.I. (2018) β-lactam/β-lactamase inhibitor combinations: an update. *Med. Chem. Comm.,* **9**: 1439–1456.

164. Bahr, G., González, L.J., and Vila, A.J. (2021) Metallo-*β*-lactamases in the Age of Multidrug Resistance: From Structure and Mechanism to Evolution, Dissemination, and Inhibitor Design. *Chem. Rev.,* **121**: 7957–8094.

165. Venatorx Pharmaceuticals. (2022) Cefepime-Taniborbactam. [Online]. Retrieved June 2022 from: https://www.venatorx.com/cefepime-taniborbactam/.

166. Rawat, D. and Nair, D. (2010) Extended-spectrum β-lactamases in Gram Negative Bacteria. *J. Glob. Infect. Dis.,* **2**: 263–274.

167. Lahiri, S.D., Mangani, S., Jahić, H., et al. (2015) Molecular Basis of Selective Inhibition and Slow Reversibility of Avibactam against Class D Carbapenemases: A Structure-Guided Study of OXA-24 and OXA-48. *ACS Chem. Biol.*, **10**: 591–600.

168. Maragakis, L.L. and Perl, T.M. (2008) *Acinetobacter baumannii*: Epidemiology, Antimicrobial Resistance, and Treatment Options. *Clin. Infect. Dis.,* **46**: 1254–1263.

169. Pang, Z., Raudonis, R., Glick, B.R., Lin, T.J., and Cheng, Z. (2019) Antibiotic resistance in *Pseudomonas aeruginosa*: mechanisms and alternative therapeutic strategies. *Biotechnol. Adv.*, **37**: 177–192.

170. Peleg, A.Y., Seifert, H., and Paterson, D.L. (2008) *Acinetobacter baumannii*: Emergence of a Successful Pathogen. *Clin. Microbiol. Rev.*, **21**: 538–582.

171. Ruffin, M. and Brochiero, E. (2019) Repair Process Impairment by *Pseudomonas aeruginosa* in Epithelial Tissues: Major Features and Potential Therapeutic Avenues. *Front. Cell. Infect. Microbiol.*, **9**: 182.

172. Diggle, S.P. and Whiteley, M. (2020) Microbe profile: *Pseudomonas aeruginosa*: opportunistic pathogen and lab rat. *Microbiology*, **166**: 30–33.

173. Morin, C.D., Déziel, E., Gauthier, J., Levesque, R.C., and Lau, G.W. (2021) An Organ System-Based Synopsis of *Pseudomonas aeruginosa* Virulence. *Virulence*, **12**: 1469–1507.

174. Wright, G.D. (2016) Antibiotic Adjuvants: Rescuing Antibiotics from Resistance. *Trends Microbiol.*, **24**: 862–871.

175. Cox, G., Sieron, A., King, A.M., De Pascale, G., Pawlowski, A.C., Koteva, K., and Wright, G.D. (2017) A Common Platform for Antibiotic Dereplication and Adjuvant Discovery. *Cell Chem. Biol.*, **24**: 98–109.

176. Zubyk, H.L., Cox, G., and Wright, G.D. (2019) Antibiotic Dereplication Using the Antibiotic Resistance Platform. *J. Vis. Exp.*, **2019**: e60536.

177. Biswas, I. (2015) Genetic tools for manipulating Acinetobacter baumannii genome: An overview. *J. Med. Microbiol.*, **64**: 657–669.

178. Schweizer, H.P. and de Lorenzo, V. (2004) Molecular Tools for Genetic Analysis of Pseudomonads. Ramos, J.L., editor. *Pseudomonas*. Boston, MA: Springer. pp. 317–350.

179. Yarlagadda, V., Medina, R., and Wright, G.D. (2020) Venturicidin A, A Membrane-active Natural Product Inhibitor of ATP synthase Potentiates Aminoglycoside Antibiotics. *Sci. Rep.*, **10**: 8134.

180. Yarlagadda, V., Rao, V.N., Kaur, M., Guitor, A.K., and Wright, G.D. (2021) A Screen of Natural Product Extracts Identifies Moenomycin as a Potent Antigonococcal Agent. *ACS Infect. Dis.*, **7**: 1569–1577.

181. Sánchez, M.B. (2015) Antibiotic resistance in the opportunistic pathogen *Stenotrophomonas maltophilia*. *Front. Med.*, **6**: 658.

182. González, L.J. and Vila, A.J. (2012) Carbapenem resistance in *Elizabethkingia meningoseptica* is mediated by metallo-*β*-lactamase BlaB. *Antimicrob. Agents Chemother.*, **56**: 1686–1692.

183. Russ, D., Glaser, F., Shaer Tamar, E., et al. (2020) Escape mutations circumvent a tradeoff between resistance to a beta-lactam and resistance to a beta-lactamase inhibitor. *Nat. Commun.*, **11**: 2029.